ISBN 978-1-960740-44-1

COMPUTER SCIENCE AND INFORMATION TECHNOLOGY - ADVANCES AND APPLICATIONS

Research Based Book Chapter

2D-3D-NUMERICAL COMPUTATIONAL INTELLIGENCE RADIOTHERAPY OPTIMIZATION FOR HYPERFRACTIONATED RADIATION TREATMENT PLANNING WITH BIOLOGICAL EFFECTIVE DOSE MODELS

Publication Date
May 09, 2025
doi: 10.5281/zenodo.14830054

Scientific Knowledge Publisher (SciKnowPub), USA
info@sciknowpub.com

RESEARCH BASED BOOK CHAPTER

2D-3D-NUMERICAL COMPUTATIONAL INTELLIGENCE RADIOTHERAPY OPTIMIZATION FOR HYPERFRACTIONATED RADIATION TREATMENT PLANNING WITH BIOLOGICAL EFFECTIVE DOSE MODELS

Francisco Casesnoves[1]

[1]PhD Engineering, MSc Physics-Mathematics, Physician. Bioengineering Laboratory Director. Independent Research Scientist. International Association of Advanced Materials, Sweden. UniScience Global Scientific Member, Wyoming, USA. Some former important affiliations: SIAM (Society for Industrial and Applied Mathematics) and ASME (American Society of Mechanical Engineers)

For Correspondence
casesnoves.research.emailbox@gmail.com

Author's Biography

Dr Francisco Casesnoves earned the Engineering and Natural Sciences PhD by Talllinn University of Technology (started thesis in 2016, thesis Defence/PhD earned in December 2018, official graduate Diploma 2019). He works as independent research scientist in computational-engineering/physics, and actually is Director of Independent Bioengineering Laboratory. Dr Casesnoves earned MSc-BSc, Physics/Applied-Mathematics (Public Eastern-Finland-University, MSc Thesis in Radiotherapy Treatment Planning Optimization, which was developed after graduation in a series of Radiation Therapy Optimization-Modelling publications [2007-present]). Dr Casesnoves earned Graduate-with-MPhil, in Medicine and Surgery [1983] (Madrid University Medicine School, MPhil in Radioprotection Low Energies Dosimetry [1985]). Casesnoves resigned definitely to his original nationality in 2020 for ideological reasons, anti-monarchy-corruption, democratic-republican ideology, and ethical-professional reasons, and does not belong to Spain Kingdom anymore. His constant service to the International Scientific Community and Estonia Republic technological progress involves about 100 DOI articles, more than 120 total publications, and about 4 books. Recent advances published are in Superconductors Mathematical Modelling and Radiotherapy Brain Neurobiological Models, 3D-AI Isodosezones and Isodoselines. Among Dr. Casesnoves inventions and scientific creations are:

1. Numerical Reuleaux Method.
2. Radiotherapy Omega Factor correction for AAA model wedge filters dose delivery.
3. Integral-Differential materials erosion model.
4. Graphical Optimization.
5. Interior Optimization Methods.
6. Superconductors Molecular Effect Model.
7. Superconductors Multifunctional Transmission Line.
8. BED radiotherapy model GA and Graphical Optimization Isodoselines and Isodosezones.

Abstract

Several radiotherapy optimization methods were developed in a large number of contributions. Among them, 2D-3D Interior and Graphical Optimization. Likewise, and recently, Pareto-Multiobjective Optimization applied/set on Genetic Algorithms methods were implemented in a series of publications. Modern computational intelligence Genetic Algorithms, combined with Inverse Objective Functions, provide fast and precise

calculations for Biological Effective Dose hyperfractionated dose-delivery planning techniques. Just remark that the design of the chapter is mainly focused on hyperfractionated BED-TPO because that is the publication series focus. There are very few discussions about the controversy of hyperfractionated versus hypofractionated TPO, that is/was not the objective of the research. In this line, this work constitutes a selection-compilation of results, significant paragraphs/algorithms/images of the articles series for prevalent/incident tumors whose cancer treatment often involves radiation therapy. Selected series of 2D-3D image processing charts are included. Selected chosen formulas, objective functions, algorithms, and radiotherapy models are explained. The selection criteria were focused on including varied important parts of radiotherapy TPO models foundations, models, algorithms, and efficacious formulas applications. Beam modification static wedges dosimetry with AAA model and Omega factor is included with essential initial formulation, Part 5. That is set after all main Parts 1-4, and intended for easy-learning of every mathematical-computational Part. Every section is presented with the improved results for each and every tumor related to computational BED-hyperfractionated Treatment Planning Optimization (TPO). Along all text, it is emphasized the clarity and practical tools to obtain acceptable/fast TPO results applied on modern radiation oncology. Today, Artificial Intelligence applications for Treatment Planning Optimization have become important and useful.

Keywords

Radiation Dose, Attenuation Exponential Factor (AEF), Simulations, Nonlinear Optimization, Matrix Algebra, Spherical-Spatial Analytical Geometry, Organ at Risk (OAR), Multi-Leaf Collimator (MLC), Wedge Filter (WF), Conformal Wedge Filter, Anisotropic Analytic Model AAA, Intensity Modulated Radiotherapy (IMRT), Intense Modulated Protontherapy (IMPT), Fluence Factor (FF), Treatment Planning Optimization (TPO), Breast Tumor (BT) Computarized Thomography (CT)

'To the pursuit of the Truth for itself'

1. General Introduction

This chapter deals with some selected essentials of radiotherapy optimization along recent publications. In recent years, the cancer treatment became more multidisciplinary, and Radiation therapy as a branch, has also got significant improvements with/without synergic combination with other therapies. Namely, among others, protontherapy and high-precision advances in routinary photon-dose optimization delivery. As a present/future advance, it is a must mention the trend towards Inmuno and Nano therapies that could bring in future total curation for specific tumors. The main types of tumors are divided into sections and foremost algorithms/formulations are also included. Selected 2D-3D image processing charts are shown at every section with convenient clarifications.

Among the number of advances included combined with all sections are the following:

1. 3D Isodoselines and Isodosezones
2. Hyperfractionated TPO formulation/algorithms
3. Inverse Optimization Methods for TPO
4. Pareto-Multiobjective Computational Intelligence based on Evolutionary Algorithms Methods
5. AAA Model Omega Factor Corrections
6. Brief of beam Modification Static Wedges publications
7. Tumor Survival Fraction Formulation and 3D Graphical Optimization

From these topics in the list, emphasis for their importance can be Pareto-Multiobjective Methods-results, Isodoselines and Isodosezones, 3D Genetic Algorithms Graphical Optimization and the reminder of previous AAA Omega Factor and 3D Beam Modification Static Wedges image processing techniques. The series of research work are extensive and can be consulted using the further reading references of each Section. Extensive formulation is included in Section 5. The reader can get also supplementary reading for important fundamentals in radiotherapy computational optimization treatment planning along the complete references of each Section.

2. General Mathematical and Computational Methods

Along these publication series a number of mathematical, software-engineering, and original algorithms methods were used mainly with MATLAB and GNU-Octave. Some important selected examples are as follows:

1. Inverse Optimization algorithm example, usually with Tihkonov and Chevyshev methods. The Tikhonov regularization theory constituted an essential method for radiotherapy articles series in these types of tumors. Details are included at Section 5, and the simplest objective function form reads:

$$\text{Chebyshev} \quad L_1 \text{ Optimization},$$
$$\text{for} \quad i = 1,2 \ldots \text{minimize pareto},$$
$$\left| DOSE_i - BED_{Effective} \right|_{L_1} \text{ with},$$
$$BED_{Effective} = k \times d \times \left[1 + \frac{d \times \beta}{\alpha} \right] - \ldots$$
$$\ldots - \frac{Ln(2)}{\alpha} \times \left[\frac{T_{Treatment} - T_{Delay}}{T_{Potential}} \right];$$

(Example 1. Casesnoves Bioengineering Laboratory. Software. 4577)

2. Computational Intelligence Optimization example, developed through Genetic Algorithms, both graphical and numerical. Example of this at Section 5 reads:

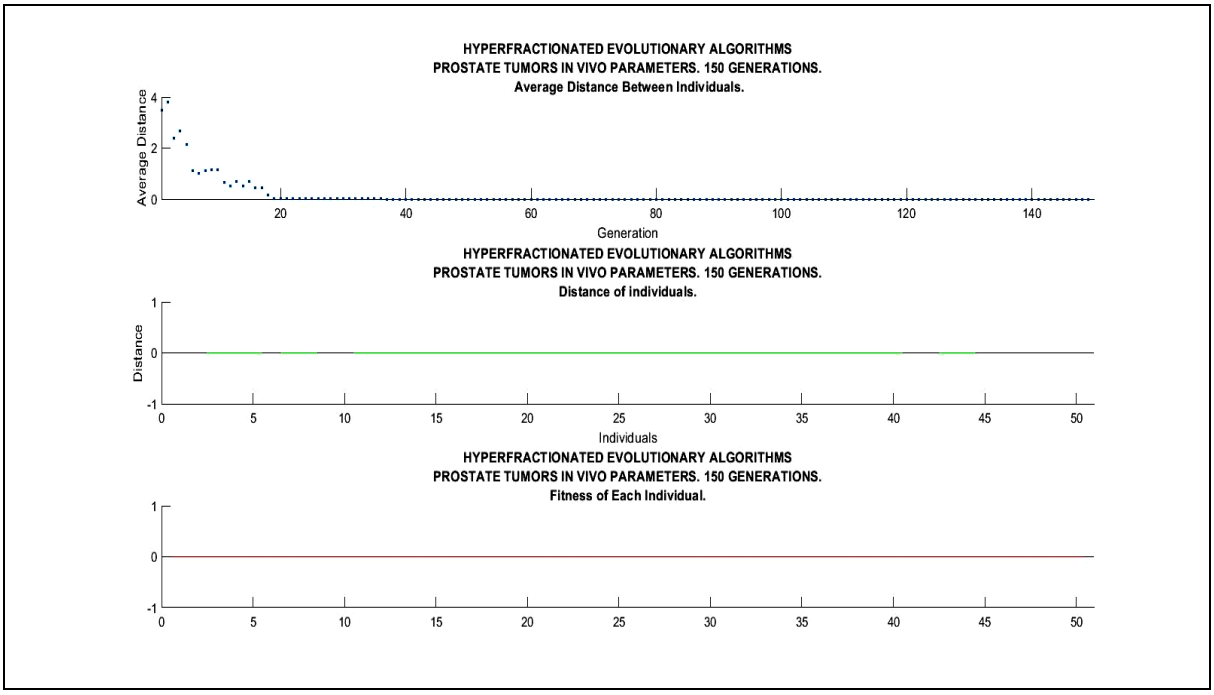

(Example 2. Casesnoves Bioengineering Laboratory. Software. 4577)

3. 2D-3D Imaging Processing Methods Example to obtain the better precise, sharp and specific graphics. This Instance from Section 2 reads:

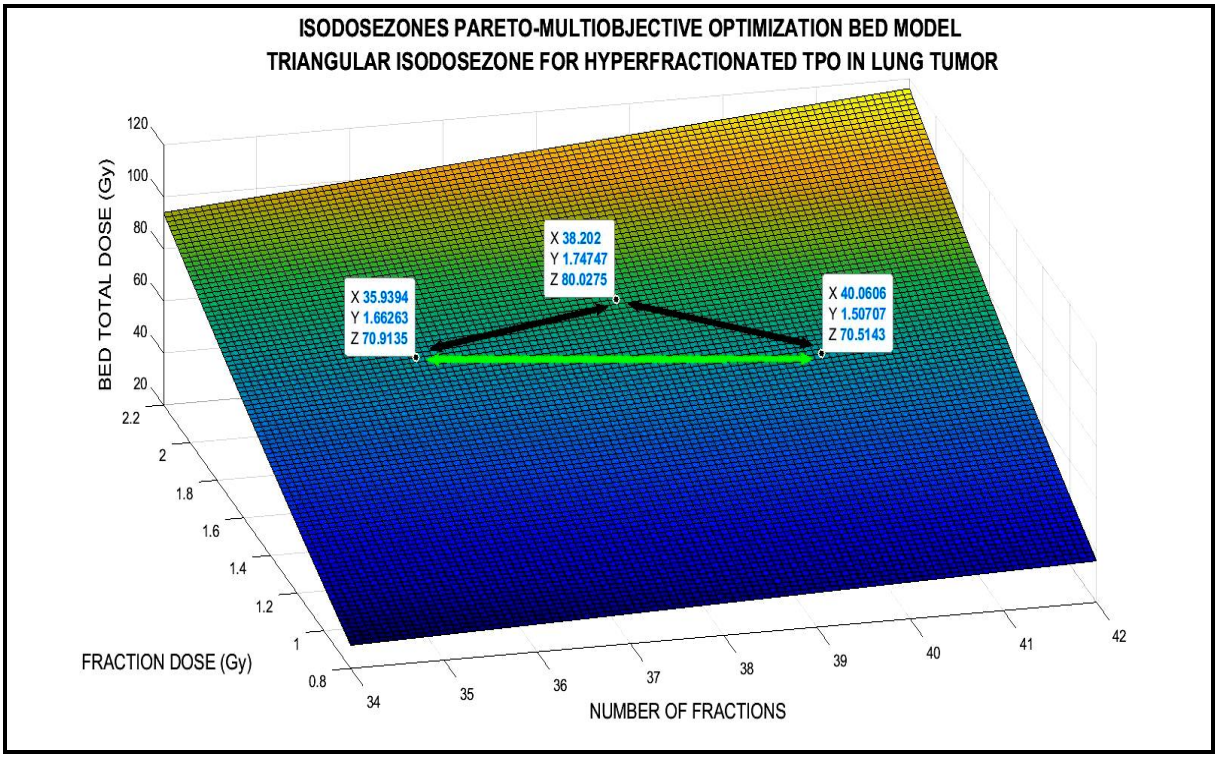

(Example 3. Casesnoves Bioengineering Laboratory. Software. 4577)

1. Breast Tumors

Abstract

Lung and breast cancer are the most frequent epidemiologically. The big difference is the survival time after treatment, in favor of the breast one. This section deals with the main previous advances in recent breast tumors publications, focused on applications of AAA model with Omega Factor for wedge filters. Namely, 3D Isodosezones-surfaces for wedge filters with AAA model. Therefore, this Section is based on selected 3D Graphical Optimization for AAA model in radiation therapy wedge filters, with Omega Factor implemented. Most important database for Isodosezones-surfaces for wedge filters with AAA model is shown with graphics and numerical details. Further formulation can be studied at Section 5.

Keywords

Radiation Dose, Attenuation Exponential Factor (AEF), Simulations, Nonlinear Optimization, Matrix Algebra, Spherical-Spatial Analytical Geometry, Organ at Risk (OAR), Multi-Leaf Collimator (MLC), Wedge Filter (WF), Conformal Wedge Filter, Anisotropic Analytic Model AAA, Intensity Modulated Radiotherapy (IMRT), Intense Modulated Protontherapy (IMPT), Fluence Factor (FF), Treatment Planning Optimization (TPO), Breast Tumor (BT) Computarized Thomography (CT)

1. Introduction and Objectives

Continuing with Anisotropic Analytic Model (AAA) radiotherapy research/improvements, new 3D Isodoses graphics are presented for beam-modification Treatment Planning Optimization TPO with Wedge Filters (WF). Results for 3D Isodose Graphics for [AAA model: z= 5, 15 cm], based on all these algorithms/software, are developed for AAA model 18 Mev intensity photon-beam. Solutions for primary demonstration of 3D Isodose Charts, in Type 1 [Vertical 3D Isodoses], and Type 2 [Horizontal 3D Isodoses are presented] in contrast to classical 2D Isodoses. 3D Isodoses radiotherapy simulations software is explained through the graphics series elaboration. TPO applications with WF, and beam modification devices in general, for breast tumors are shown.

The radiation therapy treatment for breast tumors has improved during recent clinical investigation times [1-20, 25, 74]. Optimal radiotherapy treatment dose delivery is usually a rather difficult conformal 3D operation, guided and on-time controlled by CT in 3D also [1-20, 25, 73, 74]. Therefore, the innovation of this study presents a 3D Isodoses graphics for TPO optimization with WF. These new 3D Isodoses processing images here obtained, get the dose delivery data for several depths with WF subject to 18 Mev photon-beam. They constitute a primary example for its future practical applications possibilities in TPO. It is also possible to vary in the same chart WF dimensions, LINAC output Megavoltage,

WF angles and other parameters for TPO [1-20, 73].

Consequently, the 3D Isodoses developed in this contribution involve two methodology strands. The first one is the AAA model calculations to implement data into the software [1-20, 73, 74]. The second part is the rather long programming work to obtain 3D image processing Isodoses. The type of WF dose delivery shown correspond to previous contributions types [1-20, 73, 74].

Currently radiotherapy treatment is performed in 3D commonly with Computarized Thomography (CT) imaging data before, during, and after the irradiation sessions, that is Imaging-guided radiotherapy techniques also. The OARs and normal radiosensitive tissues constitute an important part of the radiotherapy plan to improve the life quality of the patient [1-20, 73, 74].

Specifically in breast cancer [25, 38, 39, 73], the breathing movement of thorax cavity creates a precision delivery problem. Furthermore, the breast cancer patients in no few circumstances present breath difficulties that make even more complicated that movement control [73, 74]. Biological models (BM), [1, 21-24, 74], are used to modulate the dose delivery magnitude according to specific tissue radiobiological parameters. The amount of variety of BM is large, and even more the modelling corrections algorithms for hyperfractionated TPO. Normal tissue dose complications probability biological models (NTCP) are summed to the radiotherapy plan [1, 21-24, 74], to minimize the OARs radiation damage also. The mathematical optimization basis, form the primary step that was applied to develop modern TPO at both planning system and LINAC apparatus [11, 12, 67].

Therefore, the step forward from 2D to 3D for all planning systems and radiation dataset constitutes a precision requirement at present to improve the efficacy of results in radiotherapy [1-20, 73, 74]. In consequence, the innovation of this study is to present a 3D Isodoses graphics to pass on from 2D Isodoses to 3D Isodoses imaging acquisition TPO work data. In Protontherapy, 3D Isodoses could be also used. However, IMPT models are different from photon-dose ones.

When Hypo-fractionated radiation protocol is used for breast tumors cure [25], 3D Isodoses are useful. The motives, among several others, are to avoid OARs doses and increase radioprotection, and give the patient a better quality of life during radiation treatment [25]. NTCP models are essential for that purpose.

Several ideas about recent advances in cancer research, [1- 20, 73, 74], comprise pre-hypothesis about future radiation oncology. Namely, [1-20], Radiation Therapy will

remain/continue in clinical oncology future mainly for the primary/secondary attack to eliminate the tumor volume, and set/open the field for subsequent surgery, Chemo-Inmuno Therapy, or Nano-Inmunotherapy stages. Preventive Medicine Screening in early-stage diagnosis and prevention (for example, elimination of smoking, alcohol abuse, etc.), has proven be useful/significant for cancer incidence reduction [1-20]. In European Union, these early-stage screening-search for early tumor diagnosis differ rather much among different EU countries.

In summary, this chapter Section shows a software programming series for 3D Isodoses engineering software methods and graphics processing ones, focused to be applied on breast cancer [1, 25, 38, 39, 74]. Software development methods are explained according to image processing. Medical Physics applications for breast tumors, and general radiation oncology TPO are described and analyzed.

2. Mathematical and Computational Methods

In this Section, it is explained the 3D Isodoses method and shown the main programming parameters, Table 1, to be implemented in the patterns. The AAA wedge filters and radiotherapy beam modification devices software engineering is usually rather complicated.

3D Isodoses Software-Programming Method

The computational method is based on previous software works [1-20, 73, 74]. The integral equation complete analytical solution, Eq-Algorithm 1 from Section 5 is correctly simulated in dosimetry-matrices from 100 x 100 dimensions to 300 x 300 dimensions in the following results section and compared with simulations of equations of classical AEF [1-20] in AAA model foundations.

The large structure of the program comprises the summatory of every part of AAA (Erf) Equations at Section 5. Firstly, these parts of Erf functions are set independently one by one. Secondly all of them are summed. Finally, the resulting numerical values are set in the imaging subroutine. In this study, they are implemented in MATLAB. Imaging processing tools and subroutines/options are applied [1-20, 73, 74]. A number of previous publications develop WF AAA photon dose 3D graphical processed images for GNU-Octave and Freemat also [1-20]. But in these cases, the programs involve rather significant modifications [1-20].

Table 1.-AAA model main Photon-Beam Spectra parameters for 3D Isodoses Graphical simulations. Dataset is large, it is recommended to consult references [1-29, 73, 74].

NUMERICAL DOSIMETRY DATASET			
RADIATION PARAMETER	**EXPERIMENTAL REFERENCES AND SIMULATION SELECTED DATA**	**APPROXIMATED MAGNITUDE**	**AAA MODEL DATA**
SSD [cm]	Simulation dataset [1-20,73,74]	Exactly 100 cm	[1-20,73,74]
Fluence Rate [N x cm^{-2} x s^{-1}] N:number of photons	Φ_0 ϵ Experimental Data with Foilers [74]	Φ_0 ϵ [4.16 x 10^9 , 2.82 x 10^{10}] At program, 10^9 was generally implemented	[1-20,73,74]
Field Size [cm^2] WF Angle	WF Angle=15° 12 x 12 [cm] approximated field size	WF Angle=15° 12 x 12 [cm]	[1-20,73,74]
Omega Factor Angles φ1=30° φ2=30° [approximately] WF angle α	From those articles coming from Au foils experimental dosimetry measurements [1,74]	φ1=30° φ2=30° WF Angle=15°	[1-20,73,74]
Dose Rate [Gy/s]	According to [74]	1 Gy dose delivery time At [Au foils] 1 Gy delivery time ϵ [14,19] seconds	[1-20,73,74]

3. Results

The 3D Isodoses could be Type I [Vertical], Figure 1, or Type II [Horizontal]. Both types prove the utility for TPO of these 3D Isodoses graphics [1-20, 73]. Note that non-limited multiple 3D Isodoses are feasible by using the developed engineering software [1-20, 74].

Type I 3D Isodoses [Vertical]

Figures 1-2 show Type I 3D Isodoses WF graphics for [z=5 cm, z=15 cm] depth doses with AAA model. The innovation of the study involves practical use for TPO, in contrast with classical 2D Isodoses plots. The visualization 3D advantages related to 2D Isodoses are evident. The number of 3D WF dose delivery images in Figures 1-4 is two, but it is not limited to any amount superposed 3D charts in the same image.

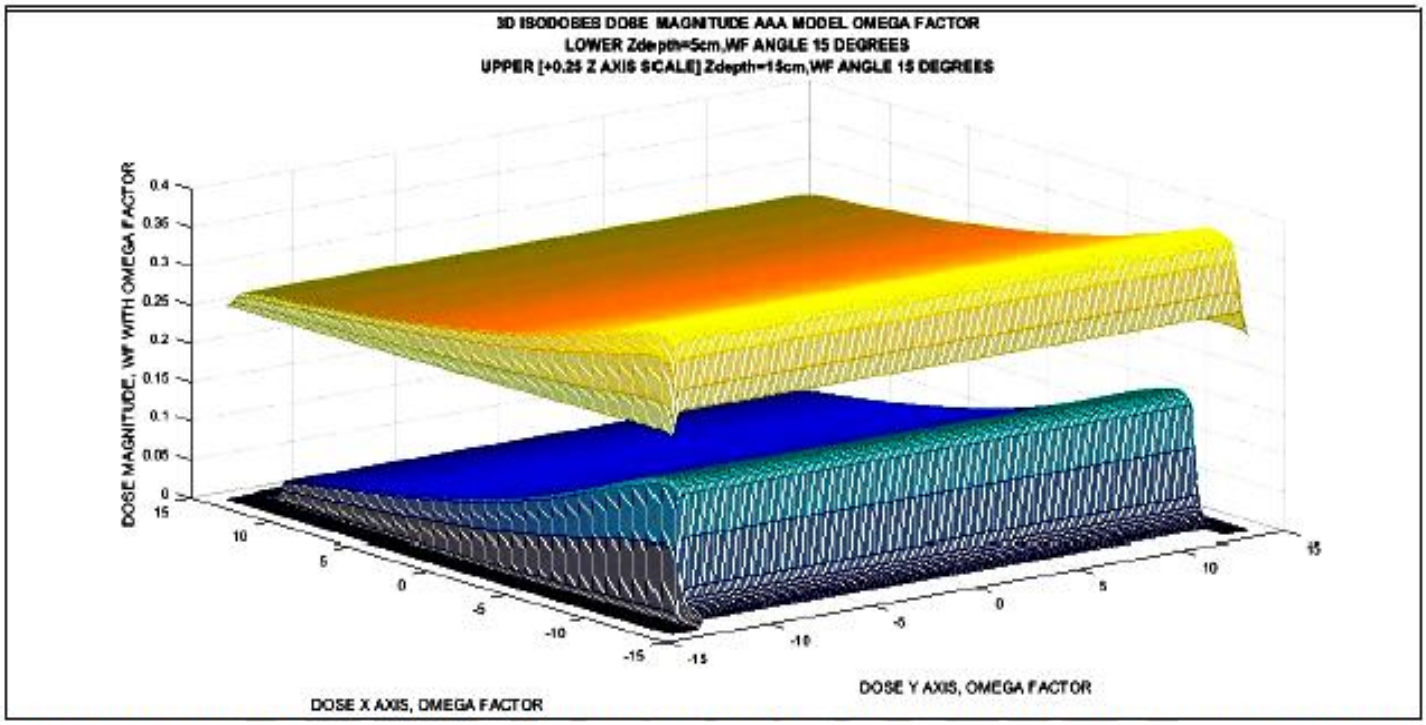

Figure 1.-Type I oblique-lateral imaging perspective of 3D Isodoses for z=15 cm [upper, scaled +0.25], and z=5 cm [lower]. It is clear the dose difference related to depth absorbed dose deposition. The precision is shown roughly watching the thickness of dose distribution, higher at z= 5 cm (blue). [Casesnoves Bioengineering Laboratory. Software. 4578]

Type II 3D Isodoses [Horizontal]

Type II 3D Isodoses WF graphics for [z=5 cm, z=15 cm] depth doses with AAA model are like Figure 1 but horizontal. The innovation of the study involves practical use for TPO, in contrast with classical 2D Isodoses plots. Figure 2. [Casesnoves Bioengineering Laboratory. Software. 4578.1]

4. Discussion and Conclusions

The objectives of the research were to demonstrate the feasibility and practical TPO usage of new 3D Isodoses for WF photon-dose delivery. The model for calculations and images was, as usual in research series, the AAA one is extensively used/improved in current photon-dose LINACs. Breast cancer TPO, based on [1-20, 73, 74] criteria, was the practical usage of 3D Isodoses proven. Figures 1-2.

Images obtained were got sharp and contrasted, Figure 1-2. The software required several combined WF calculations implemented in a unique program. However, the increase running time was less than expected. The reason was the optimal set of patterns, loops, image subroutine selected, and avoiding redundant calculations. These techniques were

rather arduous in the programming task. Method dataset is shown in Table 1. Water AAA model approaches to breast tissue adipose density with acceptable approximations.

Advantages of 3D Isodoses for TPO are the imaging perspectives, better calculations, fast calculus of dose or approximate dose delivery. Inconvenient could be the rather more difficult programming and numerical refinements to process 3D optimal Isodoses images, compared to classical 2D Isodoses graphs.

In brief, 3D Isodoses WF photon-dose graphs were presented for AAA model in water without tissue heterogeneities inset at programming. The focus was breast cancer [38, 39, 74] applications as done in [1] for TPO WF dose delivery applications.

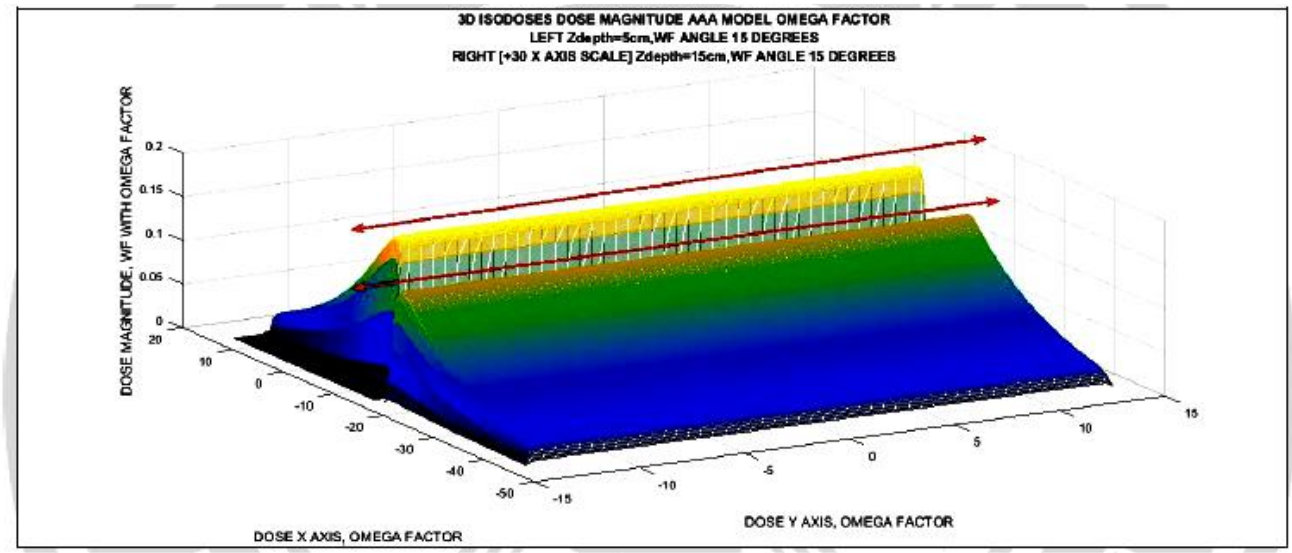

Figure 2.- Type II oblique-lateral imaging perspective of 3D Isodoses for z=5 cm [left], and z=15 cm [right, scaled +30]. It is clear, red arrows inset; the height dose difference related to depth absorbed dose deposition. [Casesnoves Bioengineering Laboratory. Software. 4579]

5. References and Further Reading

[1] Casesnoves, F. 2022. Radiotherapy Wedge Filter AAA Model 18 Mev- Dose Delivery 3D Simulations with Several Software Systems for Medical Physics Applications. Applications. Biomedical Journal of Scientific and Technical Research, 40(5).

[2] Casesnoves, F. 2016. Mathematical Exact 3D Integral Equation Determination for Radiotherapy Wedge Filter Convolution Factor with Algorithms and Numerical Simulations. Journal of Numerical Analysis and Applied Mathematics, 1(2):39-59.

[3] Casesnoves, F. 2015. Radiotherapy Conformal Wedge Computational Simulations, Optimization Algorithms, and Exact Limit Angle Approach. International Journal of Scientific Research in Science, Engineering and Technology (IJSRSET), 1(2):353-362.

[4] Casesnoves, F. 2019. Improvements in Simulations for Radiotherapy Wedge Filter dose and AAA-Convolution Factor Algorithms. International Journal of Scientific Research in Science, Engineering and Technology (IJSRSET), 6(4):194-219.

[5] Casesnoves, F. 2011. Exact/Approximated Geometrical Determinations of IMRT Photon Pencil-Beam Path Through Alloy Static Wedges in Radiotherapy Using Anisothropic Analytic Algorithm

(AAA). Peer-reviewed ASME Conference Paper. ASME 2011 International Mechanical Engineering Congress. Denver. USA. IMECE2011-65435.
[6] Casesnoves, F. 2012. Geometrical Determinations of Limit angle (LA) related to maximum Pencil-Beam Divergence Angle in Radiotherapy Wedges. Peer-reviewed ASME Conference Paper. ASME 2012 International Mechanical Engineering Congress. Houston. USA. IMECE2012-86638.
[7] Casesnoves, F. 2013. A Conformal Radiotherapy Wedge Filter Design. Computational and Mathematical Model/Simulation' Casesnoves, F. Peer-Reviewed Poster IEEE (Institute for Electrical and Electronics Engineers), Northeast Bioengineering Conference. Syracuse New York, USA. April 6th, 2013. Peer-Reviewed Poster Session on 6th April 2013. Sessions 1 and 3 with Poster Number 35. Page 15 of Conference Booklet.
[8] Casesnoves, F. 2014. Mathematical and Geometrical Formulation/ Analysis for Beam Limit Divergence Angle in Radiotherapy Wedges. Peer-Reviewed International Engineering Article. International Journal of Engineering and Innovative Technology (IJEIT), 3(7).
[9] Casesnoves, F. 2014. Geometrical Determinations of IMRT Photon Pencil-beam Path in Radiotherapy Wedges and Limit Divergence Angle with the Anisotropic Analytic Algorithm (AAA) Casesnoves, F. Peer- Reviewed scientific paper, both Print and online. International Journal of Cancer Therapy and Oncology, 2(3):02031.
[10] Casesnoves, F. 2014. Radiotherapy Conformal Wedge Computational Simulations and Nonlinear Optimization Algorithms. Peer-reviewed Article, Special Double-Blind Peer-reviewed paper by International Scientific Board with contributed talk. Official Proceedings of Bio- and Medical Informatics and Cybernetics: BMIC 2014 in the context of the 18th Multi-conference on Systemics, Cybernetics and Informatics: WMSCI 2014 July 15 - 18, 2014, Orlando, Florida, USA.
[11] Casesnoves, F. 2007. Large-Scale Matlab Optimization Toolbox (MOT) Computing Methods in Radiotherapy Inverse Treatment Planning'. High Performance Computing Meeting. Nottingham University.
[12] Casesnoves, F. 2008. A Computational Radiotherapy Optimization Method for Inverse Planning with Static Wedges. High Performance Computing Conference. Nottingham University.
[13] Casesnoves, F. 2015. Radiotherapy Conformal Wedge Computational Simulations, Optimization Algorithms, and Exact Limit Angle Approach. International Journal of Scientific Research in Science, Engineering and Technology (IJSRSET), 1(2):353-362.
[14] Casesnoves, F. 2015. Radiotherapy Standard/Conformal Wedge IMRT-Beamlet Divergence Angle Limit Exact Method, Mathematical Formulation, and Bioengineering Applications. International Article- Poster. Published in Proceedings of Conference. 41st Annual Northeast Bioengineering Conference. Rensselaer Polytechnic Institute. Troy, New York USA, April, p. 17-19.
[15] Casesnoves, F. 2015. Radiotherapy Standard/Conformal Wedge IMRT-Beamlet Divergence Angle Limit Exact Method, Mathematical Formulation, and Bioengineering Applications. IEEE (Institute for Electrical and Electronics Engineers), International Article-Poster.
[16] Casesnoves, F. 2015. Abstract-Journal. 'Radiotherapy Standard/ Conformal Wedge IMRT-Beamlet Divergence Angle Limit Exact Method, Mathematical Formulation. International Conference on Significant Advances in Biomedical Engineering. 252nd OMICS International Conference, 5(1).
[17] Casesnoves, F. 2001. Determination of Absorbed Doses in Common Radio Diagnostic Explorations. 5th National Meeting of Medical Physics. Madrid, Spain. September 1985. treatment Planning'. Kuopio University. Radiotherapy Department of Kuopio University Hospital and Radiotherapy Physics Group. Finland.
[18] Casesnoves, F. 2013. A Conformal Radiotherapy Wedge Filter Design. Computational and Mathematical Model/Simulation'. Peer-Reviewed Poster IEEE (Institute for Electrical and Electronics Engineers), Northeast Bioengineering Conference. Syracuse New York, USA. Presented in the Peer-Reviewed Poster Session on 6th April 2013. Sessions 1 and 3 with Poster Number 35. Page 15 of Conference Booklet. April 6th, 2013.
[19] Casesnoves, F. 2022. Radiotherapy Biological Tumor Control Probability Integral Equation Model with Analytic Determination. International Journal of Mathematics and Computer Research, 10(8):2840-2846.
[20] Casesnoves, F. 2022. Radiotherapy Wedge Filter AAA Model 3D Simulations For 18 MEV 5cm-Depth Dose with Medical Physics Applications", International Journal of Scientific Research in Computer Science, Engineering and Information Technology (IJSRCSEIT), 8(1):261-274.

[21] Walsh, S. 2011. Radiobiological modelling in Radiation Oncology. PhD Thesis. School of Physics. National University of Galway.
[22] Chapman, D., Nahum, A. 2015. Radiotherapy Treatment Planning, Linear- Quadratic Radiobiology. CRC Press.
[23] Mayles, W., Nahum, A. 2015. Rosenwald, J. Editors. Handbook of Radiotherapy Physics. Second Edition. CRC Press.
[24] Webb, S., Nahum, A. 1993. A Model for Calculating Tumor Control Probability in Radiotherapy Including the Effects of Inhomogeneous Distributions of Dose and Clonogenic Cell Density. Physics in Medicine and Biology, 38:653- 666.
[25] Haydaroglu, A., Ozyigit, G. 2013. Principles and Practice of Modern Radiotherapy Techniques in Breast Cancer. Springer.
[26] Casesnoves, F. 2019-20. Die numerische Reuleaux-Methode Rechnerische und dynamische Grundlagen mit Anwendungen (Erster Teil). ISBN-13: 978-620-0-89560-8, ISBN-10: 6200895600. Publishing House: Sciencia Scripts. 2019-20.
[27] Ulmer W., Harder, D. 1997. Corrected Tables of the Area Integral I(z) for the Triple Gaussian Pencil Beam Model. Journal of Medical Physics, 7:192-193.
[28] Ulmer, W., Harder, D. 1995. A Triple Gaussian Pencil Beam Model for Photon Beam Treatment Planning. Medical Physics, 5:25-30.
[29] Ulmer, W., Harder, D. 1996. Applications of a Triple Gaussian Pencil Beam Model for Photon Beam Treatment Planning. Medical Physics, 6:68-74.
[30] Ma, C., Lomax, T. 2013. Proton and Carbon Ion Therapy. CRC Press.
[31] Censor, Y., Zenios, S.A. 1997. Parallel Optimization: Theory, Algorithms and Applications'. UOP.
[32] Ulmer, W., Pyyry, J., Kaissl, W. 2005. A 3D Photon Superposition/Convolution Algorithm and Its Foundation on Results of Monte Carlo Calculations. Physics in Medicine and Biology, p. 50.
[33] Ulmer, W., Harder, D. 1997. Applications of the Triple Gaussian Photon Pencil Beam Model to Irregular Fields, Dynamical Collimators and Circular Fields. Physics in Medicine and Biology.
[34] Haddad, K., Anjak, O., Yousef, B. 2019. Neutron and High Energy Photon Fluence Estimation in CLINAC using Gold Activation Foils. Reports of Practical Oncology and Radiotherapy, 24:41-46.
[35] Sievinen, J., Waldemar, U., Kaissl, W. AAA Photon Dose Calculation Model in Eclipse™. Varian Medical Systems Report. Rad #7170A.
[36] Vagena, E., Stoulos, S., Manolopoulou, M. 2016. GEANT4 Simulations on Medical LINAC Operation at 18MV: Experimental Validation based on Activation Foils. Radiation Physics and Chemistry.
[37] Ethics for Researchers. 2013. EU Commission. Directorate-General for Research and Innovation. Science in society/Capacities FP7.
[38] Casesnoves, F. 1981. Surgical Pathology I Course Class Notes and Clinical Practice of Surgical Pathology Madrid Clinical Hospital [Professor Surgeon Dr Santiago Tamames Escobar]. 4th academic year course for graduation in Medicine and Surgery. Lessons and practice Breast Cancer Surgical and Medical Treatment. 1980-1981. Madrid Complutense University.
[39] Tamames., Escobar, S. 2000. Cirugia/ Surgery: Aparato Digestivo. Aparato Circulatorio. Aparato Respiratorio/ Digestive System. Circulatory System. Respiratory System (Spanish Edition).
[40] Silvia, C., Formenti, S.D. 2013. Combining Radiotherapy and Cancer Immunotherapy: A Paradigm Shift Silvia C. Formenti, Sandra Demaria. Journal of the National Cancer Institute, 105:256-265.
[41] Numrich, R.W. 2010. The Computational Energy Spectrum of a Program as it Executes. Journal of Supercomputing, 52.
[42] European Commission, Directorate-General for Research. 2021. Unit L3. Governance and Ethics. European Research Area. Science and Society.
[43] ALLEA. 2017. The European Code of Conduct for Research Integrity, Revised Edn.; ALLEA: Berlin Barndenburg Academy of Sciences.
[44] Good Research Practice. 2017. Swedish Research Council.
[45] Ulmer, W., Schaffner, B. 2011. Foundation of an Analytical Proton Beamlet Model for Inclusion in a General Proton Dose Calculation System. Radiation Physics and Chemistry, 80:378-389.
[46] Sharma, S.C. 2008. Beam Modification Devices in Radiotherapy. Lecture at Radiotherapy Department, PGIMER. India.
[47] Barrett, A.C. 2009. Practical Radiotherapy Planning. Fourth Edition. Hodder Arnold.

[48] Ahnesjö, A., Saxner, M., Trepp, A. 1992. A Pencil Beam Model for Photon Dose Calculations. Medical Physics, pp. 263-273.
[49] Brahime, A. 2000. Development of Radiation Therapy Optimization. Acta Oncologica, 39(5).
[50] Bortfeld, T., Hong, T., Craft, D., Carlsson, F. 2008. Multicriteria Optimization in Intensity-Modulated Radiation Therapy Treatment Planning for Locally Advanced Cancer of the Pancreatic Head. International Journal of Radiation Oncology and Biology Physics, 72(4).
[51] Brown, Bernardette, and all members of Research Group. 2014. Clinician-led Improvement in Cancer Care (CLICC) - Testing a Multifaceted Implementation Strategy to Increase Evidence-Based Prostate Cancer Care: Phased Randomised Controlled Trial - Study Protocol. Implementation Science, 9:64.
[52] Bortifield, T. 2006. IMRT: A Review and Preview. Physics in Medicine and Biology, 51(2006):R363–R379.
[53] Censor, Y. 2005. Mathematical Optimization for the Inverse Problem of Intensity-Modulated Radiation Therapy. Laboratory Report, Department of Mathematics, University of Haifa, Israel.
[54] Capizzello, A., Tsekeris, P.G., Pakos, E.E., Papathanasopoulou, V., Pitouli, E.J. 2006. 'Adjuvant Chemo-Radiotherapy in Patients with Gastric Cancer. Indian Journal of Cancer, 43(4).
[55] Dawod, T., Abdelrazek, E.M., Elnaggar, M., Omar, R. 2014. Dose Validation of Physical Wedged symmetric Fields in Artiste Linear Accelerator. International Journal of Medical Physics, Clinical Engineering and Radiation Oncology, 3:201-209.
[56] Do, S.Y, David, A., Bush, J.D.S. 2010. Comorbidity-Adjusted Survival in Early-Stage Lung Cancer Patients Treated with Hypofractioned Proton Therapy. Journal of Oncology.
[57] Ehrgott, M., & Burjony, M. 2001. Radiation Therapy Planning by Multicriteria Optimization. In Proceedings of the 36th Annual Conference of the Operational Research Society of New Zealand (Vol. 244, p. 253).
[58] Ezzel, G.A. 1996. Genetic and Geometric Optimization of Three-dimensional Radiation Therapy Treatment Planning. Medical Physics, 23:293- 305.
[59] Effective Health Care, 2008. Number 13. Comparative Efectiveness of Therapies for Clinically Localized Prostate Cancer. Bookshelf ID: NBK554842.
[60] Hansen, P. 1998. Rank-deficient and Discrete Ill-posed Problems: Numerical Aspects of Linear Inversion'. SIAM Monographs on Mathematical Modelling and Computation.
[61] Hashemiparast, S.M., Fallahgoul, H. 2011. Modified Gauss Quadrature for Ill-posed Integral Transform. International Journal of Mathematics and Computation, 13(11).
[62] Isa, N. 2014. Evidence Based Radiation Oncology with Existing Technology. Reports of Practical Oncology and Radiotherapy, 19:259-266.
[63] Johansson, K.A., Mattsson, S., Brahme, A., Turesson, I. 2003. Radiation Therapy Dose Delivery'. Acta Oncologica, 42(2):2003.
[64] Khanna, P., Blais, N., Gaudreau, P.O., Corrales-Rodriguez, L. 2016. Immunotherapy Comes of Age in Lung Cancer, Clinical Lung Cancer.
[65] Küfer, K. H., Hamacher, H. W., & Bortfeld, T. 2001. A Multicriteria Optimization Approach for Inverse Radiotherapy Planning. In Operations Research Proceedings: Selected Papers of the Symposium on Operations Research (OR 2000) Dresden, September 9–12, 2000 (pp. 3-7). Springer Berlin Heidelberg.
[66] Kirsch, A. 1996. An introduction to the Mathematical Theory of Inverse Problems. Springer Applied Mathematical Sciences.
[67] Luenberger, D.G. 1989. Linear and Nonlinear Programming (2nd Edn.)., Addison-Wesley.
[68] Moczko, J.A., Roszak, A. 2006. Application of Mathematical Modeling in Survival Time Prediction for Females with Advanced Cervical cancer treated Radio-chemotherapy. Computational Methods in Science and Technology, 12(2).
[69] Ragaz, J., Olivotto, I. A., Spinelli, J. J., Phillips, N., Jackson, S. M., Wilson, K. S., ... & Manji, M. 2005. Loco-regional Radiation Therapy in Patients with High-risk Breast Cancer Receiving Adjuvant Chemotherapy: 20-Year Results of the Columbia Randomized Trial'. Journal of National Cancer Institute, 97(2):116-126.
[70] Steuer, R. 1986. Multiple Criteria Optimization: Theory, Computation and Application. Wiley.
[71] Spirou, S.V, Chui, C.S. 1998. A Gradient Inverse Planning Algorithm with Dose-Volume Constraints. Medical Physics, 25: 321-323.

[72] Das, I.J, Colls. 1997. Patterns of Dose Variability in Radiation Prescription of Breast Cancer. Radiotherapy and Oncology, 44: 83-89.
[73] Casesnoves, F. 2018. Practical Radiotherapy TPO Course with Cyberknife. Robotic Simulations for Breathing Movements during Radiotherapy Treatment. Sigulda Radiotherapy Cyberknife Center. Latvia. Riga Technical University Bioengineering Training-Course Nonlinear Life.
[74] Casesnoves, F. 2022. Radiotherapy Linear Quadratic Bio Model 3D Wedge Filter Dose Simulations for AAA Photon-Model [18 Mev, Z=5,15 cm] with Mathematical Method System. Biomedical Journal of Scientific and Technical Research, 46(2).

2. LUNG TUMORS

Abstract

Lung cancer is epidemiologically the most frequent and one of the most aggressive tumors. Its anatomical zone location makes RT treatment difficult for a number of reasons. Namely, proximity of crucial organs (such as heart), aorta, cava, and principal arteries/veins, the emerging sympathic and parasympathic main nerve branches, breathing thorax and lung movements, and others. The wide difference related to a rather high number of tumors is its relatively short survival time after treatment, very opposite to breast one. However, recently new treatment techniques, either combined or not, have obtained more survival time. These are immunotherapy, personalization biomarkers-based diagnosis/treatment and innovative Nanoinmunotherapy, among several. This section deals with some of the selected-specific main previous published advances in recent lung tumors publications. Namely, 2D-3D Isodoselines and Isodosezones, both triangular and rectangular Isodosezones. Most important database is shown with graphics and numerical details. Further formulation can be seen/compared at Section 5.

Keywords

Radiation Dose, Attenuation Exponential Factor (AEF), Simulations, Nonlinear Optimization, Matrix Algebra, Spherical-Spatial Analytical Geometry, Organ at Risk (OAR), Multi-Leaf Collimator (MLC), Wedge Filter (WF), Conformal Wedge Filter, Anisotropic Analytic Model AAA, Intensity Modulated Radiotherapy (IMRT), Intense Modulated Protontherapy (IMPT), Fluence Factor (FF), Treatment Planning Optimization (TPO), Breast Tumor (BT) Computarized Thomography (CT)

1. Introduction and Objectives

In recent contributions [102], precise 3D imaging-processing Isodosezones [101, 102], delimited by 3D Isodoselines were developed/explained in lung, head and neck, and prostate cancer. The radiotherapy model applied was the classical/initial BED one algorithm. Modern biological-model-based Treatment Planning Optimization can get objective improvements by using high-precision Isodosezones/lines when selecting the optimal dose delivery/schedule for any personalized treatment. This paper demonstrates improved imaging-processing programming techniques [101-102], and engineered software which is developed for numerical hyperfractionated 3D TPO lung cancer treatment planning optimization database. Mathematical algorithms are detailed. Results show a series of graphics results obtained with the 3D Imaging-Isodosezones Pareto-Multiobjective Optimization programming is shown and detailed. Significances are complemented with a concise introductory/comparative section to explain/discuss the

recent formulation/equations for tissue-repair factors in BED basic equation is initiated. Applications in radiotherapy medical physics are subsequently briefed.

3D Isodosezones Rectangular (Casesnoves imaging-software and optimization invention, 2022) are developed from a previous Rectangular 3D Isodoselines and 3D Isodosezones published definition-invention [101, 102]. This new computational radiotherapy application is developed for lung tumors treatment planning optimization (TPO). The study continues further with programming and 3D graphical-numerical results as an enhancement stage, namely Rectangular and Triangular 3D Isodosezones. The further innovation constitutes this image/processing with corresponding software for Triangular 3D Isodosezones. A primary 3D Rectangular group of demonstrating graphs were shown [101, 102], and here is top-up developed. Isodoselines and Isodosezones are in this study proven be practical and complementary useful for individual TPO, because they allow multiple numerical choices in TPO. The 3D images are acquired with functional combinations of BED model parameters [84]. The BED function is a several variables one, and a brief mathematical analysis is included, related to programming precision, clarity, smooth and running time [1-21, 28, 84, 86, 88, 89, 99, 101].

Epidemiologicaly, the importance of lung cancer screening among smokers and individuals with risk factors, has been proven recently. The reason is that survival rate after 5 years among early-stage diagnosed lung tumors is significantly higher. Surgical resection of lung tumors at stage I (T1–2, N0) NSCLC yields satisfying outcome results with 5-year survival rates of 60–70%, and remains at present the golden standard in this population. After resection, radiotherapy is optional.

Lung tumors are a heterogeneous type of cancer. Their incidence and prevalence are statistically among the highest percent of all tumors and constitute the highest deaths cancer rate at present. In general [96], Non-Small-Cells-Lung carcinoma has a prevalence of approximately 85% of all lung tumors, while Small-Cells-Lung carcinoma shows about 15% of prevalence. In addition, lung and breast cancer show be the highest incidence in brain metastases. For example, 234,000 Primary Lung cancer cases in USA in 2018 with 154,050 deaths. In 1990 the incidence peak was [70/100,000 population], in 2018 [57/100,000 population]. This specific decrease of incidence in that developed country is probably due to healthier population habits related to tobacco consumption and contact with other toxic substances/chemicals. The most important oncological causal factor for lung cancer is proven be tobacco consumption, even in passive smokers. However, further pathogenesis factors are mainly chemical, from the external media intake/contact.

Namely, radon gas, passive smoking, prior radiation from any radiation source, inhaled chemicals (polycyclic aromatic hydrocarbons), heavy metal inhaled particles and/or micro-nano particles. Among previous diseases, for instance pulmonary fibrosis. If any potential patient is smoker and at the same time is in contact with carcinogenetic chemicals, the oncogenetic synergism factor increases the probability of lung cancer. Therefore, although the tobacco consumption is decreasing in developed countries, it does not happen so in underdeveloped ones. This has caused an incidence/prevalence social-geographic-pathology rate displacement towards those countries. In addition, when smoking, the oral cavity can accumulate tobacco and alcohol as oncogenetical factors. This pathogenesis can cause concomitant diseases associated to the main lung tumor.

Therefore, the objectives of the study are to get and demonstrate 3D graphical optimization for BED model isodosezones and isodoselines, both Triangular and Rectangular. Programming is based in Pareto-Multiobjective software dataset from previous contributions [101, 102]. Secondly, to demonstrate the efficacy of the improved program writing that was developed [101, 102] by showing the diverse-geometry charts with their numerical precise data, e.g., Equations 4-5. It is not an objective of this paper to discuss the deliberation between hyper and hypo fractionated dose delivery.

An additional part of the study comprises a short review of BED models adapted on Tissue-Repair relatively recent models, algorithms, and correction factors [104-106]. Nonetheless, this is a brief considered for future analysis /applications in later contributions. Equations 1-3.

The radiotherapy TPO applications outcome for this Isodosezones involves optimization of main parameter magnitudes, namely, number of fractions, total dose, treatment total time, $T_{Potential}$ and others for BED model. In this research, Figures 1-2, it is proven the 3D different selection of BED parameters, [Algorithm 1, 101, 102].

Results show 3D Isodosezones and Isodoselines imaging-processing visuals for lung cancer with a total dose in the interval: $D_{Total} \approx [30, 115]$ Gy. However, Isodosezones within graphs are related to standard lung cancer dose magnitudes, namely $D_{Total} \approx [70, 80]$ Gy. Numerical values are detailed in Figures 1-2. Table 1 shows BED *in vivo* parameters selection.

Grosso modo, both for Triangular and Rectangular 3D Isodosezones with improved software for imaging-processing in isodosezones/lines in lung cancer were obtained. Results comprise new series of 3D graphics, mathematical method, algorithms, and

radiotherapy TPO medical physics applications. A complementary review/discussion for relatively recent Tissue-Repair equations was shown.

2. Mathematical and Computational Methods

This section comprises the dataset that was used for programming improvements from [101-102]. The mathematical algorithms and software methods are also developed from [86, 88, 89, 99,101-102]. The basic dataset reminder of *in vivo* is included in Table 1 from [98]. Remark: Both alpha and beta parameters are subject of modern research and precise magnitude determinations for every type of tumor.

From [101, 102], the following essential concepts are highlighted:

Definition 1.- In RT-3D Treatment Planning, a 3D Isodoseline is demarcated by a line whose dose-distribution parameters can vary for optimal planner choice while keeping constant the total dose delivery magnitude [101-102].

Definition 2.- In RT-3D Treatment Planning, a 3D Isodosezone is demarcated by a polygon whose dose-distribution parameters can vary for optimal planner choice while keeping constant the total dose delivery magnitude [101-102].

The mathematical method constitutes an evolution from the previous lung and prostate cancer publications [101, 102]. The main algorithm formulation for imaging-processing and developments of improved 3D isodosezones/lines charts is based on Tikhonov regularization algorithms presented in a number of previous studies [Algorithms 1-5 from 86, 88, 89, 98, 99, 101, 102] and literature records [20-25, 68, 74, 75, 80, 81, 85-94, 99, 101]. Table 1 shows the numerical data implemented in software in MATLAB. Just to remark that BED model is a nonlinear several variables function, with implications in numerical results analysis.

BED nonlinear-quadratic model has been adapted for in vivo parameter T_{Pot} magnitude. Then, PMO in lung [24, 88, 89, 98, 101, 102] tumors simplest BED model reads:

$$\text{Chebyshev} \quad L_1 \text{ Optimization,}$$
$$\text{for} \quad i = 1,2 \ldots \text{minimize pareto,}$$
$$\left| DOSE_i - BED_{Effective} \right|_{L_1} \text{ with,}$$
$$BED_{Effective} = k \times d \times \left[1 + \frac{d \times \beta}{\alpha} \right] - \ldots$$
$$\ldots - \frac{Ln(2)}{\alpha} \times \left[\frac{T_{Treatment} - T_{Delay}}{T_{Potential}} \right];$$

(Algorithm 1)

where,

BED: The basic algorithm for Biological Effective Dose initially developed by Fowler et al. [22-25, 89-94, 98].

k: Optimal Number of fractions for hyperfractionated TPO. Optimization parameter [22-25, 89-94, 98].

d: Optimal Dose magnitude for every fraction. Optimization Parameter [Gy] [22-25, 89-94].

a: The basic algorithm constant for Biological Effective Dose models. Radiobiological experimental parameter in vivo [Gy^{-1}] [22-25, 89-94].

β: The basic algorithm constant for Biological Effective Dose models in vivo. Radiobiological experimental parameter [Gy^{-2}]. Note that it is very usual to set in biological models [a/β in Gy].

Ttreatment: The overall TPO time. This parameter varies according to authors' and institutions/hospitals criteria [22-25, 89-94, 98].

Tdelay: The overall TPO time delay for clonogens re-activation. This parameter varies according to authors' experimental research.

Tpotential: The potential time delay for tumor cell duplication. This parameter varies according to authors' experimental-theoretical research.

DOSE: The dose magnitudes for lung cancer simulation algorithm for Biological Effective Dose [22-25, 89-94, 98]. Software patterns were calculated around intervals DOSE ϵ [70, 80] Gy.

A number of necessary, rather mandatory, conditions in software design to obtain a convenient imaging-processing graphics are:
Setting an ordered code for fast running time of images.

Avoid excessive arrays and subroutines.
Select the optimal subroutine imaging-processing commands in the program, and well-ordered [1-20, 24, 68, 74, 88, 89, 98, 99, 101,102].

In the following sections, results and applications are presented. The imaging quality of the demonstrating Figures 1-2 was intended be good. In Table 1, software implemented dataset *in vivo* for programming with source references [38, 43-45, 98, 100, 101, 102, 103].

GRAPHICAL OPTIMIZATION PARAMETER INTERVALS FOR LUNG TUMORS [1-20,24,68,74,88,89,98,99, 101,102, 103]		
PARAMETERS WITH PROGRAMMING INTERVALS	**MAGNITUDE INTERVAL**	**ADDITIONAL**
Dose fractions number	[34, 42]	Usual protocol in literature [1-21,74-86, 101-103].
Dose fraction magnitude	[0.8, 2.2] Gy	Usual protocol in literature [1-21,74-86]. Set with intervals according to different criteria.
$T_{Treatment}$	[30,40] Days	Usual protocol in literature [1-21,74-86]. Set with intervals according to different criteria. The RT treatment varies according to weekends breaks, secondary effects, patient circumstances, etc.
T_{Delay}	[20,25] Days	Usual protocol in literature [1-21,74-86]. Set with intervals according to different criteria.
$T_{Potential}$	[22, 32] Days	Usual protocol in literature [1-21,74-86]. Set with intervals according to different criteria.
Dose interval in Objective Function	[70, 80] Gy	Usual protocol in literature [1-21,74-86, 101, 102]. Set with two total dose Pareto Functions according to different criteria. Note: at graphic for imaging-processing reasons the interval is wider.
α, α/β	0.38 Gy^{-1}, 8.2 Gy	From [89,103]. Remark, for average between early and medium tumor, it is acceptable to set alpha as 0.3 Gy^{-1}
β	0.042 Gy^{-2}	From [89,103]

Table 1.-Software implemented dataset for programming with source references [38, 43-45, 98, 101, 102, 103].

3. Results

This section comprises the new Triangular Isodosezones with mathematical precision validation and the improved rectangular ones. All of them are conveniently detailed. Note: this is a selected paper, there are in this series a large number of lung cancer TPO contributions at Google Scholar, Semantics, and published literature online and in journals/books.

Triangular Isodosezones

The innovation of this study, Figure 1, comprises also the introduction of triangular 3D Isodosezones, which get specific applications for a different parameter interval when planning the RT optimal treatment. Precision is detailed at (4-5).

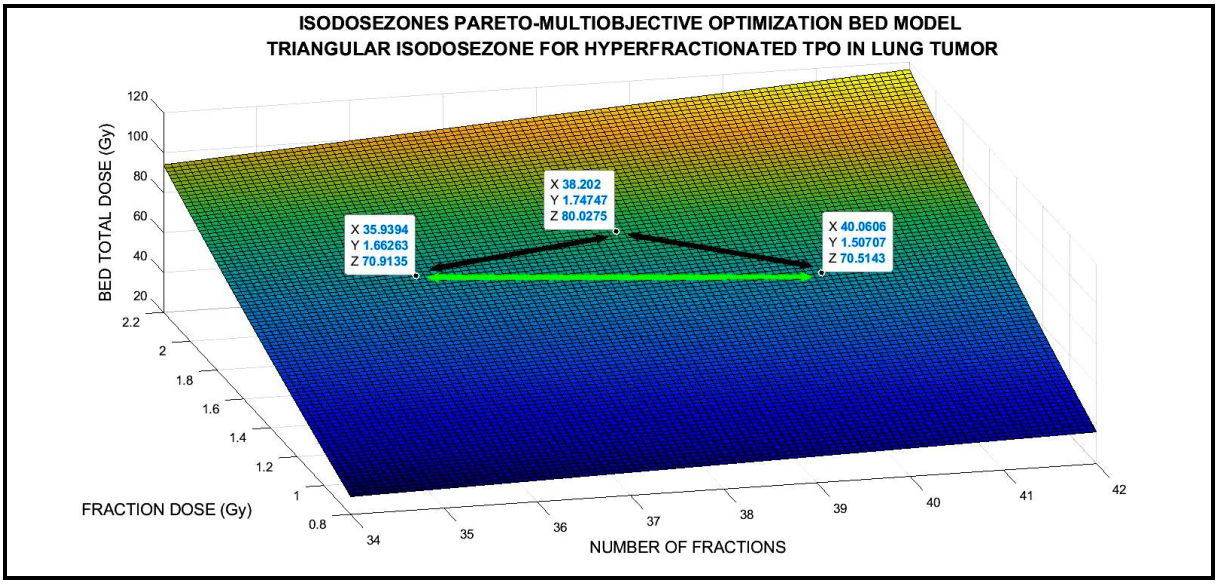

Figure 1.- [Casesnoves Bioengineering Laboratory. Software. 45710]. Triangular 3D Isodosezone for two variables. Namely, the choice is number of fractions dose and total treatment time in lung TPO. Namely, marked inset, [70, 80] Gy triangular isodosezone (yellow boundaries). Fraction dose interval is set [0.8, 2.2] Gy. In literature, Tpotential is usually set as 28 days for early-stage lung cancer. However, here an interval of [22, 32] days is programmed to cover other tumor stages. Precision can be checked setting in Algorithm (1) these extreme values at any long isodosezone. The 3D Isodosezone fundamentals for IO calculations [101, 102], are implemented into this 3D surfactal isodosezone. Pattern intervals for plotting were taken from PMO but with *in vivo* lung tumor parameters. **Formulation Precision Remark**: For calculations over the 3D graph, it is mandatory take into account that the BED model is quadratic with the dose fraction and fractions number such as: $\mathbf{K \times d + K \times d^2 \times (\beta/\alpha)}$. Therefore, it is straightforward to check at Figure 1 the following:

$$\mathbf{35.9 \times 1.6 = 59.6438 \quad Gy}$$

$$\mathbf{40.0 \times 1.5 = 60.4906\ Gy} \tag{4}$$

Therefore, the Figure 1 mathematical set for BED total dose corresponding to that defined Triangular isodose zone, taking positive differences at all, is,

ISODOSEZONE $[\ x_0\ y_0\ z_0\ ,\ x_n\ y_n\ z_n\ ] \in [\ 35.93\ 1.66\ 70.51\ ,\ 40.06\ 1.74\ 80.02\ ]$;

where

x: Fractions Number . (adimensional).

y: Fraction Dose (Gy).

z: Total Dose (Gy).

(5)

The same method/calculations can be applied for Figures 2-3. The Isodosezones geometry can be selected for TPO, RT planning optimization at any convenient shape compatible with 3D mathematical fundamentals.

Rectangular Isodosezones

This section-part demonstrates the utility of the obtained Rectangular 3D graphics for precision when planning a possible personalized TPO. In other words, once determined the proper patient radiobiological tests for the tumor, a, β, and the rest of BED model parameters, the software in seconds can provide with sharp graphics to select desirable isodosezones/lines. Then, the TPO schedule, in terms of fractions number total treatment time and/or rest of BED parameters can be determined in very short time. That is, given a specific patient at any stage subject to radiotherapy TPO and with proper biological-tissue radiosensitivity parameters, TPO schedule in isodosezones/lines is displayed in seconds, Figures 2-3.

In this extended study, 3D Interior and Graphical Optimization methods are used in parallel-refinement to confirm results from [98, 101], with the in vivo dataset from [23, 24, 97, 98, 101]. The 3D imaging process, Figures 2-3, programming demonstrate the results got with 3D IO in [101]. 3D Rectangular Isodosezones are cursor-marked inset within every 3D graph. The radiotherapy planner obtains the desired combination of fractions (k), and fraction dose (d), for a fixed total BED dose delivery. That is considered a consistent, easy, fast, and simple advance in modern TPO and RT research.

4. Discussion and Conclusions

The objective of the study was to develop new precise Triangular and Rectangular 3D imaging-processing charts for isodosezones/lines. Complementary, the mathematical part comprised algorithm and programming specific characteristics and conditions. In addition, to put forward a brief of radiotherapy medical physics applications. A theoretical discussion about Tissue Repair modelling is included, (1-3). Namely, T factor algorithms [104-106].

Isodosezones charts, Figures 1-3, can give perfected and sharpened evidence and verify the results from [98, 101, 102, 103] in protate cancer, but now for lung tumors hyperfractionated RT treatment with BED-LQ model and in vivo parameters dataset.

The relatively recent T factors are not discussed profoundly, and that brief can be considered an introduction of mathematical details for further research.

The programming method has the inconvenient that the 3D surfaces are specific for each and every model and cancer type. However, to change formulas and/or parameters in software is not complicated. Running time for Triangular and Rectangular 3D surfactal Isodose lines is satisfactory.

Results can be considered acceptable. The 3D image quality is clear and sharp. The programming software, therefore, is proven be functional and fast-running. The average time for graphs display is about 2-5 seconds, thanks to the explained conditions, and order to design the codes. An improvement related to previous studies [98, 101, 102, 103] is the development of a parameter's selection variety within the BED model implemented data and 3D visual graphics. The mathematical analysis for the model variables was justified.

In summary, further research for 3D Triangular and Rectangular imaging-procesing isodosezones/lines in lung tumors was presented. Brief of T factors for tissue repair is included in original paper, but here set at Section 5. Mathematical algorithms and software were detailed. Radiotherapy medical physics applications are described.

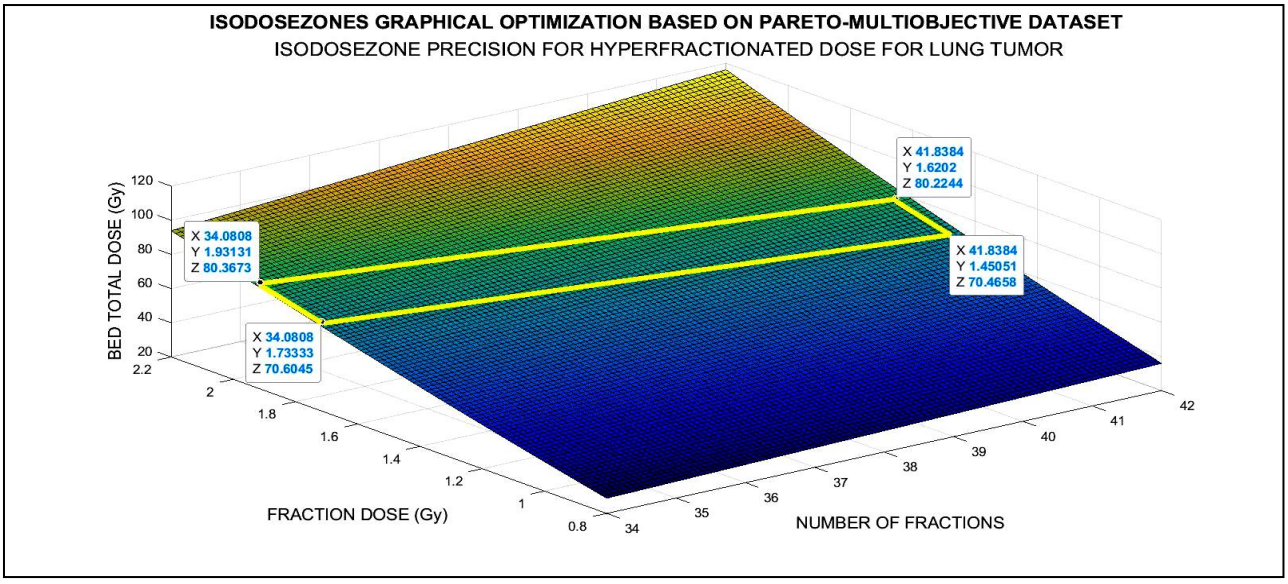

Figure 2.- 3D Isodosezone for two variables, at XY plane, number of fractions and dose per fraction, the choice. Namely, Number of fractions and dose per fraction in lung TPO. Marked inset, [70, 80] Gy isodosezone delimited by isodoselines. The precision can be checked calculating the product between fraction dose and number of fractions at each

extreme of the long isodoselines. For instance, at lower isodoseline (yellow), 34 x 1.7 is approximately equal to 41 x 1.4 (taking one digit is exactly equal). The Isodosezones fundamentals from IO calculations, [30, 100] Gy for BED total dose, are implemented into this 3D surface. Pattern intervals for plotting were taken from PMO but with *in vivo* lung tumor parameters. Each BED total dose is fixed along 3D Isodozone, while (k) and (d) parameters vary when cursor is moved over this Isodosezone. This software numerical method was also developed in F # and Fortran. [Casesnoves Bioengineering Laboratory. Software. 45711]

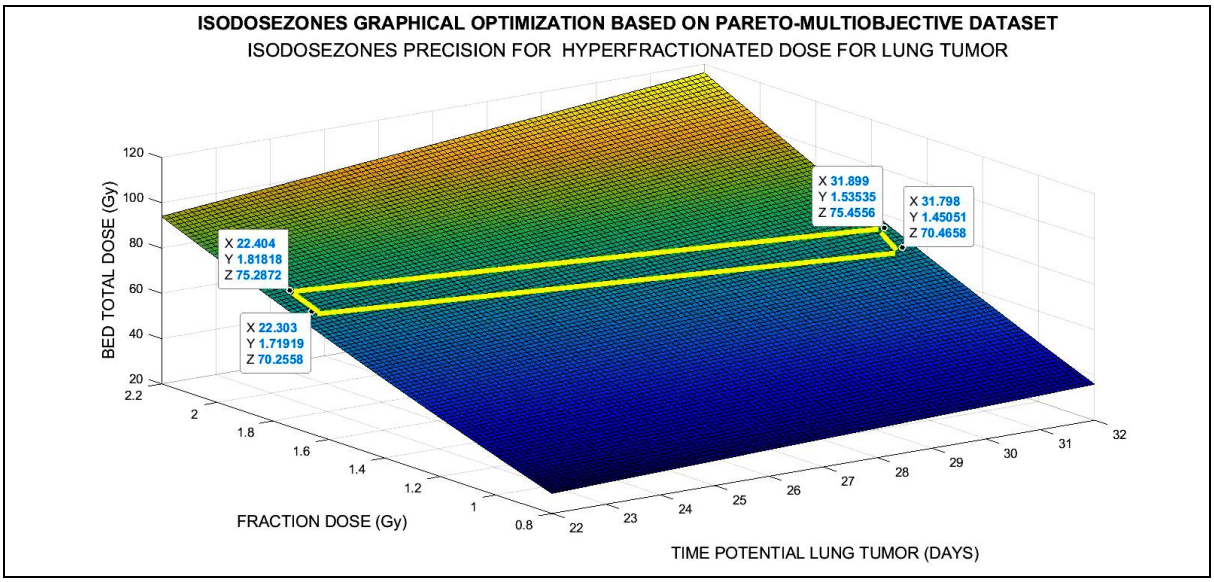

Figure 3.- Matlab 3D Isodosezone for two variables. Namely, the choice is number of fractions dose and total treatment time in lung TPO. Namely, marked inset, [70, 75] Gy isodosezone (yellow boundaries). In literature, Tpotential is usually set as 28 days for early-stage lung cancer. However, here an interval of [22, 32] days is programmed to cover other tumor stages. Precision can be checked setting in Algorithm (1) these extreme values at any long isodosezone. The 3D Isodosezone fundamentals for IO calculations, [30, 100] Gy for BED total dose, are implemented into this 3D surfactal Rectangular Isodosezone. Pattern intervals for plotting were taken from PMO but with *in vivo* lung tumor parameters. [Casesnoves Bioengineering Laboratory. Software. 45712]

5. References and Further Reading

[1] Casesnoves, F. 2022. Radiotherapy Wedge Filter AAA Model 18 Mev- Dose Delivery 3D Simulations with Several Software Systems for Medical Physics Applications. Applications. Biomedical Journal of Scientific and Technical Research, 40(5).

[2] Casesnoves, F. 2016. Mathematical Exact 3D Integral Equation Determination for Radiotherapy Wedge Filter Convolution Factor with Algorithms and Numerical Simulations. Journal of Numerical Analysis and Applied Mathematics, 1(2):39-59.

[3] Casesnoves, F. 2015. Radiotherapy Conformal Wedge Computational Simulations,Optimization Algorithms, and Exact Limit Angle Approach. International Journal of Scientific Research in Science, Engineering and Technology (IJSRSET), 1(2):353-362.

[4] Casesnoves, F. 2019. Improvements in Simulations for Radiotherapy Wedge Filter dose and AAA-Convolution Factor Algorithms. International Journal of Scientific Research in Science, Engineering and Technology (IJSRSET), 6(4):194-219.

[5] Casesnoves, F. 2011. Exact/Approximated Geometrical Determinations of IMRT Photon Pencil-Beam Path Through Alloy Static Wedges in Radiotherapy Using Anisothropic Analytic Algorithm

(AAA). Peer-reviewed ASME Conference Paper. ASME 2011 International Mechanical Engineering Congress. Denver. USA. IMECE2011-65435.
[6] Casesnoves, F. 2012. Geometrical Determinations of Limit angle (LA) related to maximum Pencil-Beam Divergence Angle in Radiotherapy Wedges. Peer-reviewed ASME Conference Paper. ASME 2012 International Mechanical Engineering Congress. Houston. USA. IMECE2012-86638.
[7] Casesnoves, F. 2013. A Conformal Radiotherapy Wedge Filter Design. Computational and Mathematical Model/Simulation' Casesnoves, F. Peer-Reviewed Poster IEEE (Institute for Electrical and Electronics Engineers), Northeast Bioengineering Conference. Syracuse New York, USA. April 6th, 2013. Peer-Reviewed Poster Session on 6th April 2013. Sessions 1 and 3 with Poster Number 35. Page 15 of Conference Booklet.
[8] Casesnoves, F. 2014. Mathematical and Geometrical Formulation/Analysis for Beam Limit Divergence Angle in Radiotherapy Wedges. Peer-Reviewed International Engineering Article. International Journal of Engineering and Innovative Technology (IJEIT). 3(7).
[9] Casesnoves, F. 2014. Geometrical Determinations of IMRT Photon Pencil-beam Path in Radiotherapy Wedges and Limit Divergence Angle with the Anisotropic Analytic Algorithm (AAA) Casesnoves, F. Peer- Reviewed scientific paper, both Print and online. International Journal of Cancer Therapy and Oncology, 2(3):02031.
[10] Casesnoves, F. 2014. Radiotherapy Conformal Wedge Computational Simulations and Nonlinear Optimization Algorithms. Peer-reviewed Article, Special Double-Blind Peer-reviewed paper by International Scientific Board with contributed talk. Official Proceedings of Bio- and Medical Informatics and Cybernetics: BMIC 2014 in the context of the 18th Multi-conference on Systemics, Cybernetics and Informatics: WMSCI 2014 July 15 - 18, 2014, Orlando, Florida, USA.
[11] Casesnoves, F. 2007. Large-Scale Matlab Optimization Toolbox (MOT) Computing Methods in Radiotherapy Inverse Treatment Planning'. High Performance Computing Meeting. Nottingham University.
[12] Casesnoves, F. 2008. A Computational Radiotherapy Optimization Method for Inverse Planning with Static Wedges. High Performance Computing Conference. Nottingham University.
[13] Casesnoves, F. 2015. Radiotherapy Conformal Wedge Computational Simulations, Optimization Algorithms, and Exact Limit Angle Approach. International Journal of Scientific Research in Science, Engineering and Technology (IJSRSET), 1(2):353-362.
[14] Casesnoves, F. 2015. Radiotherapy Standard/Conformal Wedge IMRT-Beamlet Divergence Angle Limit Exact Method, Mathematical Formulation, and Bioengineering Applications. International Article- Poster. Published in Proceedings of Conference. 41st Annual Northeast Bioengineering Conference. Rensselaer Polytechnic Institute. Troy, New York USA, April, p. 17-19.
[15] Casesnoves, F. 2015. Radiotherapy Standard/Conformal Wedge IMRT-Beamlet Divergence Angle Limit Exact Method, Mathematical Formulation, and Bioengineering Applications. IEEE (Institute for Electrical and Electronics Engineers), International Article-Poster.
[16] Casesnoves, F. 2015. Abstract-Journal. 'Radiotherapy Standard/ Conformal Wedge IMRT-Beamlet Divergence Angle Limit Exact Method, Mathematical Formulation. International Conference on Significant Advances in Biomedical Engineering. 252nd OMICS International Conference, 5(1).
[17] Casesnoves, F. 2001. Determination of Absorbed Doses in Common Radio Diagnostic Explorations. 5th National Meeting of Medical Physics. Madrid, Spain. September 1985. treatment Planning'. Kuopio University. Radiotherapy Department of Kuopio University Hospital and Radiotherapy Physics Group. Finland.
[18] Casesnoves, F. 2001. Master Thesis in Medical Physics. Eastern Finland University. Radiotherapy Department of Kuopio University Hospital and Radiotherapy Physics Grouversity-Kuopio. Defense approved in 2001. Library of Eastern finland University. Finland.
[19] Casesnoves, F. 2013. A Conformal Radiotherapy Wedge Filter Design. Computational and Mathematical Model/Simulation' Casesnoves, F. Peer-Reviewed Poster IEEE (Institute for Electrical and Electronics Engineers), Northeast Bioengineering Conference. Syracuse New York, USA. April 6th, 2013. Peer-Reviewed Poster Session on 6th April 2013. Sessions 1 and 3 with Poster Number 35. Page 15 of Conference Booklet.
[20] Casesnoves, F. 2022. Radiotherapy Biological Tumor Control Probability Integral Equation Model with Analytic Determination. International Journal of Mathematics and Computer Research, 10(8):2840-2846.

[21] Casesnoves, F. 2022. Radiotherapy Wedge Filter AAA Model 3D Simulations For 18 Mev 5 cm-Depth Dose with Medical Physics Applications", International Journal of Scientific Research in Computer Science, Engineering and Information Technology (IJSRCSEIT), 8(1):261-274.
[22] Ernits, The Marika. 2017. Applications of Power Engineering Optimization Cuts Programming with Evolutionary Preventive Fraudulent Algorithms.
[23] Walsh, S. 2011. Radiobiological modelling in Radiation Oncology. PhD Thesis. School of Physics. National University of Galway.
[24] Chapman, D., Nahum, A. 2015. Radiotherapy Treatment Planning, Linear- Quadratic Radiobiology. CRC Press.
[25] Mayles, W., Nahum, A. 2015. Rosenwald, J. Editors. Handbook of Radiotherapy Physics. Second Edition. CRC Press.
[26] Nahum, A., Webb, S. 1993. A Model for Calculating Tumour Control Probability in Radiotherapy Including the Effects of Inhomogeneous Distributions of Dose and Clonogenic Cell Density. Physics in Medicine and Biology; v. 38(6); p. 653-666.
[27] Haydaroglu, A., Ozyigit, G. 2013. Principles and Practice of Modern Radiotherapy Techniques in Breast Cancer. Springer.
[28] Casesnoves, F. 2019-20. Die numerische Reuleaux-Methode Rechnerische und dynamische Grundlagen mit Anwendungen (Erster Teil). ISBN-13: 978-620-0-89560-8, ISBN-10: 6200895600. Publishing House: Sciencia Scripts. 2019-20.
[29] Ulmer W., Harder, D. 1997. Corrected Tables of the Area Integral I(z) for the Triple Gaussian Pencil Beam Model. Journal of Medical Physics, 7:192-193.
[30] Ulmer, W., Harder, D. 1995. A Triple Gaussian Pencil Beam Model for Photon Beam Treatment Planning. Medical Physics, 5:25-30.
[31] Ulmer, W., Harder, D. 1996. Applications of a Triple Gaussian Pencil Beam Model for Photon Beam Treatment Planning. Medical Physics, 6:68-74.
[32] Ma, C., Lomax, T. 2013. Proton and Carbon Ion Therapy. CRC Press.
[33] Censor, Y., Zenios, S.A. 1997. Parallel Optimization: Theory, Algorithms and Applications'. UOP.
[34] Ulmer, W., Pyyry, J., Kaissl, W. 2005. A 3D Photon Superposition/ Convolution Algorithm and Its Foundation on Results of Monte Carlo Calculations. Physics in Medicine and Biology, p. 50.
[35] Ulmer, W., Harder, D. 1997. Applications of the Triple Gaussian Photon Pencil Beam Model to Irregular Fields, Dynamical Collimators and Circular Fields. Physics in Medicine and Biology.
[36] Haddad, K., Anjak, O., Yousef, B. 2019. Neutron and High Energy Photon Fluence Estimation in CLINAC using Gold Activation Foils. Reports of Practical Oncology and Radiotherapy, 24:41-46.
[37] Sievinen, J., Waldemar, U., Kaissl, W. AAA Photon Dose Calculation Model in Eclipse™. Varian Medical Systems Report. Rad #7170A.
[38] Vagena, E., Stoulos, S., Manolopoulou, M. 2016. GEANT4 Simulations on Medical LINAC Operation at 18MV: Experimental Validation based on Activation Foils. Radiation Physics and Chemistry.
[39] Ethics for Researchers. 2013. EU Commission. Directorate-General for Research and Innovation. Science in society/Capacities FP7.
[40] Casesnoves, F. 1981. Surgical Pathology I Course Class Notes and Clinical Practice of Surgical Pathology Madrid Clinical Hospital [Professor Surgeon Dr Santiago Tamames Escobar]. 4th academic year course for graduation in Medicine and Surgery. Lessons and practice Breast Cancer Surgical and Medical Treatment. 1980-1981. Madrid Complutense University.
[41] Tamames., Escobar, S. 2000. Cirugia/ Surgery: Aparato Digestivo. Aparato Circulatorio. Aparato Respiratorio/ Digestive System. Circulatory System. Respiratory System (Spanish Edition).
[42] Silvia, C., Formenti, S.D. 2013. Combining Radiotherapy and Cancer Immunotherapy: A Paradigm Shift Silvia C. Formenti, Sandra Demaria. Journal of the National Cancer Institute, 105:256-265.
[43] Numrich, R.W. 2010. The Computational Energy Spectrum of a Program as it Executes. Journal of Supercomputing, 52.
[44] European Commission, Directorate-General for Research. 2021. Unit L3. Governance and Ethics. European Research Area. Science and Society.
[45] ALLEA. 2017. The European Code of Conduct for Research Integrity, Revised Edn.; ALLEA: Berlin Barndenburg Academy of Sciences.
[46] Good Research Practice. 2017. Swedish Research Council.

[47] Ulmer, W., Schaffner, B. 2011. Foundation of an Analytical Proton Beamlet Model for Inclusion in a General Proton Dose Calculation System. Radiation Physics and Chemistry, 80:378-389.
[48] Sharma, S.C. 2008. Beam Modification Devices in Radiotherapy. Lecture at Radiotherapy Department, PGIMER. India.
[49] Barrett, A.C. 2009. Practical Radiotherapy Planning. Fourth Edition. Hodder Arnold.
[50] Ahnesjö, A., Saxner, M., Trepp, A. 1992. A Pencil Beam Model for Photon Dose Calculations. Medical Physics, pp. 263-273.
[51] Brahime, A. 2000. Development of Radiation Therapy Optimization. Acta Oncologica, 39(5).
[52] Bortfeld, T., Hong, T., Craft, D., Carlsson, F. 2008. Multicriteria Optimization in Intensity-Modulated Radiation Therapy Treatment Planning for Locally Advanced Cancer of the Pancreatic Head. International Journal of Radiation Oncology and Biology Physics, 72(4).
[53] Brown, Bernardette, and all members of Research Group. 2014. Clinician-led Improvement in Cancer Care (CLICC) - Testing a Multifaceted Implementation Strategy to Increase Evidence-Based Prostate Cancer Care: Phased Randomised Controlled Trial - Study Protocol. Implementation Science, 9:64.
[54] Bortifield, T. 2006. IMRT: A Review and Preview. Physics in Medicine and Biology, 51(2006):R363–R379.
[55] Censor, Y. 2005. Mathematical Optimization for the Inverse Problem of Intensity-Modulated Radiation Therapy. Laboratory Report, Department of Mathematics, University of Haifa, Israel.
[56] Capizzello, A., Tsekeris, P.G., Pakos, E.E., Papathanasopoulou, V., Pitouli, E.J. 2006. 'Adjuvant Chemo-Radiotherapy in Patients with Gastric Cancer. Indian Journal of Cancer, 43(4).
[57] Dawod, T., Abdelrazek, E.M., Elnaggar, M., Omar, R. 2014. Dose Validation of Physical Wedged symmetric Fields in Artiste Linear Accelerator. International Journal of Medical Physics, Clinical Engineering and Radiation Oncology, 3:201-209.
[58] Do, S.Y, David, A., Bush, J.D.S. 2010. Comorbidity-Adjusted Survival in Early-Stage Lung Cancer Patients Treated with Hypofractioned Proton Therapy. Journal of Oncology.
[59] Ehrgott, M., & Burjony, M. 2001. Radiation Therapy Planning by Multicriteria Optimization. In Proceedings of the 36th Annual Conference of the Operational Research Society of New Zealand (Vol. 244, p. 253).
[60] Ezzel, G.A. 1996. Genetic and Geometric Optimization of Three-dimensional Radiation Therapy Treatment Planning. Medical Physics, 23:293- 305.
[61] Effective Health Care, 2008. Number 13. Comparative Efectiveness of Therapies for Clinically Localized Prostate Cancer. Bookshelf ID: NBK554842.
[62] Hansen, P. 1998. Rank-deficient and Discrete Ill-posed Problems: Numerical Aspects of Linear Inversion'. SIAM Monographs on Mathematical Modelling and Computation.
[63] Hashemiparast, S.M., Fallahgoul, H. 2011. Modified Gauss Quadrature for Ill-posed Integral Transform. International Journal of Mathematics and Computation, 13(11).
[64] Isa, N. 2014. Evidence Based Radiation Oncology with Existing Technology. Reports of Practical Oncology and Radiotherapy, 19:259-266.
[65] Johansson, K.A., Mattsson, S., Brahme, A., Turesson, I. 2003. Radiation Therapy Dose Delivery'. Acta Oncologica, 42(2):2003.
[66] Khanna, P., Blais, N., Gaudreau, P.O., Corrales-Rodriguez, L. 2016. Immunotherapy Comes of Age in Lung Cancer, Clinical Lung Cancer.
[67] Küfer, K. H., Hamacher, H. W., & Bortfeld, T. 2001. A Multicriteria Optimization Approach for Inverse Radiotherapy Planning. In Operations Research Proceedings: Selected Papers of the Symposium on Operations Research (OR 2000) Dresden, September 9–12, 2000 (pp. 3-7). Springer Berlin Heidelberg.
[68] Kirsch, A. 1996. An introduction to the Mathematical Theory of Inverse Problems. Springer Applied Mathematical Sciences.
[69] Luenberger, D.G. 1989. Linear and Nonlinear Programming (2nd Edn.)., Addison-Wesley.
[70] Moczko, J.A., Roszak, A. 2006. Application of Mathematical Modeling in Survival Time Prediction for Females with Advanced Cervical cancer treated Radio-chemotherapy. Computational Methods in Science and Technology, 12(2).
[71] Ragaz, J., Olivotto, I. A., Spinelli, J. J., Phillips, N., Jackson, S. M., Wilson, K. S., ... & Manji, M. 2005. Loco-regional Radiation Therapy in Patients with High-risk Breast Cancer Receiving Adjuvant

Chemotherapy: 20-Year Results of the Columbia Randomized Trial'. Journal of National Cancer Institute, 97(2):116-126.
[72] Steuer, R. 1986. Multiple Criteria Optimization: Theory, Computation and Application. Wiley.
[73] Spirou, S.V., Chui, C.S. 1998. A Gradient Inverse Planning Algorithm with Dose-Volume Constraints. Medical Physics, 25:321-323.
[74] Das, I.J, Colls. 1997. Patterns of Dose Variability in Radiation Prescription of Breast Cancer. Radiotherapy and Oncology, 44: 83-89.
[75] Casesnoves, F. 2018. Practical Radiotherapy TPO Course with Cyberknife. Robotic Simulations for Breathing Movements during Radiotherapy Treatment. Sigulda Radiotherapy Cyberknife Center. Latvia. Riga Technical University Bioengineering Training-Course Nonlinear Life.
[76] Casesnoves, F. 2022. Radiotherapy Linear Quadratic Bio Model 3D Wedge Filter Dose Simulations for AAA Photon-Model [18 Mev, Z=5,15 cm] with Mathematical Method System. Biomedical Journal of Scientific and Technical Research, 46(2).
[77] Casesnoves, F. 1985. Master in Philosophy Thesis at Medical Physics Department. Protection of the Patient in Routinary Radiological Explorations. Experimental Low Energies RX Dosimetry. Medicine Faculty. Madrid Complutense University. 1984-85.
[78] Casesnoves, F. 1983-5. Ionization Chamber Low Energies Experimental Measurements for M-640 General Electric RX Tube with Radcheck ionization camera, Radcheck Beam Kilovoltimeter and TLD dosimeters. Radiology Department practice and measurements. Madrid Central Defense Hospital. Medical Physics Department. Master in Philosophy Thesis. Medicine Faculty. Complutense University. Madrid.
[79] Casesnoves, F. 1985. Determination of Absorbed Doses in Routinary Radiological Explorations. Medical Physics Conference organized by Medical Physics Society Proceedings Printed. San Lorenzo del Escorial. Madrid. September 1985.
[80] Greening, J. 1985. Fundamentals of Radiation Dosimetry. Taylor and Francis. Second Edition. 1985.
[81] International Commission of Radiation Protection. 1977. Bulletin 26th. The International Commission on Radiological Protection. Recommendations of the International Commission on Radiological Protection. Pergamon Press.
[82] Stanton, P., Colls. 1996. Cell Kinetics in vivo of Human Breast Cancer. British Journal of Surgery, 83:98-102.
[83] Hedman, M., Björk-Eriksson, T., Brodin, O., & Toma-Dasu, I. 2013. Predictive Value of Modelled Tumour Control Probability based on Individual Measurements of in vitro Radiosensitivity and Potential Doubling Time. The British Journal of Radiology, 86(1025):20130015.
[84] Fowler, J. 2010. 21 Years of Biologically Effective Dose. The British Journal of Radiology, 83: 554–568.
[85] Marcu, L. G., Toma-Dasu, I., Dasu, A., & Mercke, C. 2018. Radiotherapy and Clinical Radiobiology of Head and Neck Cancer. CRC Press.
[86] Casesnoves, F. 2022. Radiotherapy 3D Isodose Simulations for Wedge Filter 18 MEV-DOSE [z= 5, 15 cm] with AAA Model with Breast Cancer Applications. International Journal on Research Methodologies in Physics and Chemistry, 9(2):08-17.
[87] Garden, A., Beadle, B., Gunn, G. 2018. Radiotherapy for Head and Neck Cancers. Fifth Edition. Wolters Kluwer.
[88] Casesnoves, F. 2023. Radiotherapy Genetic Algorithm Pareto-Multiobjective Optimization of Biological Efective Dose and Clonogens Models for Head and Neck Tumor Advanced Treatment. International Journal of Mathematics and Computer Research, 11(01):3156-3177.
[89] Casesnoves, F. 2023. Radiotherapy Effective Clonogens Model Graphical Optimization Approaching Linear Quadratic Method for Head and Neck Tumors. International Journal of Molecular Biology and Biochemistry, 5(1):33-40.
[90] Casesnoves, F. 2023. Training Course Stereotactic Radiotherapy and Radiosurgery in Management of Metastatic Brain Tumors. Sigulda Stereotactic, Radiosurgery and Cyberknife Hospital. International Society of Radiosurgey. Sigulda, Latvia.
[91] Joiner, M., Kogel, A. 2019. Basic Clinical Radiobiology. CRC Press.
[92] Cher, M., Raz, A. 2002. Prostate Cancer: New Horizons in Research and Treatment. Kluwer Academic Publishers.
[93] Sureka, C., Armpilia, C. 2017. Radiation Biology for Medical Physicists. CRC Press.

[94] Ramon, J., Denis, L. 2007. Prostate Cancer. Springer-Verlag Berlin Heidelberg.
[95] Andisheh, B., Alt. 2013. A Comparative Analysis of Radiobiological Models for Cell Surviving Fractions at High Doses. Technology in Cancer Research and Treatment. 12(2).
[96] Casesnoves, F. 2018. Training Work. Nonlinear Life Biomedical Training-Course. Riga Technical University and Riga Oncology Hospital.
[97] Carini, H., Fidock, M., Van Gooland, A. 2019. Handbook of Biomarkers and Precision Medicine. CRC Press.
[98] Joiner, M., Kogel, A. 2019. Basic Clinical Radiobiology. CRC Press.
[99] Casesnoves, F. 2023. Radiotherapy BED Model 2D Pareto- Multiobjective Evolutionary Optimization for Prostate Cancer Hyperfractionated Treatment. Biomedical Journal of Scientific and Technical Research, 51(2).
[100] Chen, A., Vijayakumar, S. 2011. Prostate Cancer. Radiation Medicine Rounds, 2(1).
[101] Casesnoves, F. 2023. Radiotherapy BED Model Multiobjective Pareto-Interior Dual-Optimization for Prostate Cancer Hyperfractionated Treatment Planning and Isodoselines Invention. International Journal of Mathematics and Computer Research, 11(08):3651-3667.
[102] Casesnoves, F. 2024. Radiotherapy Hyperfractionated 3D Isodosezones Planning Optimization Method for Lung Tumors with BED Pareto-Multiobjective Model. International Journal of Mathematics and Computer Research, 12(02):4022-4032.
[103] Alttman, K., Lett, J. 1992. Advances in Radiation Biology. Relative Radiation Sensitivities of Human Organ Systems, Part III. Academic Press.
[104] Nikzad, S., Alter. 2015. Estimation of Cell Response in Fractionation Radiotherapy using Different Methods Derived from Linear Quadratic Model. Radiology and Oncology, 49(4):347-356.
[105] Keall, P., Alter. 2008. Investigating the Temporal Effects of Respiratory-gated and Intensity-modulated Radiotherapy Treatment Delivery on in vitro Survival: An Experimental and Theoretical Study. International Journal of Radiation Oncology - Biology - Physics, 71(5):1547-1552.
[106] Mu, X., Löfroth, P. O., Karlsson, M., & Zackrisson, B. 2003. The Effect of Fraction Time in Intensity Modulated Radiotherapy: Theoretical and Experimental Evaluation of an Optimisation Problem. Radiotherapy and Oncology, 68(2):181-187.

3. PROSTATE TUMORS

Abstract

Prostate cancer belongs epidemiologically to the most frequent tumors. This type of cancer belongs to the hormone- associated tumors type, such as breast and ovarian, for example. Its significant characteristics/differences are the TPO routinary higher radiation doses about 80Gy and the survival large time after treatment, related to other cancer types. This section deals with selected previous published advances in recent prostate tumors publications. Namely, 2D-3D Isodoselines and Isodosezones, and Computational Intelligence Pareto Multiobjective Optimization based on Genetic Algorithms. Additionally, some selected biomarkers recent Author's Proposal for prostate cancer and tumors in general which are currently under applications are briefed. Most important database is shown with graphics and numerical details. Supplemental formulation can be seen at Section 5 and further reading references.

Keywords

Pareto-Multiobjective Optimization (PMO), Mathematical Methods (MM), Biological Models (BM), Radiation Therapy (RT), Initial Tumor Clonogenes Number Population (N_0), Effective Tumor Population Clonogenes Number ($N_{Effective}$), Linear Quadratic Model (LQM), Integral Equation (IE), Tumor Control Probability (TCP), Normal Tissue Complications Probability (NTCP), Biological Effective model (BED), Tumor Control Cumulative Probability (TCCP), Radiation Photon-Dose (RPD), Nonlinear Optimization, Interior Optimization (IO), Radiotherapy Treatment Planning Optimization (TPO), Nonlinear Optimization, Treatment Planning Optimization (TPO), Artificial Intelligence (AI), Pareto-Multiobjective Optimization (PMO), Genetic Algorithms (GA) .

1. Introduction and Objectives

In a previous publication, constrained evolutionary algorithms for IN-VITRO-BED-LQ model (Linear Quadratic Biological Effective Dose Model) in prostate cancer Hyperfractionation radiotherapy TPO were optimized with Pareto-Multiobjective (PMO) methods. This study improves the research with a further comparative IN-VIVO-BED-LQ model optimization followed by a precision-refinement with Interior Optimization (IO) methods. Complex software is developed based on hyperfractionation constraints, but with *in vivo* main parameters dataset, and IO programming. Results with software design algorithmic method take in handle subroutines functions and matrix-algebra method for setting constraints and 3D IO surfaces. Results with 3D Interior Optimization by using the Genetic Algorithms (GA) previous numbers show get very good precision with new-invention of isodoselines sharp determination. Solutions dataset is shortly compared with previous *in vitro* study. Findings prove comparative PMO 2D imaging charts and numerical values of PMO prostate cancer hyperfractionated TPO parameters. Applications for prostate tumors

radiotherapy planning, especially with new Surfactal-Isodoselines, brain prostate metastases and stereotactic radiosurgery treatments are briefed.

From a previous publication [98], the objective of this contribution is applying Constrained Genetic Algorithms and 3D Interior Optimization on radiotherapy BED-LQ model for prostate tumors [1-24, 87-94] with *in vivo* dataset for an hyperfractionated schedule. The BED-LQ model [1-24, 40, 74-79, 87-94], is useful for low dose fractions, while LQL and PTL ones are more appropriate for high dose delivery RT treatment schedules—namely, hypofractionated treatment [94]. The numerical difference between *in vitro* LQ parameters for prostate LQ model can be considered important [1-24, 40, 74-79, 87-99]. It is not subject of this article any discussion about hyperfractionation versus hypofractionation dose delivery. Prostate cancer epidemiology statistics-figures are within the group of highest incidence-prevalence cancers, but lower than lung and breast tumors [99].

Therefore, the objective of the study is to carry out a double optimization process. Firstly, 2D GA optimization with in vivo data for LQ model. Secondly, making the most of the firstly GA obtained results, to get an improved refinement by using 3D Interior Optimization methods. Numerically, T_{Pot} magnitude difference *in vivo* values, prostate cancer, are about 28 days *in vivo* and [2, 19] *in vitro* ones are lower. In general, also, both *in vitro* and *in vivo* T_{Pot} parameters for prostate tumors are greater than other types of cancer [20-25]. This fact implies a longer survival time with several proper characteristics related to different treatment stages. Namely, surgical, RT, radiosurgical, chemotherapy, inmunotherapy, hormonal therapy, combinations of all of them. Today, biomarkers are getting an important role in order to predict the survival time, optimal chemotherapy, and both characteristics at the same time [95]. Table 1 shows a biomarkers classification into P-Biomarkers (Biomarkers for Prognosis, [96]), T-Biomarkers (Biomarkers for Optimal Treatment), and H-Biomarkers (Hybrid Biomarkers Group), [Author's proposal].

The programming design has two parts: Nonlinear GA-PMO engineering software with matrix algebra constraints, similar to the previous publication in codes/patterns for PMO-BED models. Second part is rather more difficult. That is, 3D Interior Optimization with the new useful-practical finding of isodoselines for radiotherapy planning hyperfractionated schedule. Those new Isodoselines along the Interior Optimization surface constitute a TPO advance and innovation of this contribution.

Results comprise Graphical and Numerical TPO hyperfractionated RT treatment planning. 2D GA graphics are presented in several formats, for 100, 150, and 250 generations. 3D Interior Optimization charts are illustrated with Isodoselines, optimal areas, and numerical

data inset. Numerical results show first GA figures and Interior Optimization refined values. Therefore, the novelty of this article, based on the previous evolutionary optimization paper [98], is its GA algorithms and computational optimization with *in vivo* parameters, 3D Interior Optimization improvements, and the practical definition of 3D Isodoselines for RT planning hyperfractionated schedule. It is objective, according to the precision of numbers obtained, that the mathematical and software developed is considered appropriate.

Grosso modo, a double constrained optimization based on previous Nonlinear Pareto-Multiobjective GA optimization was developed with the addition of 3D Interior Optimization refinement and the new-practical Isodoselines definition. Applications for radiotherapy hyperfractionated BED-TPO planning are presented. Numerical Analysis precision results are going to be promising for improvements of the method.

BIOMARKERS GENERAL CLASSIFICATION FOR CANCER RADIOTHERAPY TREATMENT
[Author's proposal]

TYPE	APPLICATION	ADDITIONAL	EXAMPLES
P-BIOMARKER (PROGNOSIS BIOMARKER)	Prediction of approximate survival time subject to optimal treatment	Prediction for approximate survival based on specific tumor cell histology, and according to the relation histology-efficacy of drugs. Drug failure investigation utility.	Research clinical trial example, [from 96]: investigation data show that patient survival time in PD-L1–positive patients who are treated with combined anti-CTLA-4 and anti-PD-1 is not superior to nivolumab monotherapy. That implied that was necessary further research. This clinical-trial study area is difficult
T-BIOMARKER (TREATMENT BIOMARKER)	Selection of approximate optimal choice for effective chemo-inmuno drug-target treatment	Optimization of the best effective drug type for personalized tumor at every patient. Detection of optimal drug-target and pharmacokinetics. Drug failure patient-personalization investigation. Target characterization.	HSP90α is an inducible molecular chaperone that functions as a homodimer [ref 96, Chapter 2.4, Table 2.4.2]
H-BIOMARKER (HYBRID BIOMARKER)	Both prediction of survival time and optimal treatment	Those ones that can make both functions, or one of them better than the other	Nano-Biomarkers actually in investigation can modify the inmuno-cells and efficacy of drugs over cells tumor

Table 1.-General Biomarkers classification, [Author's proposal]. Nano-Biomarkers is an open research field with potential perspectives in future [96, 99]. Just remark that Biomarkers are is extent, diverse and difficult as involves biochemistry, molecular biology, medicine-pharmacology, medical physiology and several other fields. Therefore, this Table is simple based on Author's proposal classification. [Casesnoves Bioengineering Laboratory. Database-creation 7.4]

2. Mathematical and Computational Methods

Following previous studies, mainly the prostate cancer one [98], and publications for Breast, Head-Neck cancer, here the Pareto-Multiobjective Optimization Fowler-foundation $BED_{Effective}$ model was programmed, [1-24, 40, 68, 74-79, 87-94, 98, 99]. Alpha, Betha, and rest of parameters intervals are detailed in Table 2. Algorithms 1-5 set the 2D GA and 3D IO formulas and constraints [85-88]. Radiobiological parameters Alpha and Betha are implemented independently, not in quotient [alpha/beta] because of the programming pattern's purpose. This low-dose LQ-BED model constitutes the foundations for hyperfractionated radiotherapy TPO, though there are dissimilarities among authors [20-25]. Therefore, the Pareto-Multiobjective [Algorithm 1] that was set, with Chebyshev L_1 norm, [Algorithms 2-4] is presented firstly. The IO method is explained secondly.

Evolutionary Algorithms Mathematical Method

The GA algorithms used are approximately the same than in previous prostate cancer publication, [98]. The sequence of the formula's development is as follows:

$$\text{Minimize,}$$
$$F(\vec{x}) = (f_1(\vec{x}), f_2(\vec{x}), \ldots . f_N(\vec{x})),$$
$$\text{subject to,}$$
$$K_i(\vec{x}) \geq 0 \text{ , for } i = 1, \ldots . . M$$

(Algorithm 1)

where,

F (x): Main function to be optimized
f_i (x): Every function of same variables (x)
K_i (x): Constraints functions such as in general $N \neq M$

BED nonlinear-quadratic model has been adapted for *in vivo* parameter T_{Pot} magnitude. Then, PMO in Prostate [24, 88, 89, 98] tumors simplest BED model reads:

$$\text{Chebyshev} \quad L_1 \text{ Optimization,}$$
$$\text{for} \quad i = 1,2 \ldots \text{minimize pareto,}$$
$$\left|DOSE_i - BED_{Effective}\right|_{L_1} \text{ with,}$$
$$BED_{Effective} = k \times d \times \left[1 + \frac{d \times \beta}{\alpha}\right] - \ldots$$
$$\ldots - \frac{Ln(2)}{\alpha} \times \left[\frac{T_{Treatment} - T_{Delay}}{T_{Potential}}\right];$$

(Algorithm 2)

where,

BED: The basic algorithm for Biological Effective Dose initially developed by Fowler et al. [22-25, 89-94, 98].

k: Optimal Number of fractions for hyperfractionated TPO. Optimization parameter [22-25, 89-94, 98].

d: Optimal Dose magnitude for every fraction. Optimization Parameter [Gy] [22-25, 89-94].

a: The basic algorithm constant for Biological Effective Dose models. Radiobiological experimental parameter *in vivo* [Gy^{-1}] [22-25, 89-94].

β: The basic algorithm constant for Biological Effective Dose models *in vivo*. Radiobiological experimental parameter [Gy^{-2}]. Note that it is very usual to set in biological models [α/β in Gy].

$T_{Treatment}$: The overall TPO time. This parameter varies according to authors' and institutions/hospitals criteria [22-25, 89-94, 98].

T_{Delay}: The overall TPO time delay for clonogens re-activation. This parameter varies according to authors' experimental research.

$T_{Potential}$: The potential time delay for tumor cell duplication. This parameter varies according to authors' experimental-theoretical research.

DOSE: The dose magnitudes for lung cancer simulation algorithm for Biological Effective Dose [22-25, 89-94, 98]. Software patterns were calculated around intervals prostate DOSE ϵ [70, 78] Gy.

Algorithm 2 [Fowler mainly, 89-94, 98]. -Prostate PMO algorithm [1-25, 85-90] implemented in software. Table 2 shows these intervals for optimization parameters details. Programming was developed in Matlab® system. At programming trials, it was found that precision was

increased related to *in vitro* parameters [98]. The constraints algebraic algorithm developed for Pareto-Multiobjective problem [Algorithms-3-5, 89-94, 21] reads:

$$\begin{aligned}&\text{Constraints,}\\&\text{For Pareto Functions}\quad i=1,2,\\&\text{and lower}-\text{upper limits of}\\&\text{optimization parameters,}\\&S_{Lower}\le K_i+d_i+T_{(Treatment)i}\le S_{Upper},\end{aligned}$$

(Algorithm 3)

Where,

S_{LOWER}: Summatory of all lower constraints for parameters [K, d, T].

S_{UPPER}: Summatory of all upper constraints for parameters [K, d, T].

K_i: Dose fraction number parameter for [i = 1, 2].

d_i: Dose fraction magnitude parameter for [i = 1, 2].

$T_{TREATMENT}$: Treatment time magnitude parameter for [i = 1, 2].

The subroutines programming strategy, as in [98], which are implemented reads:

$$\begin{aligned}&\text{Matrix Algebra Subroutines}\\&\text{For Constraints,}\\&[A_1]\times\begin{pmatrix}K\\d\\T\end{pmatrix}\le\begin{pmatrix}S_{K\max}\\d_{d\max}\\T_{T\max}\end{pmatrix},\\&[A_2]\times\begin{pmatrix}K\\d\\T\end{pmatrix}\ge\begin{pmatrix}S_{K\min}\\d_{d\min}\\T_{T\min}\end{pmatrix},\end{aligned}$$

(Algorithm 4)

where,

$S_{K,d,T}$: Upper (maximum) and Lower boundaries for parameters [K, d, T], according to Algorithms 1-2.

$A_{1,2}$: Matrices for numerical values, Table 2.

Software used for this study continues previous algorithms papers [1-20, 24, 68, 74, 88, 89, 98] with modifications, and addition of IO programs. For GA-PMO modeling, Equation 1 and Algorithms 1-4 are implemented on 2D programs, with application of Algorithm 5 basic model formula. Algorithm 2 was programmed with Algorithm 3 matrix constraints subroutines-functions. Table 2 shows Constrained GA Optimization *in vivo* parameters, different from [98], implemented in Algorithms 1-5. From Table 3 results, after IO implementation, 3D IO dataset for Table 4 is got. From all these numbers, 3D IO and 2D Genetic Algorithms Graphical Optimization imaging-processing charts, error determinations, pareto-distance, get precise approximations for hyperfractionated PMO-BED model. In general, precision obtained is more than expected, Tables 3-4.

Interior Optimization Computational Method

3D Interior and Graphical Optimization methods are used to confirm and refine the *in vivo* precision of the GA results from [98]. This is an advance as it was found that by using Interior Optimization the precision is increased and Isodoselines can be set for TPO. The method and software developed is a potential new application for accurate TPO.

Programming Dataset

Table 2 shows Matlab Constrained GA optimization dataset is detailed, for first optimization stage. As in [98], constraints matrix algebra is implemented through [Algorithms 3-5]. All these simulation techniques come from [20-25, 68, 74, 75, 80, 81, 85-94, 98]. The *in vivo* $T_{Potential}$ in prostate cancer for setting data is $T_{Potential} \in [26, 30]$ days. The reason to use *in vivo* dataset in this second prostate study is that, although currently the *in vivo* radiobiological differences differ in the literature, more realistic results are going to get.

IN VIVO LQ MODEL PARAMETERS IMPLEMENTED	
LQ MODEL PARAMETERS [Chapman, Nahum, 2015, Joiner, Kogel, 2019]	
BED-PARAMETER	MAGNITUDE/INTERVAL
T_{Pot}	[26.00 , 30.00] (Days)
T_K	21 (Days)
$T_{Treatment}$	[30 , 40] (Days)
α [Gy^{-1}]	[0.09 , 0.43] [Gy^{-1}]
β [Gy^{-2}]	0.0313 [Gy^{-2}]
Number of Fractions	[37 , 45] (Fractions)
Fraction Dose	[1.00 , 2.00] (Gy)
Pareto Total Prostate Dose Objective Function [89]	Pareto 1 : 70 Gy Pareto 2 : 78 Gy

Table 2.-Software implemented dataset for GA programming with source references [38, 43-45, 96, 97, 98]. Prostate cancer actual PMO routinary delivery doses.

3. Results

2D Evolutionary Algorithms Optimization Results

2D GA Graphical results are shown in Figures 1-4. The constrained optimization results are presented sharply in 2D multifunctional charts. This constrained optimization with *in vivo* parameters, [Algorithms 1-5] gets better results than *in vitro* one in the previous prostate cancer study [98].

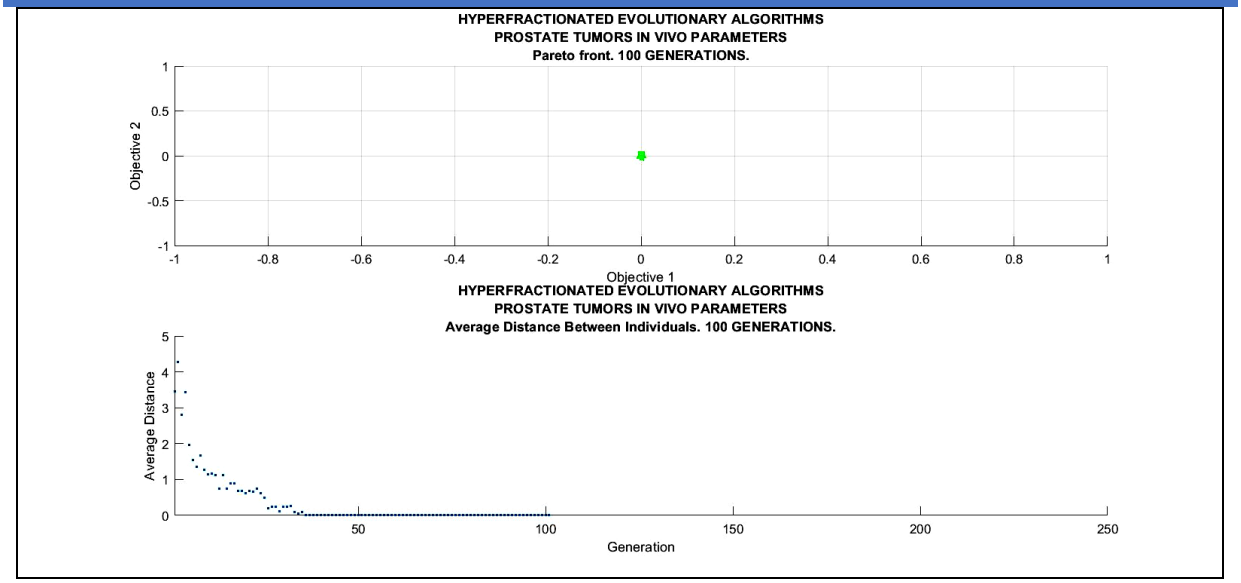

Figure 1.-High precision, almost null average distance, reached with 100 generations constrained optimization Multifunctional GA 2D graph. Note the total accomplishment of both pareto functions. The upper chart is the most important graph given by software when PMO is performed to validate the GA-optimization precision. In this study all programmed optimizations show null residuals, therefore, results are better than [98]. [Casesnoves Bioengineering Laboratory. Software. 45713]

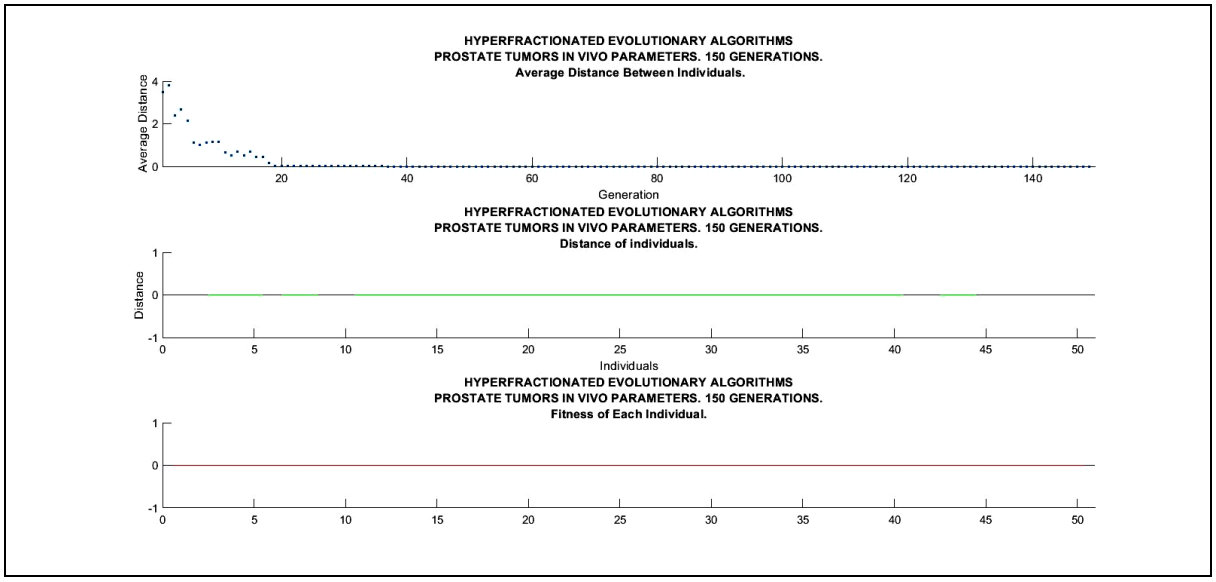

Figure 2.-Stepping up to 150 generations, image shows triple-graph for GA constrained optimization. The first one is the most important graph given by software when PMO is performed to validate the GA-optimization precision. Average distance among individuals is almost null, exact fitness. The fundamentals of Nonlinear PMO calculations are usually based on 2D PMO functions charts. [Casesnoves Bioengineering Laboratory. Software. 45714]

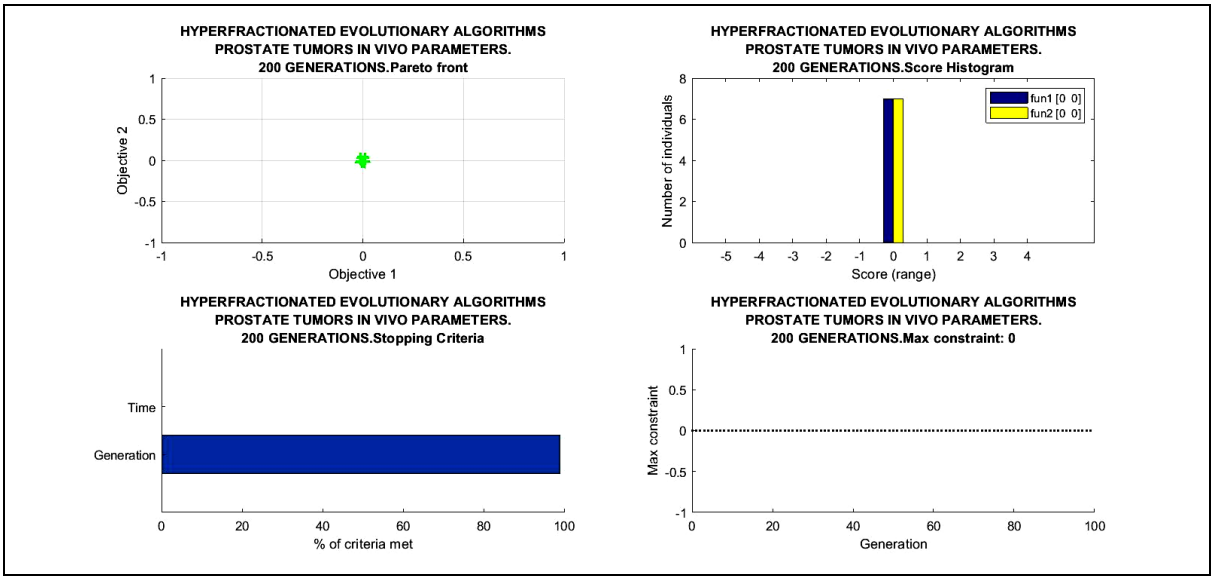

Figure 3.- 200 generations constrained optimization Multifunctional GA 2D graph. Score Histogram shows the accuracy. The upper-left image is the most important graph given by software when PMO is performed to validate the GA-optimization precision. 100% of criteria is met. [Casesnoves Bioengineering Laboratory. Software. 45715]

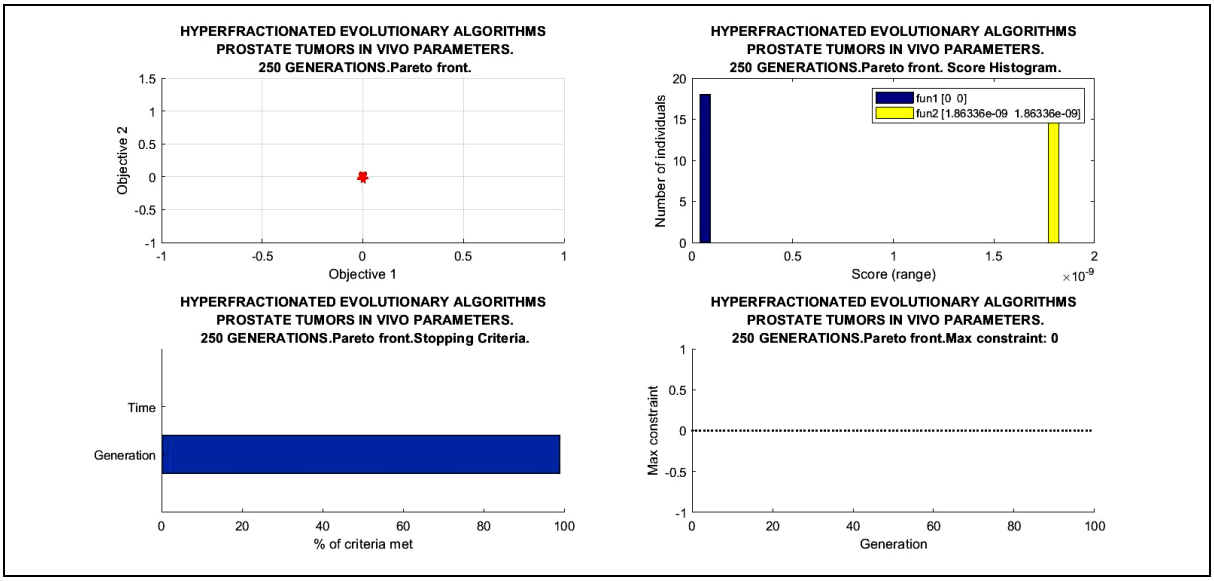

Figure 4.- 250 generations constrained optimization Multifunctional GA 2D graph. Score Histogram shows the accuracy. The upper-left image is the most important graph given by software when PMO is performed to validate the GA-optimization precision. 100% of criteria is met. [Casesnoves Bioengineering Laboratory. Software. 45716]

3D Interior Optimization Results

The imaging process software shows the results got with 3D Interior Optimization, Figures 5-7. Results are very acceptable. Isodoselines are marked inset every image. The radiotherapy planner gets multiple choices by using this 3D IO method.

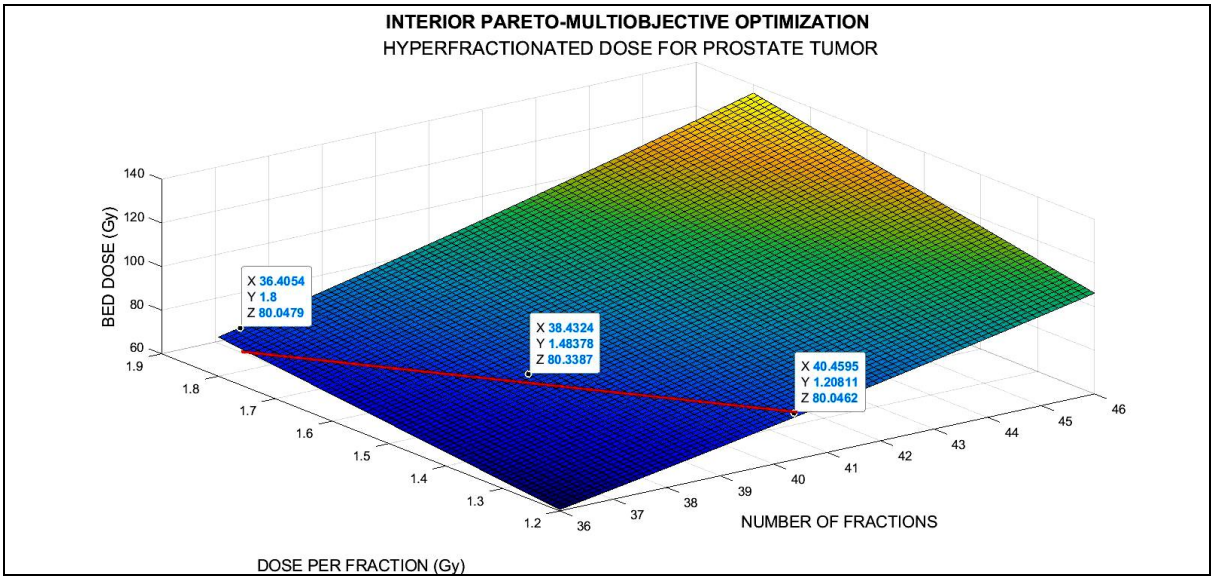

Figure 5.- The fundamentals of IO calculations are implemented into a 3D surface. Pattern intervals for plotting were taken from PMO Table 3 figures. Note that about 80 Gy BED total dose is fixed along Isodoseline, while (k) and (d) parameters vary when cursor is moved along this Isodoseline. [Casesnoves Bioengineering Laboratory. Software. 45717]

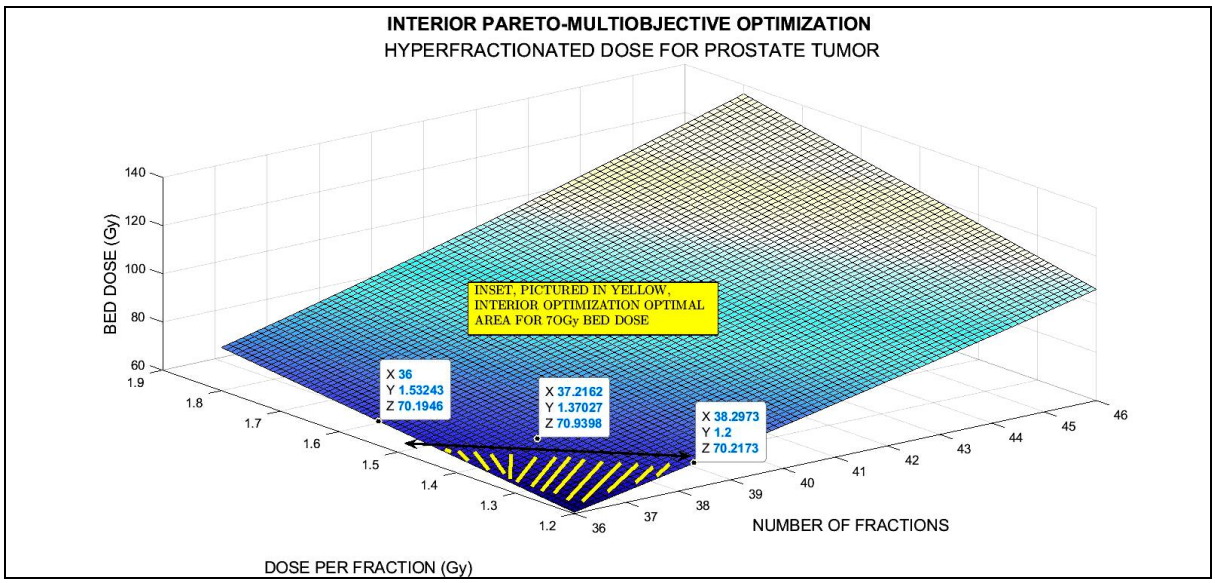

Figure 6.- Area for BED doses lower/equal than 70 Gy is marker in yellow inset. That is under the Isodoseline. Pattern intervals for plotting were taken from PMO Table 3 figures. Note that about 70 Gy BED total dose is fixed along Isodoseline, while (k) and (d) parameters vary when cursor is moved along this Isodoseline. [Casesnoves Bioengineering Laboratory. Software. 45718]

Invention of Interior Optimization Isodoselines

When performing the 3D Interior Optimization refinement, it was found that Isodoselines can be feasible and useful. Figure 7 can be considered a definite demonstration. It shows

a number of selected Isodoselines for a number of TPO-dose magnitudes to prove the new utility found. For IO, the algorithm to be set on program patterns reads,

$$BED_{Effective} = k \times d \times \left[1 + \frac{d \times \beta}{\alpha}\right] - \ldots$$

$$\ldots - \frac{Ln(2)}{\alpha} \times \left[\frac{T_{Treatment} - T_{Delay}}{T_{Potential}}\right];$$

Algorithm (5)

where all the parameters description are at Algorithms 1-4.

An image processing showing the utility for PTO of this IO with several Isodoselines is presented, Figure 7. Note that Algorithm 5 is converted when running software in a nonlinear-quadratic system of equations. As it is quadratic, the rationale of the precise results is justified.

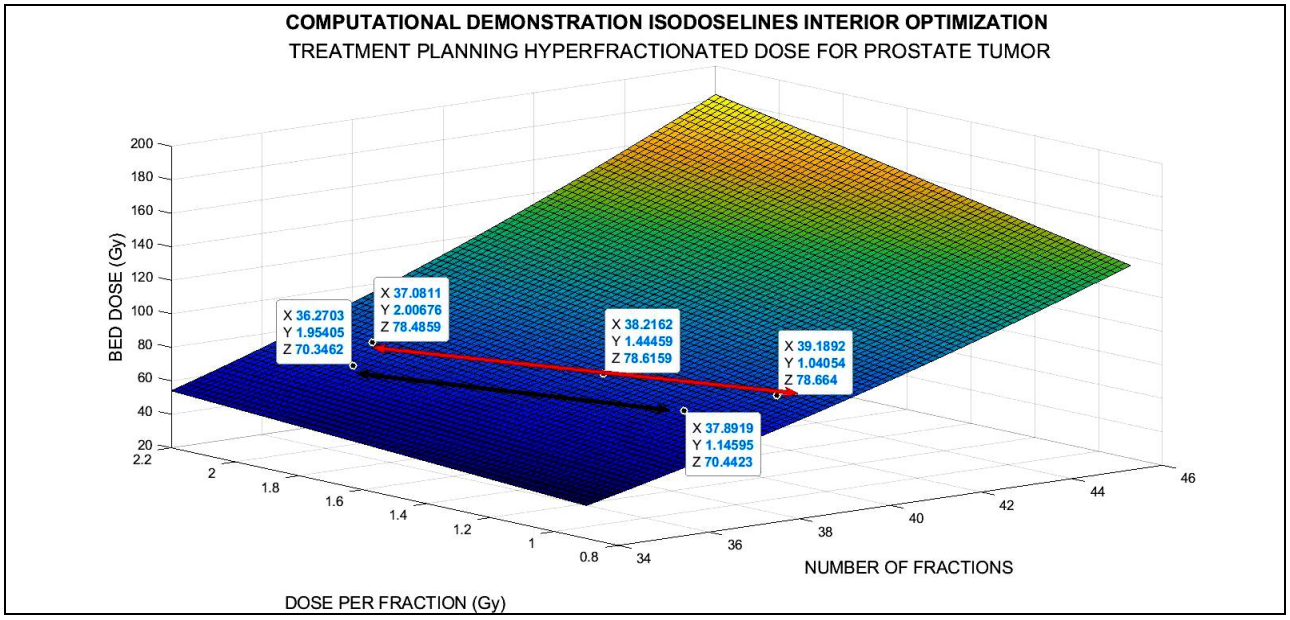

Figure 7.- The Isodoselines fundamentals for IO calculations are implemented into a 3D surface with two examples. Namely, about 70 and 78 Gy. Pattern intervals for plotting were taken from PMO Table 3 Figures. Note that each BED total dose is fixed along Isodoseline, while (k) and (d) parameters vary when cursor is moved along this Isodoseline. Intermediate values are marked in-between the Isodoseline for 78 Gy. [Casesnoves Bioengineering Laboratory. Software. 45719]

Numerical Results

Numerical results can be divided into two parts. First one is the GA numerical Figures, Table 3. Secondly IO results brief based on Figure 7 mainly. In Figure 7 Isodoselines demonstrate their efficacy for TPO choice. That is, once fixed total dose, e.g., 70 or 78 Gy, any planner can select the desired number of fractions, and the convenient figure of fraction-dose along a Isodoseline, Figure 7 proof.

Genetic Algorithm Optimization Numerical Results

Numerical dataset for Figures 1-4 in constrained PMO-GA optimization is shown in Table 3. As occurred in [98], constrained optimization displays acceptable numbers within numerical intervals [1-24, 40, 68, 74-79, 87-94, 98]. Note that PMO Genetic Algorithms is a different method than Isodoselines-zones techniques.

GENETIC ALGORITHM OPTIMIZATION NUMERICAL RESULTS FOR PROSTATE TUMORS IN VIVO PARAMETERS HYPERFRACTIONATED RT TREATMENT		
PARAMETER **[Optimization with [refs 25,83] and related author's radiotherapy text books] criteria]**	**MAGNITUDE INTERVAL/EXACT NUMERICAL GA RESULT**	**ADDITIONAL**
Optimal Dose fraction number	[40] Fractions	Usual protocol in literature [1-21,74-86].
Optimal Dose fraction magnitude	[1.7319] Gy	Usual protocol in literature [1-21,74-86]. Set with intervals according to different criteria.
$T_{Treatment}$	[38] Days	Usual protocol in literature [1-21,74-86]. Set with intervals according to different criteria. The RT treatment varies according to weekends breaks, secondary effects, patient circumstances, etc.
Dose interval in Objective Function That was set at software patterns	70 Gy for Pareto F function 1 78 Gy for Pareto F function 2	Usual protocol in literature [1-21,74-86]. Set with two total dose Pareto Functions according to different criteria.
Pareto Distance	0 Almost exact	Usual protocol in literature [1-21,74-86]. Set with two total dose Pareto Functions according to different criteria.
Average Distance	0 Almost exact	Usual protocol in literature [1-21,74-86]. Set with two total dose Pareto Functions according to different criteria.

Table 3.- Constrained optimization Algorithms 1-4 numerical results. Pareto distance is almost exact, in contrast with previous *in vitro* research (in [98], was about 10^{-2} magnitude order). [Casesnoves Bioengineering Laboratory. Software. 45720]

Interior Optimization Numerical Results

Table 4 show the accurate numerical results got with IO refinement method. Example-dataset included comes from Isodoselines of Figure 7.

INTERIOR OPTIMIZATION NUMERICAL RESULTS FOR PROSTATE TUMORS IN VIVO PARAMETERS HYPERFRACTIONATED RT TREATMENT [DATASET FROM FIGURE 7]		
FRACTIONS NUMBER k [Trunkated]	**FRACTION DOSE d Gy**	**TOTAL DOSE Gy**
37	2.00	ISODOSELINE 78 Gy
38	1.44	ISODOSELINE 78 Gy
39	1.04	ISODOSELINE 78 Gy
36	1.95	ISODOSELINE 70 Gy
38	1.14	ISODOSELINE 70 Gy

Table 4.- Brief of IO constrained optimization Algorithms 1-4 numerical results, with description of two Isodoselines, Figure 7. From Table 2, Lower Isodoseline is for 70 Gy, Upper for 78 Gy. K Figures are truncated to integers. [Casesnoves Bioengineering Laboratory. Software. 45721]

4. Discussion and Conclusions

The objective of the study was to get a series of 3D Isodoselines charts to evidence and verify the results from [98, 100] in prostate cancer hyperfractionated RT treatment with BED-LQ model and in vivo parameters. An improved and rather difficult software for 3D Interior Optimization to determine optimal surfaces and Isodoselines was constructed. All imaging processing results ratify the previous studies [98, 100].

The programming method has the inconvenient that the 3D surfaces are specific for each and every model and cancer type. However, to change formulas and/or parameters in software is not complicated. Running time for 3D surfactal Isodoselines is acceptable.

Succinctly, an extensive prostate cancer constrained RT-BED hyperfractionation model with 3D imaging processing and in vivo data was performed with Isodoselines software engineering work. Isodoselines constitute a practical result for BED RT accurate planning. Applications for hyperfractionated dose delivery in prostate tumors and radiation therapy optimal TPO in general arise from all the study.

5. References and Further Reading

[1] Casesnoves, F. 2022. Radiotherapy Wedge Filter AAA Model 18 Mev- Dose Delivery 3D Simulations with Several Software Systems for Medical Physics Applications. Applications. Biomedical Journal of Scientific and Technical Research, 40(5).
[2] Casesnoves, F. 2016. Mathematical Exact 3D Integral Equation Determination for Radiotherapy Wedge Filter Convolution Factor with Algorithms and Numerical Simulations. Journal of Numerical Analysis and Applied Mathematics, 1(2):39-59.
[3] Casesnoves, F. 2015. Radiotherapy Conformal Wedge Computational Simulations, Optimization Algorithms, and Exact Limit Angle Approach. International Journal of Scientific Research in Science, Engineering and Technology (IJSRSET), 1(2):353-362.
[4] Casesnoves, F. 2019. Improvements in Simulations for Radiotherapy Wedge Filter dose and AAA-Convolution Factor Algorithms. International Journal of Scientific Research in Science, Engineering and Technology (IJSRSET), 6(4):194-219.
[5] Casesnoves, F. 2011. Exact/Approximated Geometrical Determinations of IMRT Photon Pencil-Beam Path Through Alloy Static Wedges in Radiotherapy Using Anisothropic Analytic Algorithm (AAA). Peer-reviewed ASME Conference Paper. ASME 2011 International Mechanical Engineering Congress. Denver. USA. IMECE2011-65435.
[6] Casesnoves, F. 2012. Geometrical Determinations of Limit angle (LA) related to maximum Pencil-Beam Divergence Angle in Radiotherapy Wedges. Peer-reviewed ASME Conference Paper. ASME 2012 International Mechanical Engineering Congress. Houston. USA. IMECE2012-86638.
[7] Casesnoves, F. 2013. A Conformal Radiotherapy Wedge Filter Design. Computational and Mathematical Model/Simulation' Casesnoves, F. Peer-Reviewed Poster IEEE (Institute for Electrical and Electronics Engineers), Northeast Bioengineering Conference. Syracuse New York, USA. April 6th, 2013. Peer-Reviewed Poster Session on 6th April 2013. Sessions 1 and 3 with Poster Number 35. Page 15 of Conference Booklet.
[8] Casesnoves F. 2014. Mathematical and Geometrical Formulation/Analysis for Beam Limit Divergence Angle in Radiotherapy Wedges. Peer-Reviewed International Engineering Article. International Journal of Engineering and Innovative Technology (IJEIT), 3(7).
[9] Casesnoves, F. 2014. Geometrical Determinations of IMRT Photon Pencil-beam Path in Radiotherapy Wedges and Limit Divergence Angle with the Anisotropic Analytic Algorithm (AAA) Casesnoves, F. Peer- Reviewed scientific paper, both Print and online. International Journal of Cancer Therapy and Oncology, 2(3):02031.
[10] Casesnoves, F. 2014. Radiotherapy Conformal Wedge Computational Simulations and Nonlinear Optimization Algorithms. Peer-reviewed Article, Special Double-Blind Peer-reviewed paper by International Scientific Board with contributed talk. Official Proceedings of Bio- and Medical Informatics and Cybernetics: BMIC 2014 in the context of the 18th Multi-conference on Systemics, Cybernetics and Informatics: WMSCI 2014 July 15 - 18, 2014, Orlando, Florida, USA.
[11] Casesnoves, F. 2007. Large-Scale Matlab Optimization Toolbox (MOT) Computing Methods in Radiotherapy Inverse Treatment Planning'. High Performance Computing Meeting. Nottingham University.
[12] Casesnoves, F. 2008. A Computational Radiotherapy Optimization Method for Inverse Planning with Static Wedges. High Performance Computing Conference. Nottingham University.
[13] Casesnoves, F. 2015. Radiotherapy Conformal Wedge Computational Simulations, Optimization Algorithms, and Exact Limit Angle Approach. International Journal of Scientific Research in Science, Engineering and Technology (IJSRSET), 1(2):353-362.

[14] Casesnoves, F. 2015. Radiotherapy Standard/Conformal Wedge IMRT-Beamlet Divergence Angle Limit Exact Method, Mathematical Formulation, and Bioengineering Applications. International Article- Poster. Published in Proceedings of Conference. 41st Annual Northeast Bioengineering Conference. Rensselaer Polytechnic Institute. Troy, New York USA, April, p. 17-19.
[15] Casesnoves, F. 2015. Radiotherapy Standard/Conformal Wedge IMRT-Beamlet Divergence Angle Limit Exact Method, Mathematical Formulation, and Bioengineering Applications. IEEE (Institute for Electrical and Electronics Engineers), International Article-Poster.
[16] Casesnoves, F. 2015. Abstract-Journal. 'Radiotherapy Standard/ Conformal Wedge IMRT-Beamlet Divergence Angle Limit Exact Method, Mathematical Formulation. International Conference on Significant Advances in Biomedical Engineering. 252nd OMICS International Conference, 5(1).
[17] Casesnoves, F. 2001. Determination of Absorbed Doses in Common Radio Diagnostic Explorations. 5th National Meeting of Medical Physics. Madrid, Spain. September 1985. treatment Planning'. Kuopio University. Radiotherapy Department of Kuopio University Hospital and Radiotherapy Physics Group. Finland.
[18] Casesnoves, F. 2001. Master Thesis in Medical Physics. Eastern Finland University. Radiotherapy Department of Kuopio University Hospital and Radiotherapy Physics Grouversity-Kuopio. Defense approved in 2001. Library of Eastern finland University. Finland.
[19] Casesnoves, F. 2013. A Conformal Radiotherapy Wedge Filter Design. Computational and Mathematical Model/Simulation' Casesnoves, F. Peer-Reviewed Poster IEEE (Institute for Electrical and Electronics Engineers), Northeast Bioengineering Conference. Syracuse New York, USA. April 6th, 2013. Peer-Reviewed Poster Session on 6th April 2013. Sessions 1 and 3 with Poster Number 35. Page 15 of Conference Booklet.
[20] Casesnoves, F. 2022. Radiotherapy Biological Tumor Control Probability Integral Equation Model with Analytic Determination. International Journal of Mathematics and Computer Research, 10(8):2840-2846.
[21] Casesnoves, F. 2022. Radiotherapy Wedge Filter AAA Model 3D Simulations For 18 Mev 5 cm-Depth Dose with Medical Physics Applications", International Journal of Scientific Research in Computer Science, Engineering and Information Technology (IJSRCSEIT), 8(1):261-274.
[22] Walsh, S. 2011. Radiobiological modelling in Radiation Oncology. PhD Thesis. School of Physics. National University of Galway.
[23] Chapman, D., Nahum, A. 2015. Radiotherapy Treatment Planning, Linear- Quadratic Radiobiology. CRC Press.
[24] Mayles, W., Nahum, A. 2015. Rosenwald, J. Editors. Handbook of Radiotherapy Physics. Second Edition. CRC Press.
[25] Nahum, A., Webb, S. 1993. A Model for Calculating Tumour Control Probability in Radiotherapy Including the Effects of Inhomogeneous Distributions of Dose and Clonogenic Cell Density. Physics in Medicine and Biology; v. 38(6); p. 653-666.
[26] Haydaroglu, A., Ozyigit, G. 2013. Principles and Practice of Modern Radiotherapy Techniques in Breast Cancer. Springer.
[27] Casesnoves, F. 2019-20. Die numerische Reuleaux-Methode Rechnerische und dynamische Grundlagen mit Anwendungen (Erster Teil). ISBN-13: 978-620-0-89560-8, ISBN-10: 6200895600. Publishing House: Sciencia Scripts. 2019-20.
[28] Ulmer W., Harder, D. 1997. Corrected Tables of the Area Integral I(z) for the Triple Gaussian Pencil Beam Model. Journal of Medical Physics, 7:192-193.
[29] Ulmer, W., Harder, D. 1995. A Triple Gaussian Pencil Beam Model for Photon Beam Treatment Planning. Medical Physics, 5:25-30.
[30] Ulmer, W., Harder, D. 1996. Applications of a Triple Gaussian Pencil Beam Model for Photon Beam Treatment Planning. Medical Physics, 6:68-74.
[31] Ma, C., Lomax, T. 2013. Proton and Carbon Ion Therapy. CRC Press.
[32] Censor, Y., Zenios, S.A. 1997. Parallel Optimization: Theory, Algorithms and Applications'. UOP.
[33] Ulmer, W., Pyyry, J., Kaissl, W. 2005. A 3D Photon Superposition/ Convolution Algorithm and Its Foundation on Results of Monte Carlo Calculations. Physics in Medicine and Biology, p. 50.
[34] Ulmer, W., Harder, D. 1997. Applications of the Triple Gaussian Photon Pencil Beam Model to Irregular Fields, Dynamical Collimators and Circular Fields. Physics in Medicine and Biology.

[35] Haddad, K., Anjak, O., Yousef, B. 2019. Neutron and High Energy Photon Fluence Estimation in CLINAC using Gold Activation Foils. Reports of Practical Oncology and Radiotherapy, 24:41-46.
[36] Sievinen, J., Waldemar, U., Kaissl, W. AAA Photon Dose Calculation Model in Eclipse™. Varian Medical Systems Report. Rad #7170A.
[37] Vagena, E., Stoulos, S., Manolopoulou, M. 2016. GEANT4 Simulations on Medical LINAC Operation at 18MV: Experimental Validation based on Activation Foils. Radiation Physics and Chemistry.
[38] Ethics for Researchers. 2013. EU Commission. Directorate-General for Research and Innovation. Science in society/Capacities FP7.
[39] Casesnoves, F. 1981. Surgical Pathology I Course Class Notes and Clinical Practice of Surgical Pathology Madrid Clinical Hospital [Professor Surgeon Dr Santiago Tamames Escobar]. 4th academic year course for graduation in Medicine and Surgery. Lessons and practice Breast Cancer Surgical and Medical Treatment. 1980-1981. Madrid Complutense University.
[40] Tamames., Escobar, S. 2000. Cirugia/ Surgery: Aparato Digestivo. Aparato Circulatorio. Aparato Respiratorio/ Digestive System. Circulatory System. Respiratory System (Spanish Edition).
[41] Silvia, C., Formenti, S.D. 2013. Combining Radiotherapy and Cancer Immunotherapy: A Paradigm Shift Silvia C. Formenti, Sandra Demaria. Journal of the National Cancer Institute, 105:256-265.
[42] Numrich, R.W. 2010. The Computational Energy Spectrum of a Program as it Executes. Journal of Supercomputing, 52.
[43] European Commission, Directorate-General for Research. 2021. Unit L3. Governance and Ethics. European Research Area. Science and Society.
[44] ALLEA. 2017. The European Code of Conduct for Research Integrity, Revised Edn.; ALLEA: Berlin Barndenburg Academy of Sciences.
[45] Good Research Practice. 2017. Swedish Research Council.
[46] Ulmer, W., Schaffner, B. 2011. Foundation of an Analytical Proton Beamlet Model for Inclusion in a General Proton Dose Calculation System. Radiation Physics and Chemistry, 80:378-389.
[47] Sharma, S.C. 2008. Beam Modification Devices in Radiotherapy. Lecture at Radiotherapy Department, PGIMER. India.
[48] Barrett, A.C. 2009. Practical Radiotherapy Planning. Fourth Edition. Hodder Arnold.
[49] Ahnesjö, A., Saxner, M., Trepp, A. 1992. A Pencil Beam Model for Photon Dose Calculations. Medical Physics, pp. 263-273.
[50] Brahime, A. 2000. Development of Radiation Therapy Optimization. Acta Oncologica, 39(5).
[51] Bortfeld, T., Hong, T., Craft, D., Carlsson, F. 2008. Multicriteria Optimization in Intensity-Modulated Radiation Therapy Treatment Planning for Locally Advanced Cancer of the Pancreatic Head. International Journal of Radiation Oncology and Biology Physics, 72(4).
[52] Brown, Bernardette, and all members of Research Group. 2014. Clinician-led Improvement in Cancer Care (CLICC) - Testing a Multifaceted Implementation Strategy to Increase Evidence-Based Prostate Cancer Care: Phased Randomised Controlled Trial - Study Protocol. Implementation Science, 9:64.
[53] Bortifield, T. 2006. IMRT: A Review and Preview. Physics in Medicine and Biology, 51(2006):R363–R379.
[54] Censor, Y. 2005. Mathematical Optimization for the Inverse Problem of Intensity-Modulated Radiation Therapy. Laboratory Report, Department of Mathematics, University of Haifa, Israel.
[55] Capizzello, A., Tsekeris, P.G., Pakos, E.E., Papathanasopoulou, V., Pitouli, E.J. 2006. 'Adjuvant Chemo-Radiotherapy in Patients with Gastric Cancer. Indian Journal of Cancer, 43(4).
[56] Dawod, T., Abdelrazek, E.M., Elnaggar, M., Omar, R. 2014. Dose Validation of Physical Wedged symmetric Fields in Artiste Linear Accelerator. International Journal of Medical Physics, Clinical Engineering and Radiation Oncology, 3:201-209.
[57] Do, S.Y, David, A., Bush, J.D.S. 2010. Comorbidity-Adjusted Survival in Early-Stage Lung Cancer Patients Treated with Hypofractioned Proton Therapy. Journal of Oncology.
[58] Ehrgott, M., & Burjony, M. 2001. Radiation Therapy Planning by Multicriteria Optimization. In Proceedings of the 36th Annual Conference of the Operational Research Society of New Zealand (Vol. 244, p. 253).
[59] Ezzel, G.A. 1996. Genetic and Geometric Optimization of Three-dimensional Radiation Therapy Treatment Planning. Medical Physics, 23:293- 305.

[60] Effective Health Care, 2008. Number 13. Comparative Efectiveness of Therapies for Clinically Localized Prostate Cancer. Bookshelf ID: NBK554842.
[61] Hansen, P. 1998. Rank-deficient and Discrete Ill-posed Problems: Numerical Aspects of Linear Inversion'. SIAM Monographs on Mathematical Modelling and Computation.
[62] Hashemiparast, S.M., Fallahgoul, H. 2011. Modified Gauss Quadrature for Ill-posed Integral Transform. International Journal of Mathematics and Computation, 13(11).
[63] Isa, N. 2014. Evidence Based Radiation Oncology with Existing Technology. Reports of Practical Oncology and Radiotherapy, 19:259-266.
[64] Johansson, K.A., Mattsson, S., Brahme, A., Turesson, I. 2003. Radiation Therapy Dose Delivery'. Acta Oncologica, 42(2):2003.
[65] Khanna, P., Blais, N., Gaudreau, P.O., Corrales-Rodriguez, L. 2016. Immunotherapy Comes of Age in Lung Cancer, Clinical Lung Cancer.
[66] Küfer, K. H., Hamacher, H. W., & Bortfeld, T. 2001. A Multicriteria Optimization Approach for Inverse Radiotherapy Planning. In Operations Research Proceedings: Selected Papers of the Symposium on Operations Research (OR 2000) Dresden, September 9–12, 2000 (pp. 3-7). Springer Berlin Heidelberg.
[67] Kirsch, A. 1996. An introduction to the Mathematical Theory of Inverse Problems. Springer Applied Mathematical Sciences.
[68] Luenberger, D.G. 1989. Linear and Nonlinear Programming (2nd Edn.)., Addison-Wesley.
[69] Moczko, J.A., Roszak, A. 2006. Application of Mathematical Modeling in Survival Time Prediction for Females with Advanced Cervical cancer treated Radio-chemotherapy. Computational Methods in Science and Technology, 12(2).
[70] Ragaz, J., Olivotto, I. A., Spinelli, J. J., Phillips, N., Jackson, S. M., Wilson, K. S., ... & Manji, M. 2005. Loco-regional Radiation Therapy in Patients with High-risk Breast Cancer Receiving Adjuvant Chemotherapy: 20-Year Results of the Columbia Randomized Trial'. Journal of National Cancer Institute, 97(2):116-126.
[71] Steuer, R. 1986. Multiple Criteria Optimization: Theory, Computation and Application. Wiley.
[72] Spirou, S.V, Chui, C.S. 1998. A Gradient Inverse Planning Algorithm with Dose-Volume Constraints. Medical Physics, 25: 321-323.
[73] Das, I.J, Colls. 1997. Patterns of Dose Variability in Radiation Prescription of Breast Cancer. Radiotherapy and Oncology, 44: 83-89.
[74] Casesnoves, F. 2018. Practical Radiotherapy TPO Course with Cyberknife. Robotic Simulations for Breathing Movements during Radiotherapy Treatment. Sigulda Radiotherapy Cyberknife Center. Latvia. Riga Technical University Bioengineering Training-Course Nonlinear Life.
[75] Casesnoves, F. 2022. Radiotherapy Linear Quadratic Bio Model 3D Wedge Filter Dose Simulations for AAA Photon-Model [18 Mev, Z=5,15 cm] with Mathematical Method System. Biomedical Journal of Scientific and Technical Research, 46(2).
[76] Casesnoves, F. 1985. Master in Philosophy Thesis at Medical Physics Department. Protection of the Patient in Routinary Radiological Explorations. Experimental Low Energies RX Dosimetry. Medicine Faculty. Madrid Complutense University. 1984-85.
[77] Casesnoves, F. 1983-5. Ionization Chamber Low Energies Experimental Measurements for M-640 General Electric RX Tube with Radcheck ionization camera, Radcheck Beam Kilovoltimeter and TLD dosimeters. Radiology Department practice and measurements. Madrid Central Defense Hospital. Medical Physics Department. Master in Philosophy Thesis. Medicine Faculty. Complutense University. Madrid.
[78] Casesnoves, F. 1985. Determination of Absorbed Doses in Routinary Radiological Explorations. Medical Physics Conference organized by Medical Physics Society Proceedings Printed. San Lorenzo del Escorial. Madrid. September 1985.
[79] Greening, J. 1985. Fundamentals of Radiation Dosimetry. Taylor and Francis. Second Edition. 1985.
[80] International Commission of Radiation Protection. 1977. Bulletin 26th. The International Commission on Radiological Protection. Recommendations of the International Commission on Radiological Protection. Pergamon Press.
[81] Stanton, P., Colls. 1996. Cell Kinetics in vivo of Human Breast Cancer. British Journal of Surgery, 83:98-102.

[82] Hedman, M., Björk-Eriksson, T., Brodin, O., & Toma-Dasu, I. 2013. Predictive Value of Modelled Tumour Control Probability based on Individual Measurements of in vitro Radiosensitivity and Potential Doubling Time. The British Journal of Radiology, 86(1025):20130015.
[83] Fowler, J. 2010. 21 Years of Biologically Effective Dose. The British Journal of Radiology, 83: 554–568.
[84] Marcu, L. G., Toma-Dasu, I., Dasu, A., & Mercke, C. 2018. Radiotherapy and Clinical Radiobiology of Head and Neck Cancer. CRC Press.
[85] Casesnoves, F. 2022. Radiotherapy 3D Isodose Simulations for Wedge Filter 18 MEV-DOSE [z= 5, 15 cm] with AAA Model with Breast Cancer Applications. International Journal on Research Methodologies in Physics and Chemistry, 9(2):08-17.
[86] Garden, A., Beadle, B., Gunn, G. 2018. Radiotherapy for Head and Neck Cancers. Fifth Edition. Wolters Kluwer.
[87] Casesnoves, F. 2023. Radiotherapy Genetic Algorithm Pareto-Multiobjective Optimization of Biological Efective Dose and Clonogens Models for Head and Neck Tumor Advanced Treatment. International Journal of Mathematics and Computer Research, 11(01):3156-3177.
[88] Casesnoves, F. 2023. Radiotherapy Effective Clonogens Model Graphical Optimization Approaching Linear Quadratic Method for Head and Neck Tumors. International Journal of Molecular Biology and Biochemistry, 5(1):33-40.
[89] Casesnoves, F. 2023. Training Course Stereotactic Radiotherapy and Radiosurgery in Management of Metastatic Brain Tumors. Sigulda Stereotactic, Radiosurgery and Cyberknife Hospital. International Society of Radiosurgey. Sigulda, Latvia.
[90] Joiner, M., Kogel, A. 2019. Basic Clinical Radiobiology. CRC Press.
[91] Cher, M., Raz, A. 2002. Prostate Cancer: New Horizons in Research and Treatment. Kluwer Academic Publishers.
[92] Sureka, C., Armpilia, C. 2017. Radiation Biology for Medical Physicists. CRC Press.
[93] Ramon, J., Denis, L. 2007. Prostate Cancer. Springer-Verlag Berlin Heidelberg.
[94] Andisheh, B., Alt. 2013. A Comparative Analysis of Radiobiological Models for Cell Surviving Fractions at High Doses. Technology in Cancer Research and Treatment. 12(2).
[95] Casesnoves, F. 2018. Training Work. Nonlinear Life Biomedical Training-Course. Riga Technical University and Riga Oncology Hospital.
[96] Carini, H., Fidock, M., Van Gooland, A. 2019. Handbook of Biomarkers and Precision Medicine. CRC Press.
[97] Joiner, M., Kogel, A. 2019. Basic Clinical Radiobiology. CRC Press.
[98] Casesnoves, F. 2023. Radiotherapy BED Model 2D Pareto- Multiobjective Evolutionary Optimization for Prostate Cancer Hyperfractionated Treatment. Biomedical Journal of Scientific and Technical Research, 51(2).
[99] Chen, A., Vijayakumar, S. 2011. Prostate Cancer. Radiation Medicine Rounds, 2(1).
[100] Casesnoves, F. 2023. Radiotherapy BED Model Multiobjective Pareto-Interior Dual-Optimization for Prostate Cancer Hyperfractionated Treatment Planning and Isodoselines Invention. International Journal of Mathematics and Computer Research, 11(08):3651-3667.

4. HEAD AND NECK TUMORS

Abstract

Head and neck cancer is epidemiologically varied, both in tumor types, location, survival rates after RT TPO, individual patient characteristics, optimal delivery doses, and several other factors. Those are the main differences related to other cancer types. Recently new treatment techniques, either combined or not, have obtained more survival time. Preventive medicine, for example in tobacco and alcohol consumption, and chemicals environment plays an important role in the prevalence/incidence of these tumor types. This section deals with some of the selected-specific main previous published advances in recent head and neck tumors publications. However, following the variety aim of the chapter, it is selected the papers on Survival Fraction classical model's formulation, implemented with a number of programming methods and specific patters. Namely, first and foremost, mathematical $N_{Effective}$ tumor clonogens number in Biological Effective Dose (BED) algorithms constrained to head and neck cancer is simulated initially without implementation into Linear Quadratic Biomodel equations for BED dose delivery. Secondly, 3D imaging results for $N_{Effective}$ (Effective Tumor Population Clonogenes Number) determination after passing on the standard radiotherapy treatment time are shown. For the usual equations related to parameter Effective Tumor Population Clonogenes Number, Poisson Statistical-probabilistic Methods are used/applied. Most important database is shown with graphics and numerical details. Further formulation can be seen/compared at Section 5.

Keywords

Mathematical Methods (MM), Biological Models (BM), Radiation Therapy (RT), Initial Tumor Clonogenes Number Population (N_0), Effective Tumor Population Clonogenes Number (N_{Eff}), Linear Quadratic Model (LQM), Integral Equation (IE), Tumor Control Probability (TCP), 3D Isodoses TPO System, Tumor Control Cumulative Probability (TCCP), Radiation Photon-Dose (RPD), Nonlinear Optimization, Radiotherapy Treatment Planning Optimization (TPO), Source-Surface Distance (SSD), Software Engineering Methods, Radiation Photon-Dose, Attenuation Exponential Factor (AEF), Nonlinear Optimization, Radiotherapy Wedge Filter (WF), Anisotropic Analytic Model (AAA), Fluence Factor (FF), Omega Factor (OF), Treatment Planning Optimization (TPO), Head and Neck Tumor (HANT).

1. Introduction

Classical Fowler model for $N_{Effective}$ tumor clonogens number in Biological Effective Dose (BED) algorithms constrained to head and neck cancer is simulated initially without implementation into Linear Quadratic Biomodel equations for BED dose delivery. After Fowler initial models, a different researcher large number of model variants and literature contributions was developed. RT biological models provide with a dose delivery radioprotection optimal minimization of photon-dose deposition while keeping the most efficacious dose to maximize Tumor Control Probability in head and neck tumors. Results comprise the Effective Clonogens model for head and neck cancer parameters 3D

Graphical Optimization simulations. 3D imaging results for $N_{Effective}$ (Effective Tumor Population Clonogenes Number) determination after passing on the standard radiotherapy treatment time are shown. Applications for new 3D Isodoses Graphical Optimization image processing with AAA wedge filters photon-dose model are shown. All RT uses for TPO in head and neck cancer with Fractionation-dose are explained.

Several studies were developed in radiotherapy TPO with biological models and algorithms simulations [19, 74]. The objective of this contribution is to present 3D Graphical Optimization simulations for $N_{Effective}$ clonogens population with Fowler model [82, 84]. It was set initially without implementation in Linear Quadratic Biomodel equations for BED dose delivery. Specifically for head and neck cancer with its corresponding specific parameters [22, 82, 83, 84].

Radiotherapy combined with Radiation Protection for the patient during routinary RT treatment with BMs avoids multiple risk factors. Namely, RT overdose, OARs damage, increase of radiation use for high incidence/prevalence of any type of cancer with subsequent RT oncology therapy, medical staff professional cumulative dose increase, hospital radiation contamination, environmental radiation contamination, and others [1-20, 22-25, 73-79, 82, 83]. Table 1 shows the direct effect of BMs in TPO and the precision improvements given by $N_{Effective}$ clonogens model application in Linear Quadratic models and BED ones. For head and neck cacer RT TPO, the hypofraccionated radiotherapy protocol us usually 40-50 Gy during 6-8 weeks, with about 5 fractions/weekly. However, these magnitudes/schedules vary according to hospital or Oncology center criteria.

Head and neck tumors group present a number of proper oncological, epidemiological, pathogenesis, and radiobiological characteristics [75-79, 83]. Namely, the external media intake/contact from a group of substances that have significant pathogenesis factors in the oncological origin of these cancers. These intakes could be toxic substances or biological ones, such as virus or bacteria. Among virus, for example, the Espstein-Barr one is linked to Nasopharyngeal carcinoma pathogenesis, and Papillomavirus to Tonsillar carcinomas. That is, the head, thorax cavity and neck anatomical zones catch from air many of them from exterior media into the mouth nose, and lungs. Therefore, tobacco influence is epidemiologically-statistically high. The oral cavity accumulates tobacco and alcohol as oncogenetical factors. The lungs could also take in materials that cause mesothelioma. Specific processed substances contained in food could cause oncogenesis phenomena in oral cavity, esophagus and stomach. External radiation sources show an important influence for thyroid cancer origin [83, 84]. Electromagnetic

radiation constant and daily magnitude may have epidemiological influence in specific brain cancer tumors pathogenesis.

Therefore, following the Radiation Therapy research studies series, [1-20, 73-79, 84], this study objective is the implementation of Tumor Clonogens Effective Population Number Model for head and neck cancer, [Fowler publications series,1989-2010, 82]. Photon-dose AAA model former contributions results in breast tumors Biological Models (BM) TCP parameters, [19, 74]. Development for 3D Graphical Optimization solutions from recent study [19, 74] to obtain Effective Tumor Clonogenes Survival Rate [$N_{Effective}$], constitutes the aim of this research. Photon-beam Biological Models are based mainly on exponential functions with radiobiological parameters, namely [a, β], whose magnitudes are determined in general with *in vitro* experimental [19, 21-24, 74]. These parameters are implemented in BM to obtain Survival Fraction Clonogens Rate, [N_S], [19, 21-24, 74, 82]. N_S is function of [N_0], namely, initial clonogens population number.

The innovation of this study determines the fitted to RT treatment time initial clonogens population number with the calculation of $N_{Effective}$ for head and neck tumors RT treatment [19, 22, 74, 83, 84]. Table 1 shows applications of [$N_{Effective}$] calculations for RT head and neck cancer. The new 3D Isodoses TPO charts are shown and improved from [84] with specific programming to prove the applications of this precision-step in BED and Linear Quadratic models.

Research 3D imaging and numerical results comprise simulations for $N_{Effective}$ clonogens population model related to RT treatment delay time parameters and population doubling time head and neck tumors constants [19, 74, 83].

In summary, 3D Graphical Optimization was programmed specifically for $N_{Effective}$ clonogens population model. Results comprise 3D image processing charts and numerical approximations useful in TPO in radiotherapy, Figures 1-4, Table 4. 3D Isodoses image-processing AAA model with WF developments from [84] are shown and proven, Figures 5-6.

$N_{Effective}$ MODEL FOR HEAD AND NECK TUMORS APPLICATIONS	
RT TPO METHOD IMPROVEMENTS	**DIRECT EFFECT**
Mathematical Improvements when N_{Eff} is implemented in Survival Fraction Models	With N_{Eff} Implementation TCP is numerically more accurate Without N_{Eff} TCP is falsely numerically higher With N_{Eff} Implementation NTCP is numerically more accurate Without N_{Eff} Implementation NTCP is falsely numerically lower
N_{Eff} Implementation in Survival Fraction Models	Dose Delivery Precision because it minimizes Clonogenes growth during radiotherapy Treatment Time, Maximum Effect/Maximum Tumor Control Probability [TCP]
N_{Eff} Implementation in Survival Fraction Models for exact calculation of NTCP instead N_0 . Then, TCP and NTCP are more efficacious.	Radioprotection OARs Dose Precision because it sets exact Clonogenes growth during radiotherapy Treatment Time, Maximum Effect/Maximum Normal Tissue Complications Probability [NTCP]
Optimization of Biological Models	Dose Delivery Precision, minimum dose/ maximum effect
Previous Photon-dose Optimization	Dose Delivery Precision to be implemented in BM, minimum dose/ maximum effect
Normal Tissue Complications Probability Models [NTCP]	Dose-Volume-Histogram Dose Delivery Precision to be implemented in BM, minimum dose at OARs
ON PATIENT EFFECTS	
OARs Radioprotection	Avoid Damage at any FSUs [Organ Funcional Subunits]
Radiation Therapy Secondary Effects	Hypo Fractionations decreases Radiation Undesirable Symptoms
Patient Life Quality	Not only Physical benefit but also Psychological for Patient

Table 1.-Brief of RT TPO methods and subsequent positive effects in patient cure and post-radiation life. Those are justified also for the rise of head and neck tumor survival time and complete cure got by modern RT, IMRT, IMPT, Chemo, and Inmunotherapy advances.

2. Mathematical Models and Methods

For exclusive determination of $N_{Effective}$ Clonogens population number, a standard model was selected [Fowler model, 22, 82]. The experimental parameters for breast cancer RT treatment protocol [19, 21-25, 74, 80, 81, 82] are shown in Table 2. This mathematical model for Effective Number of Clonogens population during RT treatment planning time, [Fowler 1989- 2010], whose equation was detailed from [22, 82] reads:

$$N_{Effective} = N_0 \times 2^{\left[\frac{(T - T_{Del})}{T_{Pot}}\right]};$$

(1)

Where,

$N_{Effective}$: Number of tumor clonogens in function of RT treatment protocol time.

N_0: Initial Clonogens Number at starting RT time.

T: Total RT Treatment time.

T_{Delay}: Number of delay days after standard RT treatment time.

$T_{Potential}$: Potential Tumor Doubling Clonogens time.

Dataset for head and neck implemented into Eq.1 model is shown in Table 2. From this equation, the specialist scientific community began to apply Poisson Statistic-stochastic techniques.

HEAD AND NECK TUMORS CLONOGEN REPOPULATION DURING TREATMENT RT TIME MODEL DATASET FOR SIMULATIONS		
PARAMETER	**COMPUTATION INTERVAL**	**DETAILS**
HEAD AND NECK TUMOR N_0	[10^3 , 10^{11}] clonogens	This interval was selected from [22,80,81,83]
T Standard RT Time	Fixed days [22,46]	This interval was selected from [22,80], However it varies according to authors [25], depending on Conventional, Hiper or Hypo Fraccionated RT treatment time
T_{Delay}	Fixed days, when clonogens start mitosis	It was supposed weekends or hospital break days and unpredictable delays [80,81,83]
HEAD AND NECK TUMOR $T_{Potential}$	$T_{Potential}$ ϵ [5,6] days ; [80,81,83]	Head and Neck cancer in vivo data selected from [80,81,83]

Table 2.- Computational dataset from [19, 21-25, 74, 80, 81].

Linear Quadratic Mathematical Model for $N_{Effective}$ Implementation

Here the application of this $N_{Effective}$ model simulations on further Biomodels equations depending on N_0 and $N_{Effective}$ are explained. That set can be done into Linear Quadratic model, which is based usually on exponential functions, statistical distributions [Binomial or Poisson, 21-24,74], and two radiosensitivity key parameters, namely [α and β biological modelling parameters]. An Integral Equation Model (IEM), based on new Linear Quadratic Model and Statistical Binomial Distribution approximation was published in recent contributions [19, 74]. The simplest Linear Quadratic model equation set in [19, 74] reads:

Elementary Biological Model for clonogenes survival population N_S ;

$$N_S = N_0 \times e^{-[\alpha D + \beta D^2]} ;$$

(2)

where,

Ns: Initial number of tumor clonogens

No: Surviving number of tumor clonogens

a: Clonogen radiosensitivity parameter

β: Clonogen radiosensitivity parameter

D: Total radiation dose delivered

Parameters [a and β] are interrelated each other [β/a] and to N_0 magnitude. Parameter [a] is related to N_0 magnitude [22], although an average value is generally implemented. Both [a and β] measurements are taken *in vitro* [19, 21-25, 74]. Equation (1) is more complicated in practice for a number of constraints. Firstly, the dose D is hypofractionated in clinical practice [19, 21-25, 74]. Secondly, a Lea-Catcheside function-factor K [21], has to be introduced, although that factor is discussed. However, fractional dose factors, d, and number of fractions n, [21], are omitted in (1) for simplification, and are not relevant for the mathematical method development. In the standard BM research, [19, 21-25, 74], the quotient [σ/β] is generally considered constant. In this study, however, alpha and betha radiosensitive parameters are set independently. The reason is avoiding too many approximations. By using 100% percentages and 1% rates for $N_{0,\,Survival}$, the model can be better implemented in Statistical Distributions to obtain TCP formulation, with Poisson, Binomial, and Normal-Gaussian distributions. By using this modification [1, 74,], several numerical inconvenient are sorted. This variant, using percentages and rates of N_0 implies to make calculations setting parameters [a, mainly, and β] values in function of N_0, for example [66, 74]. Figure 1 in [74] shows an original logarithmic fitness numerical equation from these values [from 22 experimental data]. Thus, the modified BM equation reads:

Percentage and rate [% or 1%],

$$N_S\,[\%] = N_0\,[100\%] \times e^{-[\alpha D + \beta K D^2]};$$

or in rate,

$$N_S\,[1\%] = N_0\,[1\% = 1] \times e^{-[\alpha D + \beta K D^2]};$$

[Casesnoves 2022];

(3)

Where,

Ns: Initial number of tumor clonogens

No: Surviving number of tumor clonogens

a: Clonogen radiosensitivity parameter

β: Clonogen radiosensitivity parameter

D: Total radiation dose delivered

K: Lea-Catcheside function-factor K [21]

This approximation [19, 74] Equations (2-3), facilitates further calculations and improved models. However, setting percentages and/or rates for N_0 is conditioned for the magnitude changes of [a, β] related N_0 [22, 74, and 2D Logarithmic Figure 1 at 74].

3. Software-Engineering Programming Method

The programming method(s) applied for this research are based in a number of previous papers [1-20, 74]. For $N_{Effective}$ in Eq. 1 implementation 3D programs adjustments were required. Table 3 shows the 3D programming method variations to obtain acceptable better calculations, and 3D Graphical Optimization processing images, error determinations, and get applied exactly the $N_{Effective}$ model [Eq. 1 formulation].

.

$N_{Effective}$ MODEL MATLAB SOFTWARE METHOD(S)		
COMPUTATIONAL OBJECTIVE	**PROGRAMMING DEVELOPMENT**	**COMMENTS**
Implementation of experimental parameters for T_{Delay} , $T_{Potential}$,N_0	Precision required to get true simulations for head and neck tumors	Those parameters differ for every type of tumor
Optimization of implementation of $N_{Effective}$ for fast running time and imaging quality	Precision required to organize and optimize correct order, loops, patterns, and exactitude of every imaging processing subroutine	It is necessary to select the most appropriate subroutine, among several imaging processing sources for getting good 3D charts
Imaging processing refinement	Logarithmic scale changes were necessary because of the high numerical magnitude of some parameters	Several imaging processing solutions can be used.
Imaging processing matrices size optimization for final 3D plots	To get good-quality 3D model images it is necessary optimize, select, and order the best imaging-tiles matrices size combination linked to imaging processing tools	Not always bigger tiles number implies better imaging quality

Table 3.- $N_{Effective}$ model main parameters for 3D Graphical simulations [1-20, 74]. Program software parts numerically calculated for Equations 1-3. The data/method from Tables 2-3 was implemented.

4. 3D $N_{Effective}$ Model Imaging-Processing and Numerical Simulations Results

Figures 1-3 show 3D results for $N_{Effective}$ magnitudes in function of N_0 and RT head and neck cancer treatment extension time. Remark that implementation of $N_{Effective}$ 3D model and corrections for BED and Linear Quadratic optimal dose delivery magnitudes will be developed in upcoming contributions [84]. Figures 1-2 are set with axes-selected logarithmic scales. Figures 3-4 are intended to show the $N_{Effective}$ magnitude to be set in biological Linear Quadratic models [74]. Figure 4 was imaging-processed in grayscale and

box format to prove a sharp calculations perspective. Table 4 presents some maxima/minima numerical data. This software is difficult because it is necessary to compute correctly all the image matrices and avoid mistake possibilities.

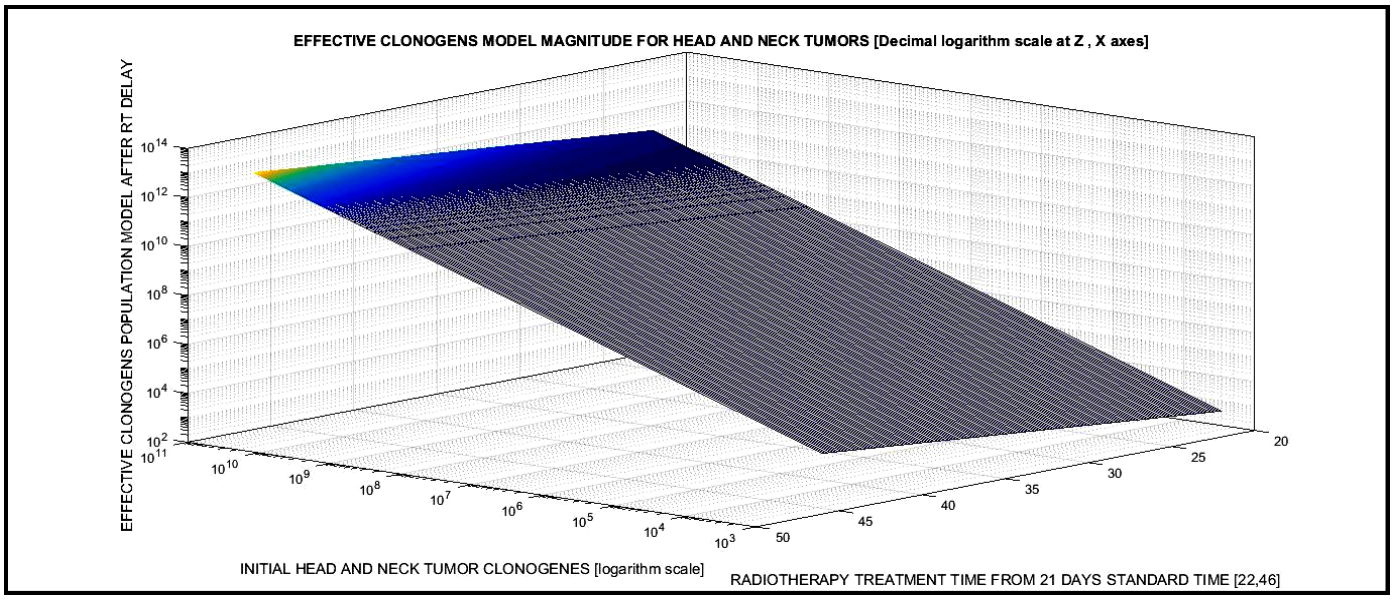

Figure 1.- Matlab $N_{Effective}$ Rate simulation 3D image for head and neck tumors. At Z, X axes, logarithmic scale. It is sharply seen that $N_{Effective}$ magnitude grows according to RT treatment delay time. Matrices for Image Processing have about [100-250 x 100-250] elements. At figure, inset, axes interval modifications explained. [Casesnoves Bioengineering Laboratory. Software. 45722].

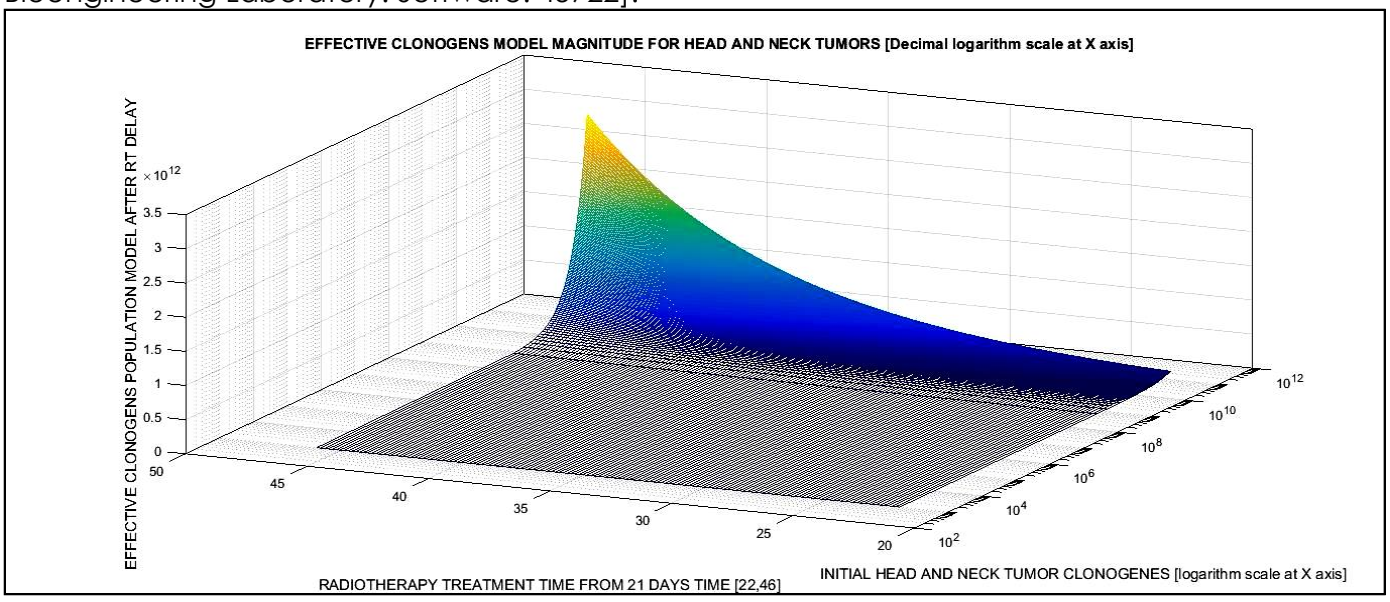

Figure 2.- Matlab $N_{Effective}$ Rate simulation 3D image for head and neck tumors. At X axis, logarithmic scale. It is sharply seen that $N_{Effective}$ magnitude grows according to RT treatment delay time. The image processing perpective was set to demonstrate the almost exponential/parabolic increase of $N_{Effective}$ magnitude from clonogenes population approximate value 10^8. The peak is better seen with this double logarithmic scale. Matrices for Image Processing have about [100-250 x 100-250] elements. At figure, inset, axes interval modifications explained. [Casesnoves Bioengineering Laboratory. Software. 45723].

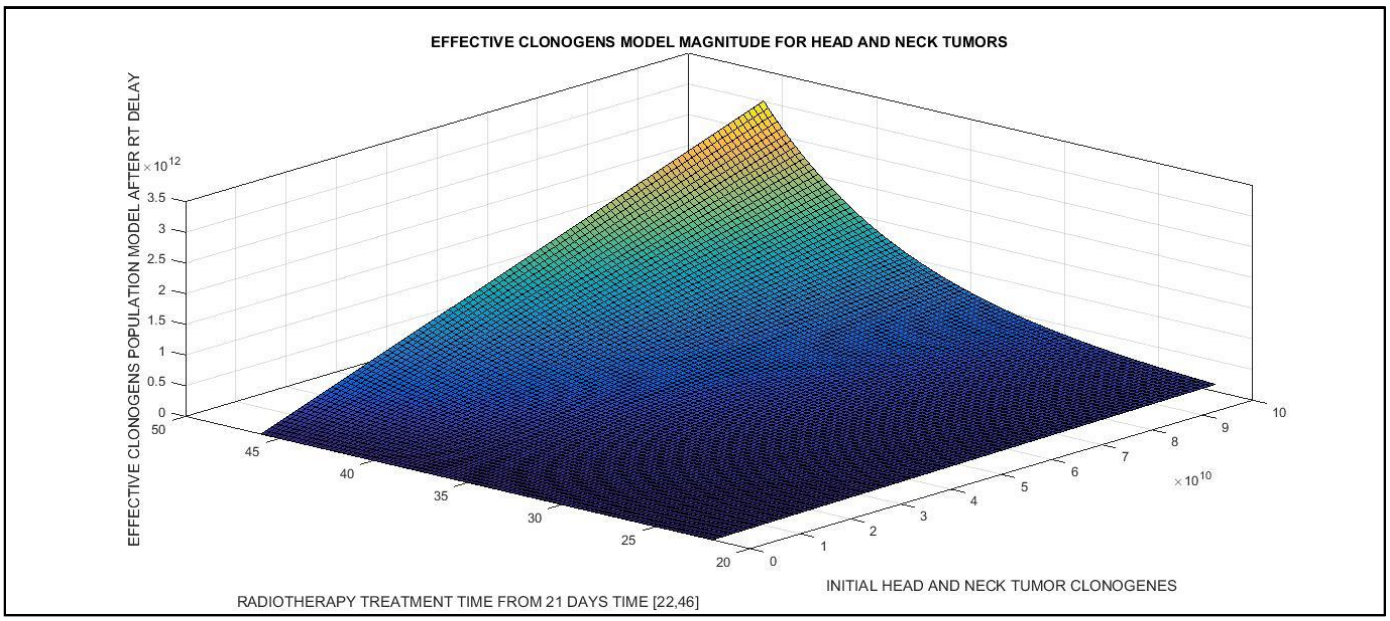

Figure 3.- Matlab $N_{Effective}$ Rate simulation 3D image for head and neck tumors. Image was set without any logarithmic scale. It is sharply seen that $N_{Effective}$ magnitude grows according to RT treatment delay time. The peak is better seen with this double logarithmic scale. Matrices for Image Processing have about [100-250 x 100-250] elements. At figure, inset, axes interval modifications explained. [Casesnoves Bioengineering Laboratory. Software. 45724].

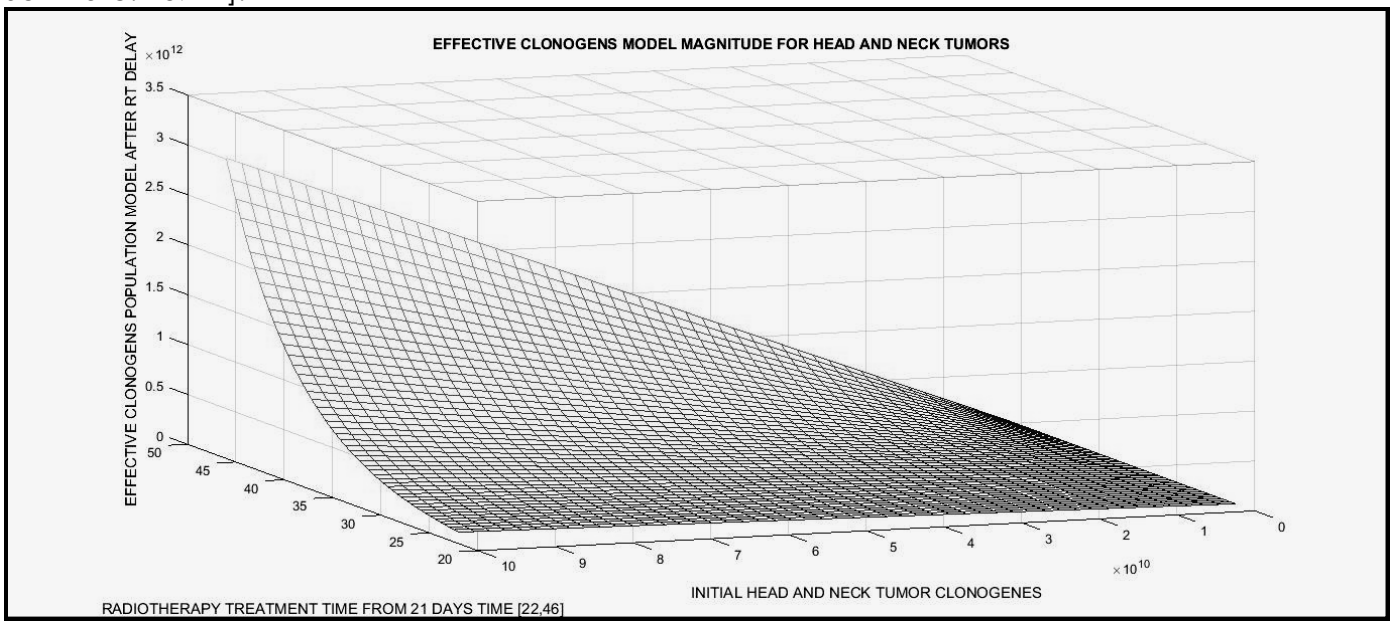

Figure 4.- Grayscale-processed with magnitude boxes Matlab $N_{Effective}$ Rate simulation. 3D image for head and neck tumors shown. Image was set without any logarithmic scale. It is sharply seen that $N_{Effective}$ magnitude grows according to RT treatment delay time. The grayscale image processing perpective was set to demonstrate the almost exponential/parabolic increase of $N_{Effective}$ magnitude from clonogenes population approximate value 10^8. The peak is better seen with this double logarithmic scale. Matrices for Image Processing have about [100-250 x 100-250] elements. At figure, inset, axes interval modifications explained. [Casesnoves Bioengineering Laboratory. Software. 45725].

NUMERICAL RESULTS FOR $N_{Effective}$ MODEL IN HEAD AND NECK TUMORS					
Minimum [N_0] Minimum [T_{Delay}]	Minimum [$N_{Effective}$] Minimum [T_{Delay}]	Maximum [N_0] Minimum [T_{Delay}]	Minimum [$N_{Effective}$] Maximum [T_{Delay}]	Maximum [N_0] Maximum [T_{Delay}]	Maximum [$N_{Effective}$] Maximum [T_{Delay}]
1000 1.49 days	1117 1.49 days	1.00×10^{11} 1.00 days	3.01×10^{4} 27-28 days	1.00×10^{11} 27-28 days	3.01×10^{12} 27-28 days

Table 4.- Some Maxima and Minima of Numerical results for model parameters. MATLAB 3D image processing data.

5. 3D Isodoses Applications for AAA Model TPO with Wedge Filters

Primary demonstration of new 3D Isodoses Treatment Planning System, [85], were published previously [84]. There are two 3D Isodoses types. Namely, Type 1 [Vertical 3D Isodoses], and Type 2 [Horizontal 3D Isodoses are presented] in contrast to classical 2D Isodoses. 3D Isodoses radiotherapy simulations software was detailed through the 3D graphics series engineering software [84]. Figures 4-5 show improved 3D Isodoses image processing for 18 Mev with [z= 5,15 cm] AAA model dose-deposition isocenter depths [1-20, 84].

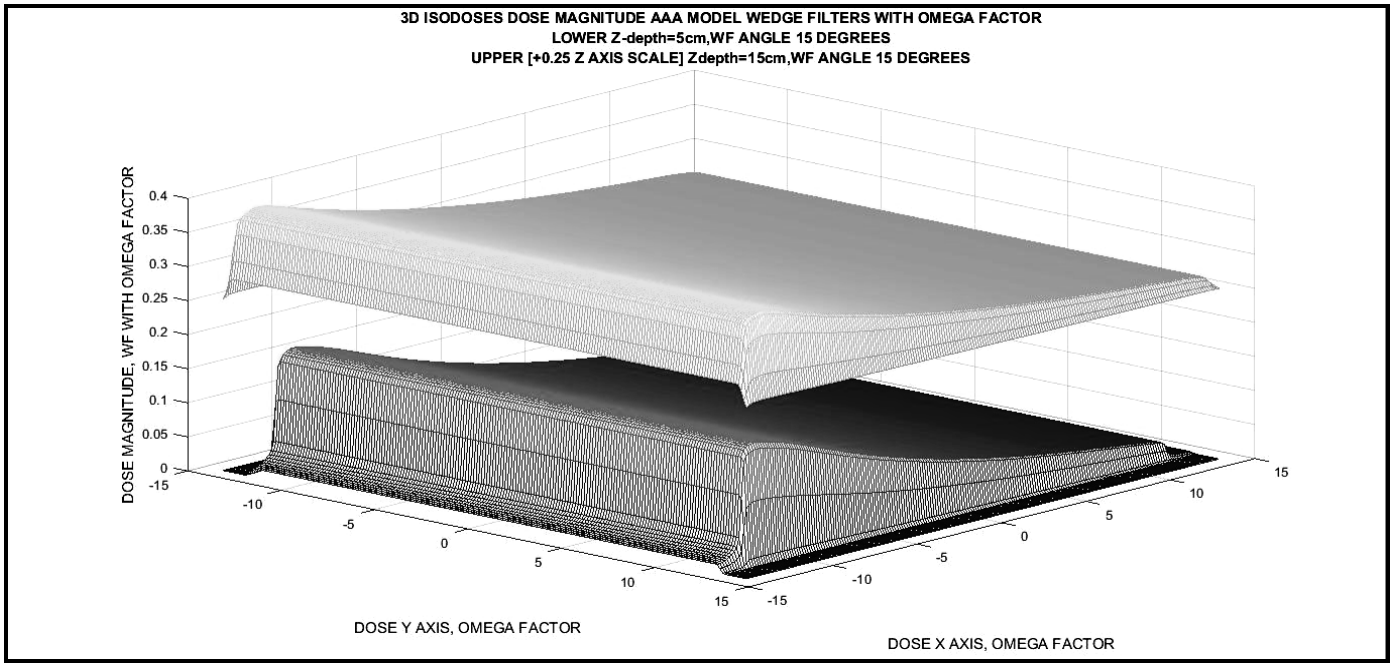

Figure 5.- A new perspective imaging-software developed from [84]. It is a Type I lateral-oblique imaging perspective of 3D Isodoses for z=5 cm [first], and z=15 cm [upper, scaled +0.25]. It is clear the height dose difference related to depth absorbed dose deposition.

This Type I lateral imaging perspective of 3D Isodoses for z=15 cm [upper, scaled +0.25], and z=5 cm [lower] demonstrate the utility and innovation [84], for TPO modern systems [85]. It is sharp the dose difference magnitudes that can be get related to depth absorbed dose deposition. Dosimetry calculations, TPO, and photon-dose approximations can be carried out with these 3D Isodoses charts. [Casesnoves Bioengineering Laboratory. Software. 45726].

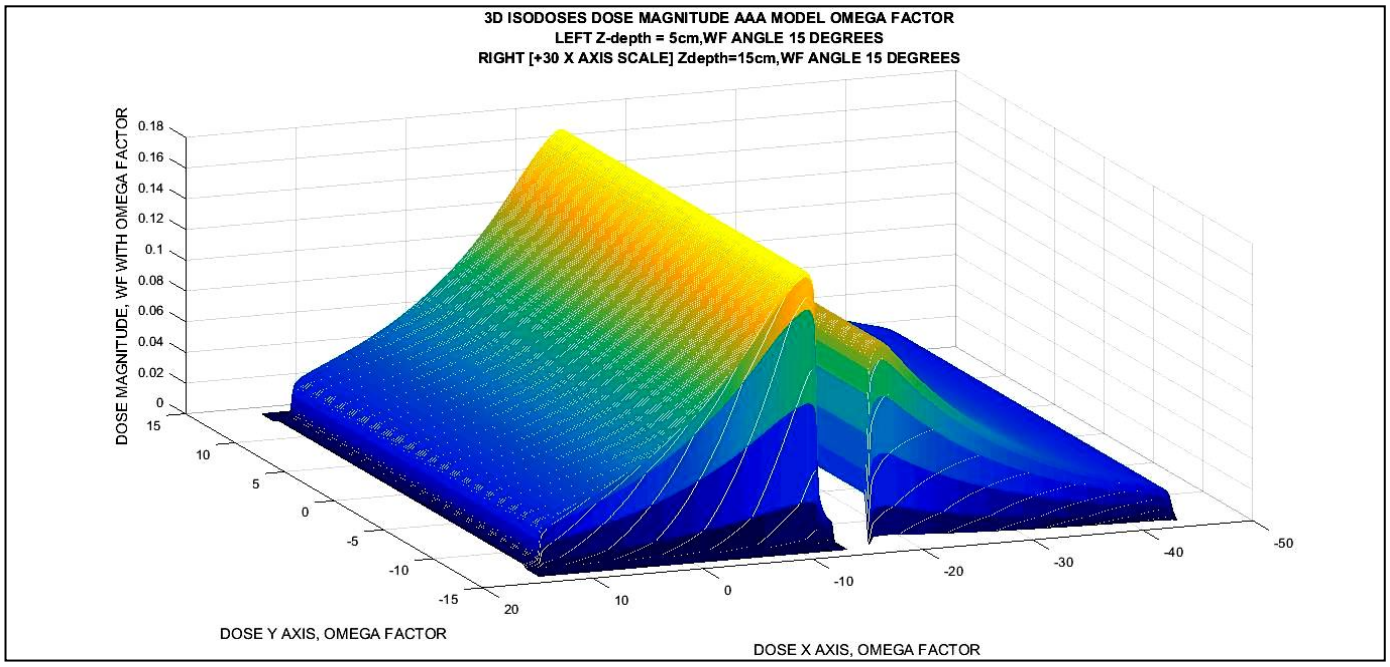

Figure 6.- A new perspective imaging-software developed from [84]. It is a Type II lateral imaging perspective of 3D Isodoses for z=5 cm [left], and z=15 cm [right, scaled +30]. It is clear the height dose difference related to depth absorbed dose deposition. [Casesnoves Bioengineering Laboratory. Software. 45727]

6. Radiotherapy Medical Physics Applications Briefing

Table 5 shows a resume of radiotherapy applications in head and neck tumors. Medical physics principal applications for radiotherapy TPO are explained concisely. Those prospective according to $N_{Effective}$ model applications are useful for radiotherapy research/applications on head and neck tumors and other types of cancer.

MODEL RESULTS APPLICATIONS FOR RADIOPROTECTION IN HEAD AND NECK TUMOR RT				
TYPE	**CLINICAL**	**RESEARCH**	**MIXED**	**COMMENTS**
BM Treatment planning optimization	TPO precise for head and neck tumors with BMs	TPO Modelling BMs developments according to $N_{Effective}$	Clinical improvements with BMs after research according to $N_{Effective}$	Inverse planning system set up on BMs according to $N_{Effective}$
LINAC OPTIMIZATION	Optimization of photon-dose for BMs	LINACs BMs Usage for IMRT, IMPT according to $N_{Effective}$	Exploration of new possibilities for $N_{Effective}$ models	Manufacturing adaptation of LINACs fro BMs according to $N_{Effective}$
Theoretical improvements for new models	Dosimetry improvements in accuracy according to radiobiology experimental $N_{Effective}$	From tumor survival clinical statistics advances in BMs according to $N_{Effective}$	According to $N_{Effective}$ new BMs research sources, both theory and clinical experimental trials	BMs got experimental evidences to be set on TPO according to $N_{Effective}$

Table 5.- Some radioprotection for RT head and neck cancer TPO Medical Physics study applications derived from results.

7. Discussion and Conclusions

3D $N_{Effective}$ clonogens population model simulations were presented as objective of the research, computationally designed for head and neck tumors [Fowler initial model, 82]. This implementation of $N_{Effective}$ 3D model and corrections are useful for BED and Linear Quadratic optimal dose delivery magnitudes that will be developed in upcoming contributions [84]. It was intended to set in software precise experimental constants [22, 81-84]. Therefore, 3D simulations could offer a realistic numerical image of $N_{Effective}$ clonogens population Fowler model for this type of cancer. Radiotherapy software improvements for new 3D Isodoses imaging processing results are detailed and shown in Figures 5-6.

Results comprise 3D Graphical Optimization imaging series, Figures 1-4, and some maxima/minima numerical dataset, Table 4. According to literature experimental parameters [22, 81-84], these 3D simulations can be considered acceptable. TPO applications for head and neck tumors are shown in Table 5. Results in improved imaging 3D Isodoses charts in AAA dose-delivery with WF are presented in Figures 5-6.

Advantages of this model are accuracy in 3D determination of N_S and easy method from the presented models to calculate Clonogenes Survival Rates for head and neck tumors, getting improved radiotherapy TPO. Inconvenients, for example, are the experimental validation of the model, Eq. 1, for large-scale clinical trials in head and neck cancers. Advantages of 3D Isodoses planning system images are extensive in TPO calculations and modern imaging-guided RT treatment.

In brief, $N_{Effcetive}$ algorithms were implemented to refine the $N_{Survival}$ magnitude determination to be set in BMs. The consequence is an improved radiation therapy treatment for head and neck RT oncology. Applications on 3D Isodose charts for AAA model TPO with WF in radiation therapy were upgraded and shown.

8. References and Further Reading

[Note: it is recommended for researchers to not restrict the search on Fowler models since the literature with models and variants is profuse]

[1] Casesnoves, F. 2022. Radiotherapy Wedge Filter AAA Model 18 Mev- Dose Delivery 3D Simulations with Several Software Systems for Medical Physics Applications. Applications. Biomedical Journal of Scientific and Technical Research, 40(5).
[2] Casesnoves, F. 2016. Mathematical Exact 3D Integral Equation Determination for Radiotherapy Wedge Filter Convolution Factor with Algorithms and Numerical Simulations. Journal of Numerical Analysis and Applied Mathematics, 1(2):39-59.
[3] Casesnoves, F. 2015. Radiotherapy Conformal Wedge Computational Simulations, Optimization Algorithms, and Exact Limit Angle Approach. International Journal of Scientific Research in Science, Engineering and Technology (IJSRSET), 1(2):353-362.
[4] Casesnoves, F. 2019. Improvements in Simulations for Radiotherapy Wedge Filter dose and AAA-Convolution Factor Algorithms. International Journal of Scientific Research in Science, Engineering and Technology (IJSRSET), 6(4):194-219.
[5] Casesnoves, F. 2011. Exact/Approximated Geometrical Determinations of IMRT Photon Pencil-Beam Path Through Alloy Static Wedges in Radiotherapy Using Anisothropic Analytic Algorithm (AAA). Peer-reviewed ASME Conference Paper. ASME 2011 International Mechanical Engineering Congress. Denver. USA. IMECE2011-65435.
[6] Casesnoves, F. 2012. Geometrical Determinations of Limit angle (LA) related to maximum Pencil-Beam Divergence Angle in Radiotherapy Wedges. Peer-reviewed ASME Conference Paper. ASME 2012 International Mechanical Engineering Congress. Houston. USA. IMECE2012-86638.
[7] Casesnoves, F. 2013. A Conformal Radiotherapy Wedge Filter Design. Computational and Mathematical Model/Simulation' Casesnoves, F. Peer-Reviewed Poster IEEE (Institute for Electrical and Electronics Engineers), Northeast Bioengineering Conference. Syracuse New York, USA. April 6th, 2013. Peer-Reviewed Poster Session on 6th April 2013. Sessions 1 and 3 with Poster Number 35. Page 15 of Conference Booklet.
[8] Casesnoves, F. 2014. Mathematical and Geometrical Formulation/Analysis for Beam Limit Divergence Angle in Radiotherapy Wedges. Peer-Reviewed International Engineering Article. International Journal of Engineering and Innovative Technology (IJEIT), 3(7).
[9] Casesnoves, F. 2014. Geometrical Determinations of IMRT Photon Pencil-beam Path in Radiotherapy Wedges and Limit Divergence Angle with the Anisotropic Analytic Algorithm (AAA)

Casesnoves, F. Peer- Reviewed scientific paper, both Print and online. International Journal of Cancer Therapy and Oncology, 2(3):02031.
[10] Casesnoves, F. 2014. Radiotherapy Conformal Wedge Computational Simulations and Nonlinear Optimization Algorithms. Peer-reviewed Article, Special Double-Blind Peer-reviewed paper by International Scientific Board with contributed talk. Official Proceedings of Bio- and Medical Informatics and Cybernetics: BMIC 2014 in the context of the 18th Multi-conference on Systemics, Cybernetics and Informatics: WMSCI 2014 July 15 - 18, 2014, Orlando, Florida, USA.
[11] Casesnoves, F. 2007. Large-Scale Matlab Optimization Toolbox (MOT) Computing Methods in Radiotherapy Inverse Treatment Planning'. High Performance Computing Meeting. Nottingham University.
[12] Casesnoves, F. 2008. A Computational Radiotherapy Optimization Method for Inverse Planning with Static Wedges. High Performance Computing Conference. Nottingham University.
[13] Casesnoves, F. 2015. Radiotherapy Conformal Wedge Computational Simulations, Optimization Algorithms, and Exact Limit Angle Approach. International Journal of Scientific Research in Science, Engineering and Technology (IJSRSET), 1(2):353-362.
[14] Casesnoves, F. 2015. Radiotherapy Standard/Conformal Wedge IMRT-Beamlet Divergence Angle Limit Exact Method, Mathematical Formulation, and Bioengineering Applications. International Article- Poster. Published in Proceedings of Conference. 41st Annual Northeast Bioengineering Conference. Rensselaer Polytechnic Institute. Troy, New York USA, April, p. 17-19.
[15] Casesnoves, F. 2015. Radiotherapy Standard/Conformal Wedge IMRT-Beamlet Divergence Angle Limit Exact Method, Mathematical Formulation, and Bioengineering Applications. IEEE (Institute for Electrical and Electronics Engineers), International Article-Poster.
[16] Casesnoves, F. 2015. Abstract-Journal. 'Radiotherapy Standard/ Conformal Wedge IMRT-Beamlet Divergence Angle Limit Exact Method, Mathematical Formulation. International Conference on Significant Advances in Biomedical Engineering. 252nd OMICS International Conference, 5(1).
[17] Casesnoves, F. 2001. Determination of Absorbed Doses in Common Radio Diagnostic Explorations. 5th National Meeting of Medical Physics. Madrid, Spain. September 1985. treatment Planning'. Kuopio University. Radiotherapy Department of Kuopio University Hospital and Radiotherapy Physics Group. Finland.
[18] Casesnoves, F. 2001. Master Thesis in Medical Physics. Eastern Finland University. Radiotherapy Department of Kuopio University Hospital and Radiotherapy Physics Grouversity-Kuopio. Defense approved in 2001. Library of Eastern finland University. Finland.
[19] Casesnoves, F. 2013. A Conformal Radiotherapy Wedge Filter Design. Computational and Mathematical Model/Simulation' Casesnoves, F. Peer-Reviewed Poster IEEE (Institute for Electrical and Electronics Engineers), Northeast Bioengineering Conference. Syracuse New York, USA. April 6th, 2013. Peer-Reviewed Poster Session on 6th April 2013. Sessions 1 and 3 with Poster Number 35. Page 15 of Conference Booklet.
[20] Casesnoves, F. 2022. Radiotherapy Biological Tumor Control Probability Integral Equation Model with Analytic Determination. International Journal of Mathematics and Computer Research, 10(8):2840-2846.
[21] Casesnoves, F. 2022. Radiotherapy Wedge Filter AAA Model 3D Simulations For 18 Mev 5 cm-Depth Dose with Medical Physics Applications", International Journal of Scientific Research in Computer Science, Engineering and Information Technology (IJSRCSEIT), 8(1):261-274.
[22] Walsh, S. 2011. Radiobiological modelling in Radiation Oncology. PhD Thesis. School of Physics. National University of Galway.
[23] Chapman, D., Nahum, A. 2015. Radiotherapy Treatment Planning, Linear- Quadratic Radiobiology. CRC Press.
[24] Mayles, W., Nahum, A. 2015. Rosenwald, J. Editors. Handbook of Radiotherapy Physics. Second Edition. CRC Press.
[25] Nahum, A., Webb, S. 1993. A Model for Calculating Tumour Control Probability in Radiotherapy Including the Effects of Inhomogeneous Distributions of Dose and Clonogenic Cell Density. Physics in Medicine and Biology; v. 38(6); p. 653-666.
[26] Haydaroglu, A., Ozyigit, G. 2013. Principles and Practice of Modern Radiotherapy Techniques in Breast Cancer. Springer.

[27] Casesnoves, F. 2019-20. Die numerische Reuleaux-Methode Rechnerische und dynamische Grundlagen mit Anwendungen (Erster Teil). ISBN-13: 978-620-0-89560-8, ISBN-10: 6200895600. Publishing House: Sciencia Scripts. 2019-20.
[28] Ulmer W., Harder, D. 1997. Corrected Tables of the Area Integral I(z) for the Triple Gaussian Pencil Beam Model. Journal of Medical Physics, 7:192-193.
[29] Ulmer, W., Harder, D. 1995. A Triple Gaussian Pencil Beam Model for Photon Beam Treatment Planning. Medical Physics, 5:25-30.
[30] Ulmer, W., Harder, D. 1996. Applications of a Triple Gaussian Pencil Beam Model for Photon Beam Treatment Planning. Medical Physics, 6:68-74.
[31] Ma, C., Lomax, T. 2013. Proton and Carbon Ion Therapy. CRC Press.
[32] Censor, Y., Zenios, S.A. 1997. Parallel Optimization: Theory, Algorithms and Applications'. UOP.
[33] Ulmer, W., Pyyry, J., Kaissl, W. 2005. A 3D Photon Superposition/ Convolution Algorithm and Its Foundation on Results of Monte Carlo Calculations. Physics in Medicine and Biology, p. 50.
[34] Ulmer, W., Harder, D. 1997. Applications of the Triple Gaussian Photon Pencil Beam Model to Irregular Fields, Dynamical Collimators and Circular Fields. Physics in Medicine and Biology.
[35] Haddad, K., Anjak, O., Yousef, B. 2019. Neutron and High Energy Photon Fluence Estimation in CLINAC using Gold Activation Foils. Reports of Practical Oncology and Radiotherapy, 24:41-46.
[36] Sievinen, J., Waldemar, U., Kaissl, W. AAA Photon Dose Calculation Model in Eclipse™. Varian Medical Systems Report. Rad #7170A.
[37] Vagena, E., Stoulos, S., Manolopoulou, M. 2016. GEANT4 Simulations on Medical LINAC Operation at 18MV: Experimental Validation based on Activation Foils. Radiation Physics and Chemistry.
[38] Ethics for Researchers. 2013. EU Commission. Directorate-General for Research and Innovation. Science in society/Capacities FP7.
[39] Casesnoves, F. 1981. Surgical Pathology I Course Class Notes and Clinical Practice of Surgical Pathology Madrid Clinical Hospital [Professor Surgeon Dr Santiago Tamames Escobar]. 4th academic year course for graduation in Medicine and Surgery. Lessons and practice Breast Cancer Surgical and Medical Treatment. 1980-1981. Madrid Complutense University.
[40] Tamames., Escobar, S. 2000. Cirugia/ Surgery: Aparato Digestivo. Aparato Circulatorio. Aparato Respiratorio/ Digestive System. Circulatory System. Respiratory System (Spanish Edition).
[41] Silvia, C., Formenti, S.D. 2013. Combining Radiotherapy and Cancer Immunotherapy: A Paradigm Shift Silvia C. Formenti, Sandra Demaria. Journal of the National Cancer Institute, 105:256-265.
[42] Numrich, R.W. 2010. The Computational Energy Spectrum of a Program as it Executes. Journal of Supercomputing, 52.
[43] European Commission, Directorate-General for Research. 2021. Unit L3. Governance and Ethics. European Research Area. Science and Society.
[44] ALLEA. 2017. The European Code of Conduct for Research Integrity, Revised Edn.; ALLEA: Berlin Barndenburg Academy of Sciences.
[45] Good Research Practice. 2017. Swedish Research Council.
[46] Ulmer, W., Schaffner, B. 2011. Foundation of an Analytical Proton Beamlet Model for Inclusion in a General Proton Dose Calculation System. Radiation Physics and Chemistry, 80:378-389.
[47] Sharma, S.C. 2008. Beam Modification Devices in Radiotherapy. Lecture at Radiotherapy Department, PGIMER. India.
[48] Barrett, A.C. 2009. Practical Radiotherapy Planning. Fourth Edition. Hodder Arnold.
[49] Ahnesjö, A., Saxner, M., Trepp, A. 1992. A Pencil Beam Model for Photon Dose Calculations. Medical Physics, pp. 263-273.
[50] Brahime, A. 2000. Development of Radiation Therapy Optimization. Acta Oncologica, 39(5).
[51] Bortfeld, T., Hong, T., Craft, D., Carlsson, F. 2008. Multicriteria Optimization in Intensity-Modulated Radiation Therapy Treatment Planning for Locally Advanced Cancer of the Pancreatic Head. International Journal of Radiation Oncology and Biology Physics, 72(4).
[52] Brown, Bernardette, and all members of Research Group. 2014. Clinician-led Improvement in Cancer Care (CLICC) - Testing a Multifaceted Implementation Strategy to Increase Evidence-Based Prostate Cancer Care: Phased Randomised Controlled Trial - Study Protocol. Implementation Science, 9:64.

[53] Bortifield, T. 2006. IMRT: A Review and Preview. Physics in Medicine and Biology, 51(2006):R363–R379.
[54] Censor, Y. 2005. Mathematical Optimization for the Inverse Problem of Intensity-Modulated Radiation Therapy. Laboratory Report, Department of Mathematics, University of Haifa, Israel.
[55] Capizzello, A., Tsekeris, P.G., Pakos, E.E., Papathanasopoulou, V., Pitouli, E.J. 2006. 'Adjuvant Chemo-Radiotherapy in Patients with Gastric Cancer. Indian Journal of Cancer, 43(4).
[56] Dawod, T., Abdelrazek, E.M., Elnaggar, M., Omar, R. 2014. Dose Validation of Physical Wedged symmetric Fields in Artiste Linear Accelerator. International Journal of Medical Physics, Clinical Engineering and Radiation Oncology, 3:201-209.
[57] Do, S.Y, David, A., Bush, J.D.S. 2010. Comorbidity-Adjusted Survival in Early-Stage Lung Cancer Patients Treated with Hypofractioned Proton Therapy. Journal of Oncology.
[58] Ehrgott, M., & Burjony, M. 2001. Radiation Therapy Planning by Multicriteria Optimization. In Proceedings of the 36th Annual Conference of the Operational Research Society of New Zealand (Vol. 244, p. 253).
[59] Ezzel, G.A. 1996. Genetic and Geometric Optimization of Three-dimensional Radiation Therapy Treatment Planning. Medical Physics, 23:293- 305.
[60] Effective Health Care, 2008. Number 13. Comparative Efectiveness of Therapies for Clinically Localized Prostate Cancer. Bookshelf ID: NBK554842.
[61] Hansen, P. 1998. Rank-deficient and Discrete Ill-posed Problems: Numerical Aspects of Linear Inversion'. SIAM Monographs on Mathematical Modelling and Computation.
[62] Hashemiparast, S.M., Fallahgoul, H. 2011. Modified Gauss Quadrature for Ill-posed Integral Transform. International Journal of Mathematics and Computation, 13(11).
[63] Isa, N. 2014. Evidence Based Radiation Oncology with Existing Technology. Reports of Practical Oncology and Radiotherapy, 19:259-266.
[64] Johansson, K.A., Mattsson, S., Brahme, A., Turesson, I. 2003. Radiation Therapy Dose Delivery'. Acta Oncologica, 42(2):2003.
[65] Khanna, P., Blais, N., Gaudreau, P.O., Corrales-Rodriguez, L. 2016. Immunotherapy Comes of Age in Lung Cancer, Clinical Lung Cancer.
[66] Küfer, K. H., Hamacher, H. W., & Bortfeld, T. 2001. A Multicriteria Optimization Approach for Inverse Radiotherapy Planning. In Operations Research Proceedings: Selected Papers of the Symposium on Operations Research (OR 2000) Dresden, September 9–12, 2000 (pp. 3-7). Springer Berlin Heidelberg.
[67] Kirsch, A. 1996. An introduction to the Mathematical Theory of Inverse Problems. Springer Applied Mathematical Sciences.
[68] Luenberger, D.G. 1989. Linear and Nonlinear Programming (2nd Edn.)., Addison-Wesley.
[69] Moczko, J.A., Roszak, A. 2006. Application of Mathematical Modeling in Survival Time Prediction for Females with Advanced Cervical cancer treated Radio-chemotherapy. Computational Methods in Science and Technology, 12(2).
[70] Ragaz, J., Olivotto, I. A., Spinelli, J. J., Phillips, N., Jackson, S. M., Wilson, K. S., ... & Manji, M. 2005. Loco-regional Radiation Therapy in Patients with High-risk Breast Cancer Receiving Adjuvant Chemotherapy: 20-Year Results of the Columbia Randomized Trial'. Journal of National Cancer Institute, 97(2):116-126.
[71] Steuer, R. 1986. Multiple Criteria Optimization: Theory, Computation and Application. Wiley.
[72] Spirou, S.V, Chui, C.S. 1998. A Gradient Inverse Planning Algorithm with Dose-Volume Constraints. Medical Physics, 25: 321-323.
[73] Das, I.J, Colls. 1997. Patterns of Dose Variability in Radiation Prescription of Breast Cancer. Radiotherapy and Oncology, 44: 83-89.
[74] Casesnoves, F. 2018. Practical Radiotherapy TPO Course with Cyberknife. Robotic Simulations for Breathing Movements during Radiotherapy Treatment. Sigulda Radiotherapy Cyberknife Center. Latvia. Riga Technical University Bioengineering Training-Course Nonlinear Life.
[75] Casesnoves, F. 2022. Radiotherapy Linear Quadratic Bio Model 3D Wedge Filter Dose Simulations for AAA Photon-Model [18 Mev, Z=5,15 cm] with Mathematical Method System. Biomedical Journal of Scientific and Technical Research, 46(2).
[76] Casesnoves, F. 1985. Master in Philosophy Thesis at Medical Physics Department. Protection of the Patient in Routinary Radiological Explorations. Experimental Low Energies RX Dosimetry. Medicine Faculty. Madrid Complutense University. 1984-85.

[77] Casesnoves, F. 1983-5. Ionization Chamber Low Energies Experimental Measurements for M-640 General Electric RX Tube with Radcheck ionization camera, Radcheck Beam Kilovoltimeter and TLD dosimeters. Radiology Department practice and measurements. Madrid Central Defense Hospital. Medical Physics Department. Master in Philosophy Thesis. Medicine Faculty. Complutense University. Madrid.
[78] Casesnoves, F. 1985. Determination of Absorbed Doses in Routinary Radiological Explorations. Medical Physics Conference organized by Medical Physics Society Proceedings Printed. San Lorenzo del Escorial. Madrid. September 1985.
[79] Greening, J. 1985. Fundamentals of Radiation Dosimetry. Taylor and Francis. Second Edition. 1985.
[80] International Commission of Radiation Protection. 1977. Bulletin 26th. The International Commission on Radiological Protection. Recommendations of the International Commission on Radiological Protection. Pergamon Press.
[81] Stanton, P., Colls. 1996. Cell Kinetics in vivo of Human Breast Cancer. British Journal of Surgery, 83:98-102.
[82] Hedman, M., Björk-Eriksson, T., Brodin, O., & Toma-Dasu, I. 2013. Predictive Value of Modelled Tumour Control Probability based on Individual Measurements of in vitro Radiosensitivity and Potential Doubling Time. The British Journal of Radiology, 86(1025):20130015.
[83] Fowler, J. 2010. 21 Years of Biologically Effective Dose. The British Journal of Radiology, 83: 554–568.
[84] Marcu, L. G., Toma-Dasu, I., Dasu, A., & Mercke, C. 2018. Radiotherapy and Clinical Radiobiology of Head and Neck Cancer. CRC Press.
[85] Casesnoves, F. 2022. Radiotherapy 3D Isodose Simulations for Wedge Filter 18 MEV-DOSE [z= 5, 15 cm] with AAA Model with Breast Cancer Applications. International Journal on Research Methodologies in Physics and Chemistry, 9(2):08-17.
[86] Garden, A., Beadle, B., Gunn, G. 2018. Radiotherapy for Head and Neck Cancers. Fifth Edition. Wolters Kluwer.
[87] Casesnoves, F. 2023. Radiotherapy Genetic Algorithm Pareto-Multiobjective Optimization of Biological Efective Dose and Clonogens Models for Head and Neck Tumor Advanced Treatment. International Journal of Mathematics and Computer Research, 11(01):3156-3177.
[88] Casesnoves, F. 2023. Radiotherapy Effective Clonogens Model Graphical Optimization Approaching Linear Quadratic Method for Head and Neck Tumors. International Journal of Molecular Biology and Biochemistry, 5(1):33-40.

5. FORMULATION BRIEFING AND BASIC ALGORITHMS FORMULATION WITH AAA MODEL BEAM MODIFICATION WEDGE FILTERS

AAA Model Example of Omega Factor Correction for Wedge Filters Dose Delivery

The most important mathematical development for AAA model was the Omega Factor. This algorithm elevates to 3D the dose delivery calculation for wedge filters. The large mathematical innovation can be found along all Author's References in all chapters. Algorithm 1 shows the main result.

$$
\begin{aligned}
&D(x,y,z)=\frac{I(z)\,A\,\Phi_0}{4(1+z/F)^2}\,x\sum_{K=1}^{K=3} e^{\left[\sigma_K'(z)S^2-2Sx\right]}\ldots x\\
&\ldots x\left[\left[Erf\left(\frac{y+b'}{\sigma_K(z)}\right)\right]-\left[Erf\left(\frac{y-b'}{\sigma_K(z)}\right)\right]\right]\ldots x\\
&\ldots x\left[\left[Erf\left(\frac{x+a'+\sigma_K^2(z)S^2}{\sigma_K(z)}\right)\right]-\left[Erf\left(\frac{x-a'-\sigma_K^2(z)S^2}{\sigma_K(z)}\right)\right]\right];\\
&\text{where } S=S\left([\Omega]_F\right), \text{ and } A=A\left([\Omega]_F\right);\\
&A\left([\Omega]_F\right)=x\,e^{\left[-\mu_w x\left[L\,x\left(\frac{\sin\alpha}{\cos(\alpha+\phi)}\right)\right]\right]x[[\Omega]_F]};\\
&S\left([\Omega]_F\right)=x\,e^{\left[-\mu_w x\left[\pm\frac{Cu}{F+z}x\left(\frac{\sin\alpha}{\cos(\alpha+\phi)}\right)\right]\right]x[[\Omega]_F]};\\
&[\Omega]_F=\left[1+\frac{\tan^2\phi_2}{1+\tan^2\phi_1}\right]^{\frac{1}{2}};
\end{aligned}
\qquad (1)
$$

Algorithm 1 for Omega Factor in AAA model. It is recommended consultation of all Sections references about AAA model and AAA Omega Factor if the reader wants to see all large mathematical development.

Evolutionary Algorithms Mathematical Method

The GA algorithms used are approximately the same than in previous prostate cancer publication [98]. The sequence of the formula's development is as follows:

$$\begin{aligned}&\text{Minimize,}\\&F(\vec{x})=(f_1(\vec{x}),f_2(\vec{x}),....f_N(\vec{x})),\\&\text{subject to,}\\&K_i(\vec{x})\geq 0\text{ , for } i=1,.....M\end{aligned}$$

(Algorithm 1.1)

Where,

F (x): Main function to be optimized.

f_i (x): Every function of same variables (x).

K_i (x): Constraints functions such as in general N ≠ M.

BED nonlinear-quadratic model has been adapted for *in vivo* parameter T_{Pot} magnitude. Then, PMO in Prostate, [24, 88, 89, 98] tumors simplest BED model reads:

$$\begin{aligned}&\text{Chebyshev}\quad L_1\text{ Optimization,}\\&\text{for}\quad i=1,2...\text{minimize pareto,}\\&\left|DOSE_i-BED_{Effective}\right|_{L_1}\text{ with,}\\&BED_{Effective}=k\times d\times\left[1+\frac{d\times\beta}{\alpha}\right]-...\\&...-\frac{Ln(2)}{\alpha}\times\left[\frac{T_{Treatment}-T_{Delay}}{T_{Potential}}\right];\end{aligned}$$

(Algorithm 2)

where,

BED: The basic algorithm for Biological Effective Dose initially developed by Fowler et al. [22-25, 89-94, 98].

k: Optimal Number of fractions for hyperfractionated TPO. Optimization parameter [22-25, 89-94, 98].

d: Optimal Dose magnitude for every fraction. Optimization Parameter [Gy] [22-25, 89-94].

a: The basic algorithm constant for Biological Effective Dose models. Radiobiological experimental parameter *in vivo*. [Gy^{-1}] [22-25, 89-94].

β: The basic algorithm constant for Biological Effective Dose models *in vivo*. Radiobiological experimental parameter [Gy^{-2}]. Note that it is very usual to set in biological models [α/β in Gy].

$T_{Treatment}$: The overall TPO time. This parameter varies according to authors' and institutions/hospitals criteria [22-25, 89-94, 98].

T_{Delay}: The overall TPO time delay for clonogens re-activation. This parameter varies according to authors' experimental research.

$T_{Potential}$: The potential time delay for tumor cell duplication. This parameter varies according to authors' experimental-theoretical research.

DOSE: The dose magnitudes for lung cancer simulation algorithm for Biological Effective Dose [22-25, 89-94, 98]. Software patterns were calculated around intervals prostate DOSE ϵ [70, 78] Gy.

Algorithm 1 [Fowler mainly, modified by Casesnoves, 98]. -Prostate PMO algorithm [1-25, 85-90] implemented in software. Table 2 shows these intervals for optimization parameters details. Programming was developed in MATLAB® system. At programming trials, it was found that precision was increased related to *in vitro* parameters [98]. The constraints algebraic algorithm developed for Pareto-Multiobjective problem, [Algorithms-3-5, 85] reads:

$$\text{Constraints,}$$
$$\text{For Pareto Functions} \quad i = 1, 2,$$
$$\text{and lower} - \text{upper limits of}$$
$$\text{optimization parameters,}$$
$$S_{Lower} \le K_i + d_i + T_{(Treatment)i} \le S_{Upper} \ ,$$

(Algorithm 3)

where

S_{LOWER}: Summatory of all lower constraints for parameters [K, d, T].

S_{UPPER}: Summatory of all upper constraints for parameters [K, d, T].

K_i: Dose fraction number parameter for [i = 1, 2].

d_i: Dose fraction magnitude parameter for [i = 1, 2].

$T_{TREATMENT}$: Treatment time magnitude parameter for [i = 1, 2].

The subroutines programming strategy, as in [98], which are implemented reads:

$$\text{Matrix Algebra Subroutines}$$
$$\text{For Constraints,}$$
$$[A_1] \times \begin{pmatrix} K \\ d \\ T \end{pmatrix} \le \begin{pmatrix} S_{K\max} \\ d_{d\max} \\ T_{T\max} \end{pmatrix},$$
$$[A_2] \times \begin{pmatrix} K \\ d \\ T \end{pmatrix} \ge \begin{pmatrix} S_{K\min} \\ d_{d\min} \\ T_{T\min} \end{pmatrix},$$

(Algorithm 4)

where,

$S_{K,d,T}$: Upper (maximum) and Lower boundaries for parameters [K, d, T], according to Algorithms 1-2.

$A_{1,2}$: Matrices for numerical values, Table 2.

Sofware used for this study continues previous algorithms papers [1-20, 24, 68, 74, 88, 89, 98] with modifications, and addition of IO programs. For GA-PMO modeling, Equation 1 and Algorithms 1-4 are implemented on 2D programs, with application of Algorithm 5 basic model formula. Algorithm 2 was programmed with Algorithm 3 matrix constraints subroutines-functions. Table 2 shows Constrained GA Optimization *in vivo* parameters, different from [98], implemented in Algorithms 1-5. From Table 3 results, after IO implementation, 3D IO dataset for Table 4 is got. From all these numbers, 3D IO and 2D Genetic Algorithms Graphical Optimization imaging-processing charts, error determinations, pareto-distance, get precise approximations for hyperfractionated PMO-BED model. In general, precision obtained is more than expected, Tables 3-4.

Mathematics of the Tissue-Repair Formulation Factor for Survival Fraction Equations [104-106]

The tissue-repair cells growth during hyperfractionated long-time RT-treatment has been discussed by several authors [104-106]. It involves the implementation of a so-called T Factor (in literature notation is G, [104-106]) within the Survival Fraction classical model, or within the quadratic part of BED basic equation. Attempted models do not demonstrate, *de facto*, complete agreement between BED classical model theoretical calculations and experimental measurements [104-106]. This new complementary sub-section presents/details the recent formulas to overcome this model relative numerical inconsistency according to some literature sources [104-106]. In literature, some kind of diatribe *in favor* and *against* [104-106], of these different correction factors implementation within BED fundamental equation remains.

Usually, the RT algorithms are automatically set in planning system commercial apparatus, and the manufacturers select models according to their TPO requirements for screen-selection of parameters. Therefore, a multiple variants of correction factors are available in the literature based on theoretical developments and their experimental validation.

Here T-Factor-Formula for Mu model is shown, because that T-Factor model is corroborated by other authors in terms of agreements between survival fraction

experimental and theoretical obtained database [104-106]. Additionally, the formulation of this MU model involves less mathematical framework than Keall and Brenner models [104-106]. Therefore, this short examination is centered in explaining some of these models with short discussion. Namely,

The most simple standard Survival Fraction equation reads,

$$SF = e^{\left[-\alpha D-\beta D^2\right]};$$

where,

SF : Tumoral cells survival fraction (adimensional) .

D : Dose magnitude, either total or for every fraction. [Gy]. [22-25, 89-94].

α : The basic algorithm constant for Biological Effective Dose models. Radiobiological experimental parameter in vivo. [Gy^{-1}]. [22-25, 89-94].

β : The basic algorithm constant for Biological Effective Dose models in vivo. Radiobiological experimental parameter . [Gy^{-2}]. Note that it is very usual to set in biological models [α / β in Gy].

(1)

The standard Survival Fraction corrected equation reads,

$$SF = e^{\left[-\alpha D-T\,\beta D^2\right]};$$

were,

T : Tissue Repair T Factor . (adimensional) .

(2)

The T parameter, Tissue-Repair Factor for Mu model reads,

$$T = \frac{2}{n^2}\left[\frac{\exp(-\mu\,\Delta t)}{(1-\exp(-\mu\,\Delta t))}\right]\bullet\left[n-\frac{(\exp(-\mu\,\Delta t))^n}{(1-\exp(-\mu\,\Delta t))}\right]+\frac{1}{n};$$

where,

Δt : Time interval between fractions. (s).

N : Subfractions number . (adimensional).

μ : is the rate constant for repair of sublethal damages. (s^{-1}) .

(3)

Some Mathematical Analysis

The T Factor was developed in a number of models. The Mu model equation is the simplest. Equation (3) can be easily set within BED model variants. For example, the T Factor of Brenner model is an integral equation more difficult to be implemented in BED model. Nevertheless, all of them result be not specially complicated for BED calculations inset.

9. Scientific Ethics Standards

All software was done by the Author along these series. This study contains improved programming for 3D Triangular Isodosezones, [Casesnoves, May 7th, 2024, 3rd November 2020 and other dates], and engineered software that was developed for numerical hyperfractionated 3D TPO lung cancer imaging-processing database. Formulas applied/included are from previous article series with *in vitro* and *in vivo* database. Provided the objective functions for optimization require, models frequently constitute a mathematically feasible modification from several authors, based also on all literature Sections related papers. RT applications methods for these publications were created by Dr Casesnoves in 2007-present. Methods from 3D Isodosezones-lines were created by Dr. Francisco Casesnoves in 3rd November 2016, and Interior Optimization Methods in 2019.

BED model setting in Algorithms and programming were developed by Dr Casesnoves from previously published BED models. This article has previous papers information, whose inclusion is essential to make the contribution understandable. This study was carried out, and their contents are done according to the International Scientific Community and European Union Technology and Science Ethics. References: 'European Textbook on Ethics in Research'. European Commission, Directorate-General for Research. Unit L3. Governance and Ethics. European Research Area. Science and Society. EUR 24452 EN. And based on 'The European Code of Conduct for Research Integrity'. Revised Edition. ALLEA. 2017. This research was completely done by the author, the computational-software, calculations, images, mathematical propositions and statements, reference citations, and text is original for the author. When a mathematical statement, algorithm, proposition or theorem is presented, demonstration is always included. When a formula is presented, all parameters are detailed or referred. If any results inconsistency is found after publication, it is clarified in subsequent contributions. When a citation such as [Casesnoves, 'year'] is set, it is exclusively to clarify intellectual property at current times, without intention to brag. The article is exclusively scientific, without any commercial, institutional, academic, any religious, religious-similar, non-scientific theories, personal opinions, political ideas, or economical influences. When anything is taken from a source, it is adequately recognized. Ideas and some text expressions/sentences from previous publications were emphasized due to a clarification aim. Number of references is large to provide literature in open access for public health care institutions. Some additional Scientific Ethic Standards sources applied are:

1. ALLEA. 2017. The European Code of Conduct for Research Integrity, Revised Edn.; ALLEA: Berlin Barndenburg Academy of Sciences.
2. Good Research Practice. 2017. Swedish Research Council.

10. AUTHOR'S BIOGRAPHY

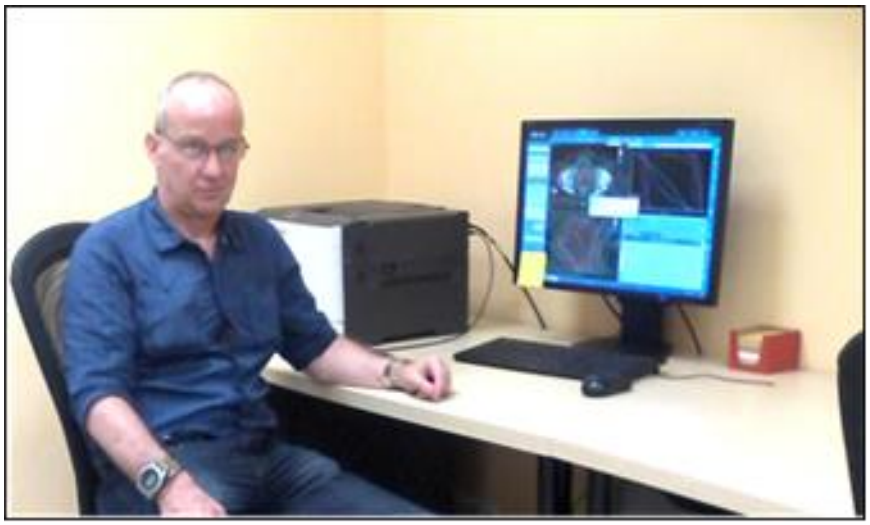

Dr Francisco Casesnoves earned the Engineering and Natural Sciences PhD by Talllinn University of Technology (started thesis in 2016, thesis Defence/PhD earned in December 2018, official graduate Diploma 2019). He works as independent research scientist in computational-engineering/physics. Dr Casesnoves earned MSc-BSc, Physics/Applied-Mathematics (Public Eastern-Finland-University, MSc Thesis in Radiotherapy Treatment Planning Optimization, which was developed after graduation in a series of Radiation Therapy Optimization-Modelling publications [2007-present]). Dr Casesnoves earned Graduate-with-MPhil, in Medicine and Surgery [1983] (Madrid University Medicine School, MPhil in Radioprotection Low Energies Dosimetry [1985]). Casesnoves resigned definitely to his original nationality in 2020 for ideological reasons, anti-monarchy-corruption, democratic-republican ideology, and ethical-professional reasons, and does not belong to Spain Kingdom anymore. His constant service to the International Scientific Community and Estonia Republic technological progress involves about 80 articles, more than 100 total publications, and about 4 books. Recent advances published are in Superconductors Mathematical Modelling and Radiotherapy Brain Neurobiological Models, 3D-AI Isodosezones and Isodoselines. Among Dr Casesnoves inventions and scientific creations are:

Numerical Reuleaux Method

Radiotherapy Omega Factor correction for AAA model wedge filters dose delivery

Integral-Differential materials erosion model

Graphical Optimization

Interior Optimization

Superconductors Molecular Effect Model

Superconductors Multifunctional Transmission Line

BED radiotherapy model GA optimization

RT Isodoselines and Isodosezones

Acknowledgement

To Natashka Kamarova, the best of my life, always with me.

Conflict of Interest

Author declares no conflict of inetrest, all was made by Author.